ALTERATION OF CEREBRAL BLOOD FLOW AFTER NEUROVASCULAR INJURY

by

Lingjue Li

BS, Sun Yat-sen University, 2012

MS, University of Pittsburgh, 2013

Submitted to the Graduate Faculty of

School of Pharmacy in partial fulfillment

of the requirements for the degree of

Doctor of Philosophy

University of Pittsburgh

2019

UNIVERSITY OF PITTSBURGH

SCHOOL OF PHARMACY

This dissertation was presented

by

Lingjue Li

It was defended on

April 5th, 2019

and approved by

Samuel M. Poloyac, Pharm D, PhD, Professor, School of Pharmacy

Mioara D. Manole, MD, Assistant Professor, School of Medicine

Patrick M. Kochanek, MD, Professor, School of Medicine

Robert B. Gibbs, PhD, Professor, School of Pharmacy

Philip E. Empey, PharmD, PhD, Assistant Professor, School of Pharmacy

Alberto L. Vazquez, PhD, Assistant Professor, Department of Radiology

Elizabeth A. Crago, RN, PhD, Assistant Professor, School of Nursing

Dissertation Advisors: Samuel M. Poloyac, Pharm D, PhD, Professor, School of Pharmacy

Mioara D. Manole, MD, Assistant Professor, School of Medicine

Copyright © by Lingjue Li

2019

ALTERATION OF CEREBRAL BLOOD FLOW AFTER NEUROVASCULAR INJURY

Lingjue Li, PhD

University of Pittsburgh, 2019

Cardiac arrest (CA) and subarachnoid hemorrhage (SAH) are devastating neurovascular diseases with high mortality. Patients who survive the initial insult frequently have long-term neurological deficits. Delayed ischemia is recognized as one of the important mechanisms underlying poor outcome; however, strategies to improve cerebral perfusion failed to demonstrate efficacy in long-term outcome. Regulation of vascular tone in the cerebral microvasculature is key in determining cerebral blood flow (CBF), therefore, the evaluation of cerebral microcirculation alterations after CA and SAH can provide insights into the pathophysiology of neurovascular diseases and aid in the discovery of promising therapeutic targets.

The aim of this dissertation is to explore the role of cerebral microvascular alterations in an animal model and patients who are subjected to neurovascular diseases. In Chapter 2, we extensively reviewed the pharmacological therapies used for CA and global ischemia. We believe that combination therapy is promising which maximizes the effect of CBF restoration and off-sets potential adverse effects on cerebral microcirculation. In Chapter 3 and 4, we established an *in-vivo* multiphoton microscopy platform to evaluate the pathophysiology and pharmacology in a pediatric CA model. We observed the capillary no-reflow phenomenon and prolonged plasma mean transit time (MTT) *in-vivo*, identified arteriolar constriction and red blood cell (RBC) stasis as two potential targets to restore cerebral perfusion after CA. Inhibition of a vessel constrictive fatty acid, 20-HETE, dilated arterioles and attenuated MTT but had no

effect on RBC stasis. Our results suggest the need for combination therapy to mitigate both the arteriolar constriction and the no-reflow phenomenon. In Chapter 5, we assessed 20-HETE and CO_2 reactivity as two microcirculatory biomarkers in SAH patients. Plasma 20-HETE was not correlated with cerebrospinal fluid level, suggesting that local production of 20-HETE might underline the pathophysiology of SAH. We also found a wide range of CO_2 reactivity in SAH patients which paved the way for future clinical biomarker investigation.

Collectively, this work identified new therapeutic targets in cerebral microcirculation, and provides rationale for CBF targeted treatment for neurovascular diseases. The clinical biomarker investigation provides novel insights in identifying vulnerable patient population to enable personalize treatment in the future.

Keywords

Cardiac arrest, subarachnoid hemorrhage, cerebral blood flow, microcirculation, 20-HETE, multiphoton microscopy.

TABLE OF CONTENTS

LIST OF TABLES

LIST OF FIGURES

PREFACE

I am dedicating this dissertation to my family, my husband and my parents, who make every effort count and whose unselfish love, sacrifice, dedication and support made this dissertation possible. I am also dedicating this work to my grandfather, who passed away in 2016; his love and persistence always encourage me in every endeavor.

For the past six years, I have been very fortunate to pursue my PhD training at the University of Pittsburgh, School of Pharmacy. This is so far the best time and most exciting adventure I have ever had which I will surely treasure for the rest of my life.

I have met so many kind people who made great impact on my professional and personal life. I could not name all of them here; however, I would like to acknowledge at least a few who have made a significant contribution to my PhD study. First, I would like to thank my advisor Dr. Samuel Poloyac, for his dedicated mentorship and tremendous support since 2012. His passion in teaching and research always encourage me to step out my comfort zone and confront the challenge bravely. He never shows me an easy way, because he believes the right way is never easy which I learned to agree with. His outstanding guidance always motivates me to think harder and try harder. It is our numerous discussions that inspired this dissertation piece by piece. Without his mentoring in science and life, I would not have been where I am today. I, like

any one of your students, might argue with you sometimes, but will always love you. I owe significant gratitude to my co-advisor, Dr. Mioara Manole, for her incredible dedication and mentoring in my PhD training. Her enthusiasm in research and patience in details always encourage me whenever I came across any difficulties. I would like to thank my dissertation committee: Drs. Kochaneck, Gibbs, Empey, Vazquez, and Crago. They represent the level of brilliance, excellence and integrity in scientific research that I always look up to and work towards.

I am very grateful to my lab mates in Poloyac's lab: Chenxiao, Trish, Pat, Beth, Junmei, Kacey, Mark and Basha. Their work helped shape my training and accompany me as family. Special thanks to Henry, for his dedication and mastery in animal surgery which is essential to this dissertation. I would regret if I did not acknowledge my friend and colleagues in School of Pharmacy: Rujuta, Fanuel, Solomon, Junyi, Alex, Yoko, Katie, Jess, Hari, Karryn, Jing and Yingfei, who made my time at Pitt wonderful and lively.

My sincere gratitude goes to University of Pittsburgh, School of Pharmacy, Safar Center for Resuscitation, Center for Biologic Imaging, all the faculty, staff and students. Special thanks to Dean Kroboth, who introduced me to Pitt initially. Her caring and encouragement strengthened my determination to be a scientist. A big thank you to Dr. Folan and Lori, who are always helpful whenever I need help. I am really fortunate to be a member of this great school and the fruitful collaboration. I am humbled by all the participants, the patients and their family, who devoted to my training and dissertation work.

Finally, I give my heartful gratitude to my family for their extraordinary love and support. My husband Zhangxian, who I owe great thanks to, joined me in the United States after three years of separation. Without his faith, sacrifice and love, this dissertation would not be

possible. Our marriage is the best gift during my graduate study. My parents Yangzhao and Shaojuan, devoted tremendous support for my education over these years. Their marvelous understanding and love give the meaning of every endeavor. Family is the most important and I owe this accomplishment to you.

1.0 INTRODUCTION AND BACKGROUND

1.1 INTRODUCTION

The theme of this dissertation is to better understand the pathophysiology of neurovascular diseases, such as cardiac arrest (CA) and subarachnoid hemorrhage (SAH). Secondary ischemia is a common complication accompanied with CA and SAH and is attributed to mortality and morbidity. We are determined to investigate the cerebral blood flow (CBF) after CA and SAH and trying to identify novel therapeutic targets to ultimately improve patient outcome. In chapter 1, we provided a brief introduction of CBF alterations after CA since it is the disease we focused on in chapter 2-4. The introduction of SAH will be illustrated with more details in chapter 5.

1.2 CARDIAC ARREST OVERVIEW

Cardiac arrest (CA) is the cessation of systemic circulation due to trauma, drug overdose, drowning, asphyxia, cardiovascular or other medical causes. More than 356,500 and 209,000 people suffer from out-of-hospital and in-hospital CA annually in the United States [1]. Despite the recent gradual improvement in survival, CA remains a significant cause of death with only 11.4% patients who survive to discharge [1].

Brain injury caused by CA contributes to 68% and 23% mortality in out-of-hospital and in-hospital CA [2, 3]. Patients that survive the initial CA often suffer from prolonged neurological dysfunction, including coma and persistent vegetative state. It was estimated that only 3-7% survivors are able to return to their previous level of function, which creates an enormous economical and societal burden on patients, their family and health care system [4, 5].

1.3 CEREBRAL BLOOD FLOW AFTER CARDIAC ARREST

The ischemic perfusion that follows CA subjects the brain tissue to hypoxia and leads to neuronal damage. Cerebral blood flow (CBF) is a key component during and after resuscitation to provide sufficient perfusion and oxygen supply. Disturbances in CBF post-CA have been recognized in numerous clinical studies as well as pre-clinical animal models [6]. Classically, CBF post-resuscitation can be described into three phases: early hyperemia, followed by hypoperfusion, and finally either resolution of normal blood flow or protracted hyperemia [7]. Recently, detailed temporal and regional CBF alterations after CA was depicted using MRI. Manole, *et al*. reported early hyperemia in the subcortical region and sustained hypoperfusion in the cortical region in a pediatric asphyxial CA model [8]. Different animal models, age, injury severity have also been attributed to CBF variations [6, 8, 9].

1.4 CBF REGULATION

Regulation of CBF is multifactorial. CBF is direct proportional to the cerebral perfusion pressure (CePP) and inversely related to cerebral vascular resistance (CVR) (Eq. 1). CePP is the driving force of blood flow in the brain and is determined by the difference between the mean arterial pressure (MAP) and intracranial pressure (ICP) (Eq. 2). As described by Poiseuille[10], CVR is affected by the length of the vessel (L), blood viscosity (η) and vessel radium (r) (Eq. 3). Change in any of these factors can impact CBF.

$$CBF = \frac{CePP}{CVR} \qquad \text{(Eq. 1)}$$

$$CePP = MAP - ICP \quad \text{(Eq. 2)}$$

$$CVR = \frac{8L\eta}{\pi r^4} \quad \text{(Eq. 3)}$$

1.5 RESUSCITATION MANAGEMENT

Ever since cardiopulmonary resuscitation (CPR) was implemented in 1960s, the guidelines for modern resuscitation have evolved based on emerging preclinical and clinical evidence. The primary goal of resuscitation during CA is to provide perfusion to critical organs (heart and brain) with a final goal of restoring and maintaining spontaneous perfusion. Pharmacologic therapies such as vasopressors, antiarrhythmic drugs, atropine, sodium bicarbonate, calcium (Ca^{2+}), and magnesium have been used clinically and in animal models to facilitate resuscitation [11]. Various therapies were utilized to optimize CBF post-resuscitation.

1.6 CARDIAC ARREST ANIMAL MODELS

CA leads to a global ischemia injury. To mimic the global ischemic status, early animal models such as aortic balloon occlusion [12] and neck tourniquet insults [12] were studied. Recently, clinically relevant animal models were established including ventricular fibrillation (VF) CA, asphyxial CA and KCL induced CA [9, 13, 14]. Most studies were conducted in small or large animal models, including rats, mice, rabbits, cats, dogs, pigs, sheep and monkeys [15-17]. Animal models enable the serial and regional assessment of CBF and also provide the advantage

of correlating CBF and CBF targeted interventions with thorough histology and outcome evaluations. On the other hand, species, age and gender differences can attribute to CBF variations observed in different studies. Cautions should be taken when interpreting results on different animal models.

1.7 DIFFERENT METHODOLOGY FOR CBF ASSESSMENT

Both invasive and non-invasive methodologies have been utilized to study CBF or perfusion post-CA. Some methodologies are only applied in animal models while some others can also be used at bedside. A more detailed description of different methodology can be found elsewhere [7]. In animal models, radiolabeled microspheres, laser-speckle flowmetry, and optical imaging are often adopted [17-20]. Multiphoton microscopy is a novel imaging method which enables detailed observation in the cerebral microcirculation [21]. Although CBF is not routinely monitored for patients who survive from CA, methods available for CBF assessment in human includes transcranial doppler, arterial spin labeling MRI, Xenon-CT, and near-infrared spectroscopy [6, 22-25]. Different methodologies provide different features as well as limitations for CBF assessment. These advantage and limitations add another layer of complexity in different studies.

CBF directed therapies post-CA have the potential to restore nutrition supply and attenuate neuronal damage. Indeed, therapies targeted at both early hyperemia and hypoperfusion have shown benefit in outcomes [13, 26-28]. We propose here to analyze the impact of previously published CBF-directed therapies on CBF and neurological outcome post-CA with special attention to details of the experimental protocol as it relates to the species used,

CA model, regional and temporal changes in perfusion, as well as specific microcirculatory alterations. The detailed presentation of CBF directed therapies grouped according to the physiological parameters impacted will be summarized in chapter 2.

2.0 PHARMACOLOGICAL THERAPIES TARGETED ON CEREBRAL BLOOD FLOW AFTER CARDIAC ARREST

2.1 INTRODUCTION

Major strides were made during the last decades in improving the rates of resuscitation from CA by optimizing CPR techniques and maximizing CPR education in laypersons. Important advances also occurred in the optimization of post-CA physiological care, including institution of hypothermia, maintenance of temperature regulation and blood pressure. While hypoxic-ischemic encephalopathy is the major limiting factor for intact neurological survival after CA, cerebral-specific therapies have not been instituted at a large scale to date. There is a pressing need for novel interventions to improve CBF after CA to prevent secondary injury and improve overall outcomes. As several pharmacological therapies have been explored in preclinical models and some therapies have been explored in patients, we identified the need to synthetize the effects of pharmacologic therapeutic interventions to date as they relate to the regulation of CBF. Development of such interventions requires a thorough understanding of the factors that are known to regulate CBF and the effects of current pharmacologic therapies. Therefore, the purpose of this chapter is to summarize the current evidence for pharmacological therapies that targeted CBF restoration after CA or global ischemia models and discuss the potential for future development.

To identify published articles on CBF-directed therapies, we initially developed a comprehensive search strategy (Appendix I). This search strategy yielded 1063 articles from PubMed database published until Dec 2018. We analyzed 665 studies in animal models and 28 clinical studies. A flowchart of our results is presented in Figure 2.1. Two reviewers screened the titles and abstracts, identified and analyzed relevant articles, and categorized these articles into five classes generated a priori based on the therapeutic mechanism and site of action. The categories included: flow promotion therapies (maximize CePP), vasodilatory (maximize CVR),

thrombolytic (mitigate capillary stasis), antioxidant and anti-inflammatory (maintain homeostasis of the endothelial cells), and other hemodynamic therapies (combination therapies or other mechanisms) (Figure 2.1). These therapies are also summarized in Appendix II.

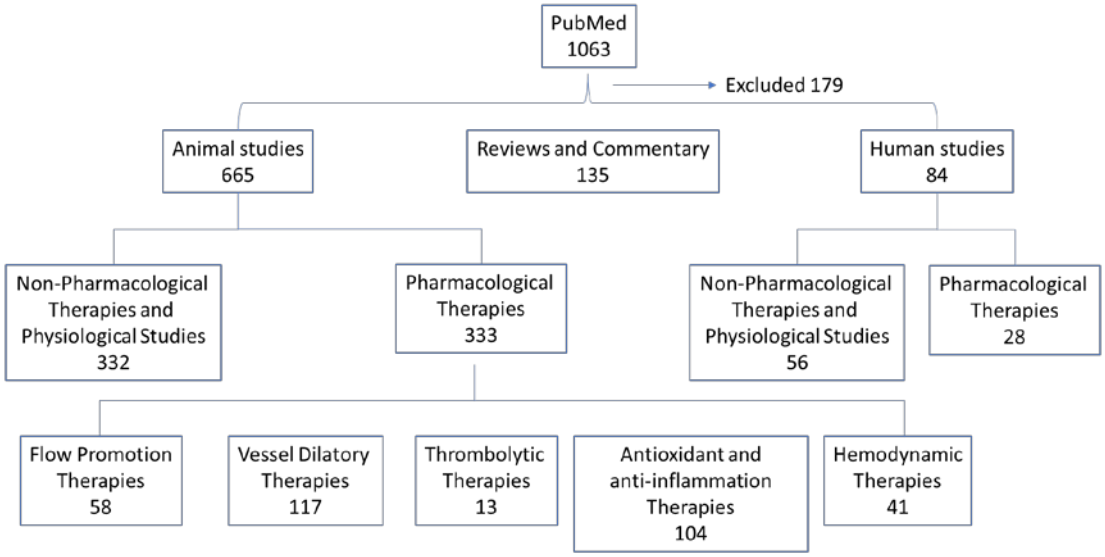

Figure 2.1 Flowchart of the results from the PubMed database

2.2 FLOW PROMOTION THERAPIES

The flow promotion therapies have the goal to improve CBF by maximizing CePP either via increasing the cardiac output or MAP s According to Eq.1 and 2, increasing MAP will enhance CePP and CBF. This class of therapies can be further categorized as adrenergic agents and non-adrenergic agents.

2.2.1 Adrenergic Agents

Most adrenergic agents exert a “fight or flight” response: increased blood pressure, vasoconstriction in most vascular beds, vasodilation in skeletal muscles, heart and brain, increased heart rate, and bronchodilation. The effect of each specific adrenergic agent is determined by the type of adrenergic receptor stimulated (ARs) and the affinity to each receptor. The four major adrenergic receptors are α-1, α-2, β-1 and β-2. Alpha-1 receptors are localized postsynaptically in sympathetic nerves and are expressed in the smooth muscle throughout the body [29, 30] They mediate the cardiovascular sympathetic responses to stress. The major effect of α-1 receptor activation is smooth muscle contraction in blood vessels including vessels of the heart and brain. Alpha-1 receptors also mediate glycogenolysis and gluconeogenesis responses. Alpha-2 adrenergic receptors are expressed in both peripheral tissue and central nervous system and are localized pre-synaptically at the terminals of the sympathetic nerves. When activated, α-2 ARs inhibit the release of endogenous agonist norepinephrine (NE) and attenuate the sympathetic response [31]. The physiological effects of α-2 ARs include decreased peripheral vascular resistances, decreased insulin release and increased glucagon release. Beta-1 adrenergic receptors are the predominant receptors in cardiac smooth muscles and control cardiac function through positive inotropic and chronotropic effects, producing increased contractility and tachycardia, while β-2 receptors mediate smooth muscle relaxation, bronchodilation and glycogenolysis when activated [30]. When autoregulation is intact, cerebral vasoconstriction mediated by vascular α receptors is not significant [30, 32]. In contrast, coronary blood flow is enhanced by both α and β-2 receptor stimulation [30]. The effects of adrenergic agents on myocardial function during resuscitation were previously described [32-34], and thus we will focus on the effect of adrenergic agents on CBF during and after resuscitation.

Epinephrine (Epi) has been used clinically as standard of care at resuscitation for more than 40 years [35]. As a non-selective adrenergic receptor agonist, Epi activates all four receptors' isoforms with different affinity. Epi has a higher affinity for β than α receptors, therefore, at low Epi doses, β-1 and β-2 receptor mediated responses dominate, while at high dose, α-1, α-2 receptor mediated responses predominate. At the Epi dose used for resuscitation, α receptor mediated response is the primary effect, manifested as enhanced aortic diastolic pressure, which increases coronary perfusion pressure (CPP) and CePP. CPP has been strongly associated with successful return of spontaneous circulation (ROSC) in both humans and animals [36, 37]. In a ventricular fibrillation (VF) CA model in piglets Epi increased CPP in a dose-dependent manner [38]. At a higher Epi dose of 0.09 mg/kg, CPP almost doubled, and survival success was approximately six times higher than at a low Epi dose of 0.015 mg/kg, suggesting the potent α-1 activation of the higher dose. The potent cardiac vasoconstriction of Epi increased blood pressure and CePP, leading to increased CBF (Eq.1). Epi administered at resuscitation increased cortical CBF more than six-fold post-CA, and increased cerebellar and midbrain CBF tenfold [39]. Similar to the effect on CPP, Epi also exerts a dose dependent effect on CBF. Pigs that received high Epi dose of 2.0 mg/kg at resuscitation from VF CA had four to five-fold higher CBF in cortex, cerebellum and midbrain compared with pigs that received a low Epi dose of 0.02 mg/kg [39]. Epi also improves CBF and cerebral O_2 uptake in pediatric CA models after resuscitation [40].

Epi has a short half-life of 2-3 minutes. To sustain its flow promoting effect, multiple dosing strategies were investigated in CA models. Studies have suggested that Epi increases CBF in a dose dependent manner: higher doses are associated with higher CBF and resuscitation rates [39-42]. The Epi doses evaluated range from 0.015 ~ 2.0 mg/kg. Different dosing regimens of

Epi and their effect on CBF were also evaluated in animal models. When dosed repeatedly after resuscitation, each bolus of Epi was observed to have a transient CBF increment [43]. Continuous Epi infusion led to more a sustained increment in cortical CBF compared with repeated doses [44]. However, long-term neurological assessments were not performed in those studies, and in the context of recent human studies showing no neurological benefit in Epi-treated groups vs. controls these evaluations are needed.

More recently, the effect of Epi on CBF has been questioned in the cerebral microcirculation, mostly due to its prolonged α-1 mediated peripheral vasoconstriction. Ristagno *et al.* found that cortical microcirculatory blood flow was largely reduced after 0.03 mg/kg Epi treatment in a pig model of CA [45]. The evaluation was based on images obtained in piglets though a cranial window placed on the surface of the cortex, and only visible surface vessels were assessed. The Ristagno group also reported that epinephrine, due to its α-1 agonist effect, decreased PbO_2 tension and increased $PbCO_2$ tension and worsened tissue ischemia[46]. Other effect of Epi in cerebral microcirculation is still under investigation. With more advanced imaging methods such as arterial spin label MRI and multiphoton microscopy, the effects of Epi treatment as it relates to dose on cerebral microcirculation after CA can be better elucidated.

In addition to the effect of Epi on CBF when given at after resuscitation, the effect of Epi during the post-CA period has been evaluated in pre-clinical studies. Epi administered at 3 h after resuscitation in a pediatric CA model markedly increased CBF in all brain regions, likely secondary to loss of autoregulation [8].

Other adrenergic agents with effect on CBF evaluated post-resuscitation from CA include **NE, phenylephrine, methoxamine** and **dexmedetomidine**. Similar to Epi, NE is also a non-selective adrenergic receptor agonist and can activate α-1, α-2 and β1-receptors, and thus can

also increase heart rate, cardiac contractile force and blood pressure, therefore promote CBF. Lindner, *et al.* reported that NE administration significantly increased CePP in a swine CA where CBF was assessed using microspheres. CBF increased from 30 mL/min/100g to 58 mL/min/100g after NE administration [47]. NE is a weak β-2 AR agonist, so NE was not expected to increase glycogenolysis after resuscitation. In this study, both NE and Epi increased CBF and oxygen delivery to a similar extent, but neither increased cerebral oxygen consumption. Phenylephrine and methoxamine are two pure α-1 agonists. They are expected to constrict cardiac smooth muscle and increase CePP during resuscitation thus promoting CBF. Phenylephrine at 10 mg/kg improves CBF post-CA to a similar extent as Epi 0.2 mg/kg administration [48], while at phenylephrine dose of 0.1 mg/kg, the cortical CBF is only 1/6 of the CBF after Epi administration [40]. Methoxamine at a dose of 10 mg/kg can only partially restore CBF up to the caudal structure such as the pons, medulla and cervical spinal cord [49]. These results suggest that α-1 activation alone produces modest increases in CBF and thus is potentially not sufficient for flow promotion to the brain after CA. The positive inotropic and chronotropic effect of β-1 AR might also play an important role. Dexmedetomidine is an α-2 AR agonist with good brain penetration profile. The rationale of using dexmedetomidine is to attenuate α-1 AR responses in the brain and reduce CRV. When dexmedetomidine was administered after resuscitation with phenylephrine in a canine model of 5 min CA, pial arterioles dilated up to 15 min post-CA but no difference was found in oxygen extraction post resuscitation [42]. Since CBF or metabolism were not directly measured in this study, the decreased oxygen extraction might be due to the impaired metabolism. Compared with Epi, other adrenergic agents have only been evaluated over a limited dose range with limited CBF assessment available. Furthermore, additional studies

to evaluate the effects of other adrenergic agents on long-term outcome assessments are needed to determine overall therapeutic efficacy.

Overall, adrenergic agents have a role in promoting CBF post-CA. It is critical to restore the spontaneous perfusion to the brain as soon as possible. Currently, adrenergic agents are the only pharmacological agents able to attain this, and need to be dosed immediately at the resuscitation. However, prolonged α-1 AR responses may lead to sustained cerebral vasoconstriction, which could result in increased CVR and compromised CBF. Prolonged α-1 and β-2 activation could also worsen ischemia by stimulating oxygen consumption. It might be plausible to use adrenergic agents at resuscitation and suspend after ROSC is achieved.

The efficacy of adrenergic agents to promote CBF after CA has been demonstrated in multiple animal models, however their direct effect on microcirculation remains an important and largely unexplored. With the emergence of more powerful methodologies such as Arterial Spin Label MRI for regional CBF assessment and in vivo multiphoton microscopy for direct microcirculatory assessment, a more thorough evaluation of the role of adrenergic agents is possible.

2.2.2 Non-adrenergic Agents

The effect of non-adrenergic agents can be mediated by both the adrenergic α1, β2 receptors, and also by specific dopaminergic, vasopressin, …etc receptors.

Dopamine (DA) plays a major role in the central nervous system by regulating motor and cognitive function. DA also has vascular effects mediated by DA receptors and cross interaction with ARs. At low concentration, DA activates vascular D1 receptors, elevates intracellular cAMP and mediate vasodilation. At intermediate concentration, DA can increase perfusion by

interactions with both β-1 receptors and D1 receptors. At high concentrations, DA has cross interaction with α receptors in the smooth muscle and produce vasoconstriction. Liu *et al.* found that DA administration improved MAP and oxygen metabolism after 30min ROSC in a 4min VFCA swine model[50]. In this study, CPP increased 33% after 1-hour ROSC but CBF measurement was not performed. The improved CPP might be a combination of both α-1 ARs and D1 activation. Similar to Epi, cautions also arise for the potential deleterious effect of prolonged α-1 receptor activation which could constrict peripheral arterioles and compromise CBF.

Vasopressin is an endogenous hormone synthesized in hypothalamus and released into the blood stream. The major effect of vasopressin includes arterial constriction and increasing water reabsorption during hypertonicity [51]. Vasopressin does not share crossover activation with ARs. There are three types of vasopressin receptors: V1a, V1b and V2. The vascular effect of vasopressin is predominantly mediated by V1a receptor expressed in smooth muscle cells [52]. V1a receptor belongs to G-protein coupled receptor family. When V1a is activated, downstream pathways, including phospholipase C (PLC), inositol-1,4,5-trphosphate (IP3), protein kinase C (PKC) pathways, will increase intracellular Ca^{2+} level, causing depolarization and muscular contraction [53]. In the heart, vasopressin can cause coronary vasoconstriction and increased CPP although controversial observation does exist [54, 55]. In the brain, vasopressin is mostly considered a potent vasoconstrictor for arteries and arterioles [56]. White topical application of vasopressin constricted pial arterioles in anesthetized rabbits [57], vasopressin also shown to exert a biphasic action with an initial potent vasoconstriction mediated by V1 receptors, followed by vasodilation mediated by V2 receptors [58]. Dose- and vessel size-dependent effect of vasopressin has been reported where vasopressin dilates large arteries at low, physiological dose

[57, 59]. Such dilatory effect has been attributed indirectly to nitric oxide (NO) pathway [60]. At a high dose of 40 mU/kg given intravenously, Faraci *et al.* showed that the resistance of large arteries decreases while resistance of small arterioles increases [57]. Vasopressin therefore could be preferred in promoting perfusion pressure with cerebral vasodilation in large cerebral arteries.

Vasopressin does not share crossover activation with ARs, therefore it could increase cardiac perfusion, but not myocardial oxygen demand. Accumulating clinical studies and animal experiments suggest the benefit of vasopressin over Epi after CPR [61-64]. Vasopressin administration increased aortic diastolic pressure after 4 min CA compared with saline control and with Epi, which suggests potent coronary vasoconstriction and increased CPP[65]. Vasopressin also ameliorated neurodegeneration in these piglets as assessed by MRI. Several other studies investigated the effect of vasopressin on CBF and found equivalent or even better results compared with Epi. In a prolonged porcine CA model, vasopressin resulted in a two-fold increase in myocardial blood flow at 90s and 5 min after ROSC compared with Epi. CBF was found to be 3.5 and 6.3 times higher as compared with Epi at 90 s and 5 min after ROSC, respectively [63]. In a pediatric 8 min asphyxial CA model, both CPP and CBF increased more than two-fold after vasopressin administration but was comparable to Epi treatment [62]. A study by Nozari, *et al.* showed in a 5 min VFCA model that vasopressin injection led to ~30% higher cortical CBF compared to Epi, while CPP and CePP are similar between two treatment groups, indicating the reduction of CVR after vasopressin treatment [66]. The exact values and extent of CPP and CBF promotion effect of vasopressin are different across studies, which could be due to different animal models and quantification methodology.

Recently, the effect of vasopressin on microcirculatory blood flow has gained more attention. Using orthogonal polarization spectral imaging through a cranial window in pigs

treated with vasopressin at resuscitation, a 5 times increase in the number of perfused cortical microvessels was observed after vasopressin treatment compared with Epi [64]. At the same time, improved microcirculatory flow index and brain tissue oxygenation were observed at 5 min after vasopressin administration compared with Epi treatment [46]. Although vasopressin has been suggested to provide advantages in cerebral microcirculatory flow and outcome after CA resuscitation, its superiority over Epi as a vasopressor has not been established. Vasopressin administration was found with suboptimal endocardial perfusion and myocardial hypoperfusion [46]. Although supportive preclinical studies exist, there is a need for additional clinical evaluation to determine if vasopressin improves overall cerebral blood flow.

Endothelin (ET) is a family of four vasoactive peptides produced in endothelium. ET-1 is the predominant isoform and constrict vessels by activating two types of ET receptors: ET_A and ET_B receptors. Both ET_A and ET_B receptors are localized in the vascular smooth muscle while ET_B receptors are also found in endothelial cells and macrophages [54, 67, 68]. Activation of both ET_A and ET_B receptors results in vasoconstriction. The mechanism of action includes PLC activation, leading to accumulation of inositol triphosphate and intracellular Ca^{2+} [69]. ET_B receptor also exerts vasodilation by stimulating NO production on the endothelium. ET_A is the predominant isoform in the heart and mediates positive inotropic effect by activating protein kinase C and the Na^+/H^+ exchanger [70]. ET receptors are also found in cerebral blood vessel, choroid plexus and peripheral nerves so ET-1 is considered a potent cerebral vasoconstrictor mediated by Ca^{2+} channels [70].

A thorough study by DeBehnke investigated the effect of ET-1 at a dose of 50, 150 and 300 µg, respectively, with or without Epi after 10min VFCA[71]. CPP was found higher (85 vs 28 mm Hg) in pigs receiving 300 µg ET-1 injection compared with pigs receiving Epi. More

than 4 times higher regional and global CBF was observed in pigs receiving 150 and 300 μg ET-1 than pigs receiving Epi. These results suggest that ET-1 promotes CBF by increasing CePP, exerting dose-dependent, positive inotropic effect mediated by ET_A. Another study by Holzer, *et al.* confirmed the dose-dependent promotion of ET-1 on CPP and CBF in a 5 min VFCA in swine [72]. In these two studies, the flow promotion effect of ET-1 manifests within 10 min after injection. However, concerns rise for ET-1 with worsened outcome post resuscitation, mainly due to the persistence of the vasoconstrictor effect. A pharmacokinetic model with radiolabeled ET revealed that ET-1 is distributed and cleared in a complicated three-compartment model and can remain in the body up to 45 hours [73]. Another study also described prolonged vasoconstrictive effect compared with ET-1 plasma concentration due to extremely slow dissociation from binding site [74]. Hilwig and colleagues reported that ET-1 substantially increased CPP during CPR but the mean pulse pressure dropped to less than 10 mm Hg after 1 hour ROSC [75]. ET_A antagonist BQ123 injected at 15 min ROSC improved long-term neurological outcome after CA, which further questioned the application of endothelin-1 as an appropriate flow promotion agent during resuscitation [76, 77].

Angiotensin (ANG) II is an endogenous octapeptide and widely involved in physiological activities including vasoconstriction, blood pressure regulation, inflammation, and platelet aggregation [78]. Two G-protein-coupled receptors, ANG type 1 receptor (AT_1R) and ANG type 2 receptor (AT_2R), have been identified as the main types of ANG receptors. Most of the effects of ANG II are mediated by AT_1R, which is distributed in various organs, including liver, heart, brain, kidney, adrenals and vasculature [79]. Acutely accumulated ANG II can activate AT1R and produce vascular smooth muscle constriction. The mechanism includes activation of downstream PLC, phospholipase A2 (PLA2), IP3 and diacylglycerol (DAG).

Within seconds, IP3 can subsequently increase intracellular Ca^{2+} level and cause smooth muscle cell contraction[79]. Meanwhile DAG can activate PKC and also contribute to vasoconstriction. In addition, activated PLA2 can further form arachidonic acid (AA) and produce a range of vasoactive metabolites: prostaglandins, leukotrienes, epoxyeicosatrienoic acids (EETs) and hydroxyeicosatetraenoic acids (HETEs). ANG II can also activate NAD(P)H oxidases and produce reactive oxygen species (ROS) [80].

Similar to other flow promotion agents, ANG II also increase blood pressure and CBF by constricting large arteries. Little and Brown showed that ANG II administration increased CBF from 6.9 mL/min per 100 g to 30.8 mL/min per 100 g in a pediatric piglet VFCA model using radiolabeled microspheres [81]. However, the CBF promotion effect has not been evaluated in comparison with other vasopressors. It is difficult to determine the relative potency and efficacy of ANG II compared with other agents based on the currently published literature. Moreover, ANG II might not serve as a preferred flow promotion agent because of its wide range of physiological effects. Unwanted effects such as ROS production, platelet aggregation and sustained vasoconstriction might compromise the benefit of ANG on flow promotion.

In summary, several non-adrenergic agents have also been used during resuscitation for CA. Their flow promotion effects provide novel mechanisms to improve CBF but also bring in new challenges. So far, no superior effect has been recognized compared with Epi. More long-term outcome and off-target effect remains to be investigated.

2.3 VASODILATORY THERAPIES

This class of therapies dilate peripheral vessels, reducing CVR and improve CBF post-CA. According to Eq.3, vasodilator strategies have the potential to have great efficacy to increase CBF. Multiple mediators participate in the change of vessel diameter such as glutamate, NO, adenosine, ions like hydrogen (H^+), potassium (K^+), Ca^{2+} and vasoactive fatty acids [82, 83]. The molecular pathways of these mediators are complex and sometimes overlapping. A single agent can improve perfusion through cross-talk activation of multiple pathways simultaneously or sequentially. As will be highlighted in the forthcoming section, it is notable that most of agents in this class also possess neuroprotection independent from the CBF effect.

2.3.1 NO Pathway

NO is a key signaling molecule in the vasculature produced by various cell types including endothelial cells, platelets, macrophages, and neurons. Three isoforms of nitric oxide synthase (NOS) are responsible for the synthesis of NO: endothelial NOS (eNOS), neuronal NOS (nNOS) and inducible NOS (iNOS). Both eNOS and nNOS transiently produce NO at nanomolar level in a Ca^{2+} dependent manner, while iNOS is less Ca^{2+} sensitive and produces NO at the micromolar range. Biochemical stimuli such as thrombin, acetylcholine and bradykinin, and mechanical stimuli such as shear stress and cyclic strain can increase NO synthesis. It is generally considered that the low local levels of NO produced by eNOS are cytoprotective and the high concentrations of NO produced by iNOS are cytotoxic [84].

After formation, NO diffuses to adjacent vascular smooth muscle cells and exerts vasorelaxation. The fundamental mechanism of NO is through guanylyl cyclase activation which

increases cGMP formation and activates PKG [85]. NO can also inhibit voltage-gated Ca^{2+} channels and activate Ca^{2+}denpendent K^+ channel [86, 87]. Both effects result in reduction in cytosolic Ca^{2+} level and vasodilation. Additional mechanisms of NO vasodilation include the inhibition of vasoconstrictive pathways, such as ANG II and 20-HETE [88, 89]. In the heart, NO exerts a dual inotropic effect and a positive chronotropic effect [90]. At low concentrations, NO enhances myocardial contractility while at high concentrations it depresses contractility. In the brain, NO is a key mediator in regulating CBF at rest, during physiological conditions, as well as under pathophysiological conditions [86]. It is generally recognized that eNOS derived NO plays an essential role in autoregulation by maintaining basal vascular tone. NO derived from nNOS appears more involved in neurovascular coupling [91]. In addition to its well-known vasodilatory effect, NO also exerts antiplatelet, antithrombotic, anti-inflammatory, and antioxidant properties.

Therapies targeting NO pathway include NO donors and various NOS inhibitors (Appendix II). The rationale to use NO donors, including **inhaled NO, L-arginine**, **sodium nitroprusside,** and **nitroglycerin,** is to increase NO level, dilate peripheral vessels and decrease CVR. Direct inhalation of NO can supply intravascular NO and has been shown greatly improved survival rate when initiated up to 2 hours in a CA model in mice [91]. However, CBF did not increase in the cortex, hippocampus or whole brain when evaluated with ASL-MRI, probably due to systemic vasorelaxation and decreased CePP. L-arginine serves as a substrate for all NOS. Hiramatsu and Tsui, both reported that L-arginine increased CBF ~50% accompanied with improved oxygen metabolism in two pediatric piglet CA models [92, 93]. Sodium nitroprusside is clinically used to treat acute hypertensive crises due to its potent vasodilatory effect. Schultz, *et al.* suggested that sodium nitroprusside produces 2-fold increased CPP and 4 -fold increased CePP in a 15 min VFCA swine model [94]. Yannopoulos, *et al.* further confirmed

improved CPP with improved survival rate and neurological outcome in an 8 min swine model [95]. **Nitroglycerin** is a prodrug which releases NO after bioactivation and cause vasodilation [96]. Nitroglycerin improved the neurological outcome given alone in an 8 min asphyxial CA model in rats [97]. However, CBF post-CA has not been assessed after nitroglycerin treatment alone. Combination therapy of nitroglycerin with either epinephrine or vasopressin has shown benefits in protection of myocardial blood flow and endocardial perfusion in two swine CA models [98, 99]. More importantly, the combination therapies lead to improved CBF and functional outcome after CA [100-102]. In a 6 min asphyxial CA study, delayed use of nitroglycerin in addition to vasopressin produced better resuscitation rate than vasopressin alone, proposing that the optimal dosing strategy of nitroglycerin to avoid MAP decrease is delayed administration, as the potential deleterious effects common for NO donors could be prolonged systemic hypotension [103].

Multiple NOS inhibitors have been investigated in the CA models focused on mitigating some of the unwanted pathophysiological effects of NO. Glutamate release in early ischemia leads to activation of nNOS and iNOS, producing massive amount of NO, which can interact in direct equimolar concentrations with superoxide to form neurotoxic peroxynitrite [102, 104]. The rationale to use NOS inhibitors is to prevent the excessive production of NO by nNOS and iNOS. On the other hand, reduction of NO by NOS inhibitors can lead to vasoconstriction both in the heart and in the brain. **L-nitro-arginine methyl ester (L-NAME),** is a non-selective NOS inhibitor which has been shown to reduce blood flow by 25% and increase resistance by 50% in humans [105]. In a swine model of CA, L-NAME injected at reperfusion showed no change in CBF[106]. Two other studies in pediatric piglets reported decreased CBF after L-NAME injection at resuscitation[94, 107], which was likely due to the observed ~2 fold increased MAP

and ~2.5 increased CVR as reported by Hiramatsu [93]. **Methylene Blue** inhibits NO synthesis as well as guanylyl cyclase activity and have been suggested to counteract with NO by attenuating cGMP mediated vasodilation [94, 108]. However, the study by Miclescu *et al.* measured cortical CBF using laser-Doppler and reported almost doubled cortical CBF after 12 min CA in pigs [109]. Such effect could be attributed to the additional inotropic effect of methylene blue as reported earlier[110]. **7-nitroindazole(7-NI)** and **L-N(5)-(1-iminoethyl)ornithine (L-NIO)** are selective nNOS and eNOS inhibitors, respectively. Several studies have shown that nNOS inhibition by 7-NI reduces NO concentration in the brain and reduced neuronal damage while eNOS inhibition by L-NIO is detrimental after global ischemia [111-113]. However, neither 7-NI nor L-NIO affected CBF, suggesting that the effect of these two NOS inhibitors are not flow dependent.

NO regulation is complex given the dichotomous effects of neuroprotection and neurotoxicity. The benefit of CBF improvement of NO could be compromised by the deleterious interaction with ROS. Elucidation of pathways to specifically increase CBF without altering the ROS generation and neuronal survival are needed to identify effective methods of neuroprotection with NO pathway modulation.

2.3.2 Adenosine

Adenosine is an endogenous purine nucleoside which exerts a wide range of physiological activities such as coronary vasodilation, antithrombotic property and regulation of the sympathetic nervous system [114]. The effects of adenosine occur through four adenosine receptors: A_1, A_{2A}, A_{2B} and A_3. Activation of A1 and A3 receptors reduces adenyl cyclase activity and decreases intracellular cAMP. A potent vasodilatory effect is mainly mediated by

A_{2A} and increase cAMP levels in the vascular bed [115]. Adenosine also shares cross interactions with the NO and adrenergic systems [116]. By dilating coronary arteries, adenosine can increase coronary flow and myocardial oxygen tension. Xu, *et al*. reported that adenosine dosed immediately after resuscitation induced hypothermia, improved CBF and survival in rats subjected to 12 min CA [117]. Such beneficial effect in CBF could be attributed to reduced temperature and/or vasodilation. Of note, adenosine administration can cause bradyarrhythmias [118], and endogenous adenosine released by myocardial cells during ischemia is also implicated to cause or perpetuate bradyasystole in CA [119]. Hence, due to its mixed cardiac profile, adenosine is not commonly used as a vasodilator after CA.

2.3.3 Calcium Channel Blockers

Calcium is a central determinant of membrane potential and regulate vascular tone [120, 121]. As mentioned in previous sections, Ca^{2+} also serves as a key secondary messenger for multiple therapeutic agents.

During ischemia, however, the Ca^{2+} hemostasis is disrupted by multiple ion channels and receptors dysfunction, which leads to a massive shift of Ca^{2+} from extracellular spaces into intracellular compartments and exacerbates the ischemic injury [122, 123]. Calcium channel blockers are expected to block the excessive influx of Ca^{2+}, reducing Ca^{2+} overload, producing membrane hyperpolarization and vasorelaxation.

Nimodipine binds specifically to L-type voltage-gated Ca^{2+}channels and acts preferentially on cerebral vessels [124]. Schindler, *et al.* reported that nimodipine injected at resuscitation produces almost twice higher CBF at 10 minutes ROSC in pigs subjected to 5min VFCA [125]. The CBF increment of nimodipine obtained in animal models was also seen in a

randomized clinical study with improved CBF 4 hours post arrest using Xenon CT [126]. **Diltiazem** is also a Ca^{2+} channel blocker with high affinity for coronary vasculature [127]. The negative inotropic, chronotropic, and dromotropic effects of diltiazem provides potential benefit of reduced oxygen consumption in the heart. When dosed at 5 min after ROSC, diltiazem increased CBF on both hemispheres over 2 hours ROSC in an asphyxial CA model [125]. In this study, the oxygen consumption index remained unchanged compared with placebo, suggesting the impaired metabolism which could not be reversed by diltiazem treatment. **Flunarizine** is a Ca^{2+} antagonist which has relative low affinity to voltage-gated Ca^{2+}channels but binds to calmodulin and dilate peripheral vessels [128]. Two canine VFCA studies demonstrated that flunarizine, given immediately after reperfusion, improved post-resuscitation CBF [125, 129]. The improved CBF persisted for 1.5 and 4 hours, respectively, in these two studies. Significant reduced neurological deficit was also reported after flunarizine treatment [130]. **Levosimendan** is a Ca^{2+} sensitizer, exerts positive inotropic effect by increasing the Ca^{2+} sensitivity in myocytes. Levosimendan can also dilate vessel by opening ATP-dependent K^{+}-channel [130]. Both positive inotropic and vasodilatory effects could potentially improve CBF by increasing perfusion pressure and reducing CVR. A study by Kelm *et al.* showed that continuous infusion of levosimendan leads to improved CBF and outcome in rats subjected to asphyxial CA [131].

Calcium homeostasis is complex because of the essential role as a secondary messenger which involves in various biological processes. Calcium channels are widely distributed, and calcium channel blockers' effect on heart calcium receptors may produce unwanted effects of reduced cardiac output. In fact, multiple randomized clinical studies in CA patients failed to find benefit in neurological outcome or survival rate after Ca^{2+} channel blocker treatments, indicating that Ca^{2+} channel blockers alone might not improve the outcome [127, 132-134]. Neurotoxicity

was also found in calcium channel blockers [135]. More investigation should be performed to explore the role of Ca^{2+} channel blockers in the cerebral microcirculation, providing mechanistic rationale to support the use of Ca^{2+} channel blockers.

2.3.4 Glutamate Receptor Antagonists

Glutamate is a prominent excitatory neurotransmitter in the central nervous system. The effect of glutamate is mediated by four classes of receptors: N-methyl-D-aspartate (NMDA), α-amino-3-hydroxy-5-methyl-4-isoxazolepropionic acid (AMPA), Kainate, and metabotropic receptors. NMDA, AMPA and Kainate receptors are ionotropic receptors which enable ion flow across membranes to maintain plasticity and potential. During early ischemia, accumulated extracellular glutamate activates glutamate receptors excessively, leading to excitotoxicity and neuronal death [136]. By antagonizing glutamate receptor activity, it is expected to reduce excitotoxicity and neuronal damage. However, glutamate receptor antagonists administration after CA has reported both beneficial [137-139] and deleterious effects [138, 140-142]. Pre-treatment with MK-801, a noncompetitive NMDA receptor antagonist, and NBQX, an AMPA receptor antagonist, increase vascular resistance and depress CBF at baseline [143, 144]. Moreover, CBF and oxygen consumption remained lower after resuscitation in NBQX group, suggesting exacerbated ischemic injury [145]. The application of glutamate receptor antagonists is not supported with current evidence, probably due to early onset of excitotoxicity.

2.3.5 Vasoactive Fatty Acids

As previous described, PLA2 cleaves AA from phospholipids under ischemic condition and other pathophysiological conditions. Released AA is quickly metabolized through cyclooxygenase (COX), lipoxygenase (LOX) pathways, and by cytochrome (CYP) P450 enzymes into vasoactive prostaglandins, leukotrienes, EETs, and HETEs [144, 146]. Strategies have targeted specific fatty acids with the goal of improving CBF in CA models. For example, the metabolite 20-HETE is a potent vasoconstrictor for small arteries playing a key role in regulating CBF in the microcirculation [147, 148]. The mechanism of 20-HETE vasoconstriction is mediated by depolarization of vascular smooth muscle membrane secondary to blocking the large-conductance Ca^{2+}-activated K^{+}-channels [149-151] and stimulation of the L-type Ca^{2+} channel [152, 153]. More recently, direct effects of 20-HETE were described in apoptosis [90], neuroinflammation and superoxide production pathways [154, 155]. Shaik, *et al.* demonstrated that treatment of **HET0016**, which specifically inhibits the formation of 20-HETE, improved cortical CBF by ~25% assessed by laser speckle flowmetry in a pediatric asphyixal CA model [156]. Favorable histological outcome and neurological outcome were also reported in the same study. 20-HETE could serve as a promising target to improve CBF due to its strong potency and relatively enriched level in the brain. A vasodilator mediator produced by the COX enzyme is Prostaglandin E2 (PGE2). In the cerebral microcirculation, PGE2 dilates microvessels in the presence of NO and counteracts the vasoconstrictive effect of 20-HETE [27]. **Indomethacin** is a non-selective COX inhibitor and **celecoxib** is a selective COX-2 inhibitor. In a swine VFCA model, both indomethacin and celecoxib significantly decreased PGE2 level and attenuated increased regional CBF at 30min post ROSC [148]. The blood flow to the heart was also reduced with decreased percentage of ejection fraction after indomethacin and celecoxib pre-treatment,

which indicates the deleterious effect in the heart post-CA. Selective inhibition of COX-2 have been associated with adverse cardiovascular effects including hypertension and stroke [157]. One potential mechanism of COX-2 adverse effects is via the shunting of AA to the formation of other metabolites upon potent COX-2 inhibition [158]. Based on this putative mechanism, any evaluation of future inhibitors of AA metabolism should include assessment of metabolite shunting and potential downstream adverse effects.

It is very common that two fatty acids produced from the same precursor exert opposite vascular effects. For example, vasodilatory EETs and vasoconstrictive 20-HETE are metabolized from AA by CYP450. Vasodilatory agents, either depressing vasoconstrictive fatty acids, or enhancing vasodilatory fatty acids, should be synthesized with high selectivity to prevent unwanted interactions.

2.3.6 Anesthetics

Anesthetics, acting on ion channels, can affect CBF by interfering with vascular tone. Ion channels on the smooth muscle cell membranes are critical to maintain active potential and normal basal vascular tone. At least 4 different types of K^+ channels, 1 to 2 types of voltage-gated Ca^{2+} channels, more than two types of Cl^- channels, store-operated Ca^{2+} channels, and stretch-activated cation channels in the smooth muscle cell membranes mediate the effects of anesthetics [159]. **Bupivacaine** is a sodium channel blocker with a biphasic vascular effect. At low doses, bupivacaine causes vasoconstriction while at clinical doses, bupivacaine is vasodilatory [122]. Li *et al.* observed normalized early hyperemia and later hypoperfusion with bupivacaine infusion in a four-vessel-occlusion rat mode [160]. **Thiopental** is a barbiturate which binds to GABA channel and decreases neuronal activity. Infusion of thiopental increases

MAP, reduces oxygen consumption and cardiac output[161]. Controversy exists regarding to the efficacy of thiopental after global ischemia. Nemoto, *et al.* found that infusion of thiopental at 90 mg/kg over an hour did not improve brain oxygenation in a neck tourniquet model of global ischemia [162]. Similarly, no significant alterations in efficacy were observed with repeated dosed thiopental in an asphxial CA canine model [163]. Conversely, Kofke *et al.* reported improved metabolism profile, regional and total CBF after thiopental infusion at 90 mg/kg initiated at 5 min post-ischemia in monkeys.[164] Ebmeyer, also observed a mitigation effect of thiopental in addition to hypothermia in a 12.5 min VFCA canine model[28]. **Desflurane** is suggested to activate GABA channel, block K^+ channel and L-type Ca^{2+} channel[165]. An earlier study indicated that desflurane increases heart rate and decreases both MAP and CVR[166]. However, Loepke *et al.* observed that desflurane improved neurological outcome independent from a CBF effect in a pediatric piglet CA model [167]. **Methyl isobutyl amiloride (MIA)** although not an anesthetic agent, also affects ion channels. MIA inhibits the Na^+/H^+ antiporter on the membrane and attenuate intracellular alkalosis to prevent neuronal death[168]. In a rat model of CA induced by KCl, CBF, rats receiving MIA decreased to ~25% of baseline in all brain regions after reperfusion, even lower than rats received vehicle[169]. The uniformly reduced CBF could be due to lower pH in the systemic circulation which can lead to vasoconstriction. Overall, given current evidence, most anesthetics are not preferred agents to increase CBF after CA. First, the efficacy of the anesthetics to improve neurological outcome remains to be validated. Second, the observed improvement in outcome could be attributed more to flow-independent factors such as metabolism or temperature, rather than CBF itself. Third, the long-term exposure under anesthetics could introduce deleterious effects such as hypotension or

neurotoxicity. Since anesthetics are used in almost all CA animal models, it is very important to consider their effects during CBF assessments.

2.4 THROMBOLYTIC THERAPIES

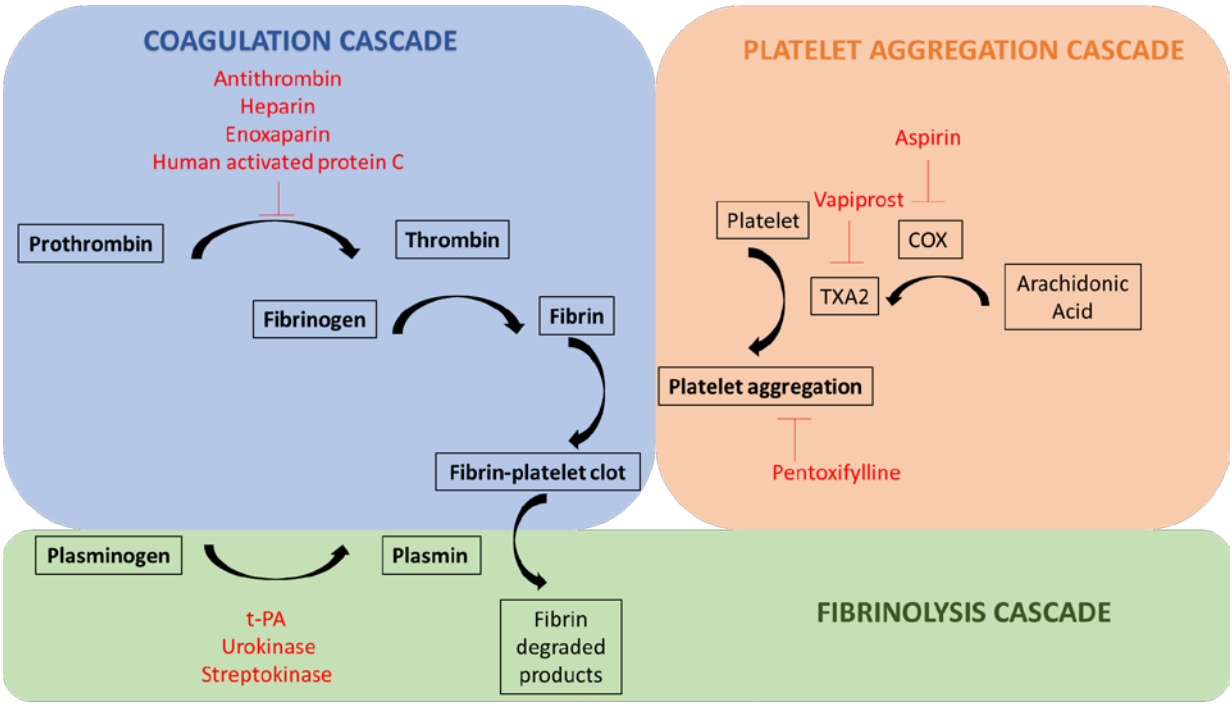

Figure 2.2 thrombolytic therapies and their roles in coagulation cascade

By thrombolytic therapies we refer here to agents which participates in the cascades of coagulation, platelet aggregation and fibrinolysis (Figure 2.2). This class of therapies are aimed to prevent/degrade the microthrombi formed during or after global ischemia, reduce CVR and improve CBF (Eq.1).

The cerebral microcirculation is impaired after global ischemia, especially the blockade of microcirculatory flow. This phenomenon is firstly described as “no-reflow phenomenon” by Ames *at al.* in 1968, where cortical capillaries failed to be reperfused after global ischemia in

rabbits [170]. Similar observations were made afterwards by other investigators [171-173]. Patients resuscitated from CA have increased systemic coagulation which could lead to microcirculation obstruction [21, 174, 175]. Increased coagulation after CA in the setting of unchanged fibrinolytsisc is thought to contribute to the formation of thrombi and block the microcirculatory flow.

2.4.1 Therapies Target on Coagulation Cascade

Antithrombin is an endogenous protein which prevents the clot formation by inactivation of multiple clotting factors, such as Xa and IIa[176]. **Heparin** and **enoxaparin** activate antithrombin and accelerate the binding of antithrombin-thrombin complex by 2000-4000 fold [177]. **Human activated protein C** (hAPC) is an endogenous anticoagulant acting by degrading the cofactors Va and VIIIa [178]. hAPC also possesses anti-inflammation properties by modulating cytokine production. The administration of heparin at resuscitation substantially decreased the no-reflow region in the forebrain (defined as absence of microvascular filling) to 7% compared with 28% in the untreated rats after 15 minutes CA [179]. Enoxaparin pre-treatment but not post-treatment improved post-CA microcirculatory perfusion mitigated the no-reflow, shortened hypoperfusion duration and increased perfusion ~50% [180]. However, injection of antithrombin after CPR did not affect CBF nor oxygen extraction post ROSC [181]. High dose of hAPC infusion after reperfusion also failed to influence cortical CBF or reduce neuron loss after 14 min global ischemia [182]. These results suggest that these agents might not be effective post-insult due to their mechanism of action of preventing thrombin complex formation. If the thrombin complex is already formed during ischemia, this class of agents may have limited effects in reducing CVR post-treatment.

2.4.2 Therapies Targeting the Platelet Aggregation Cascade

Agents that target the platelet aggregation and affect CBF include **aspirin, vapiprost,** and **pentoxifylline**. Aspirin is a clinically used non-selective COX inhibitor. Low dose of aspirin prevents platelet aggregation by inhibition of COX1, reducing formation of thromboxane A2 (TXA2) [183]. Treatment with aspirin prior to ischemia almost completely prevented hypoperfusion in a four-vessel occlusion rat model [184]. Vapiprost is a specific thromboxane A2-receptor antagonist. When vapiprost was dosed prior to cardiopulmonary bypass, CBF was found 64.3% of baseline compare with 40.2% of baseline in control group [181]. The cerebral oxygen metabolism is also improved to 80.1% compared with 50.0% in the control group. **Pentoxifylline** is a methylxanthine derivative which can decrease plasma and whole blood viscosity, increase erythrocyte deformability and prevent platelet aggregation [185]. When infused prior to CA, pentoxifylline maintained CBF similar to baseline in a feline VFCA model from 5-180 min ROSC while in the control group CBF was reduced to ~50% baseline [186]. The improved histological and neurological outcome in another four-vessel-occlusion rat model also suggests the benefit of pentoxifylline pre-treatment with improved microcirculatory flow [187]. Similar to agents targeting on the coagulation cascade, agents targeting on platelet aggregation also requires pre-treatment which limits their application in enhancing microcirculatory flow in the post-resuscitation phase.

2.4.3 Therapies Targeted on Fibrinolytic Cascade

Urokinase, recombinant tissue type plasminogen activator (rt-PA) and **streptokinase** activate plasminogen and lead to downstream fibrinolytic effect (Figure 2.2). Guo, *et al.*

performed CBF assessment using dual-slice spiral CT and found rabbits receiving urokinase infusion at resuscitation had ~16% higher CBF and ~25% greater cerebral blood volume compared to rabbits received vehicle treatment in an asphyxial CA model [188]. The administration of t-PA at resuscitation substantially reduced the no-reflow areas and homogenous microcirculatory flow post-CA in a 15min feline CA model [189]. An earlier study by Lin, *et al.* reported that streptokinase increased CBF which persisted over 3 hours in the grey matter and hippocampus in dogs subjected to 12-16 min CA [180]. A recent study by Spinelli, *et al.* demonstrated improved cardiac resuscitability, attenuated ICP and brain edema in a porcine model of prolonged CA [190]. Interestingly, an antifibrinolytic agent aprotinin also improved carotid blood flow and CBF after resuscitation, but the effect was mainly attributed to the endothelium-mediated vasodilation[191]. Compared with therapies targeting the coagulation cascade and platelet aggregation cascade, fibrinolytic agents appeared to be more applicable in post-resuscitation treatment. Detailed characterization of fibrinolytic agents is necessary to demonstrate their potency, optimal dosing time and long-term benefit for outcome assessment.

Thrombolytic therapies are promising agents to improve CBF especially advantageous in the restoration of microcirculatory flow. Fibrinolytic agents appear to be more suitable for post-resuscitation treatment compared with agents that target coagulation cascade and platelet aggregation cascade. One potential deleterious effect for thrombolytic therapies is the bleeding risk. However, multiple clinical studies have shown that thrombolytic therapy after CA is associated with improved neurological outcome in patients without increased bleeding risks [192-195]. Based on this evidence, future clinical trials to evaluate the safety and efficacy of such agents on long- and short-term outcomes are necessary to clearly identify the potential clinical utility of these drugs in CA patients.

2.5 HEMODYNAMIC THERAPIES

Hemodynamic therapies are aimed at restoring the systemic homeostasis including the hematocrit, oxygen, glucose, pH, volume and osmolarity. Stable homeostasis is essential to restore CBF post-CA because blood component can determine viscosity, which is inversely related to CBF. (Eq.3) In addition, cardiac output changes in compensation to blood volume expansion, which also affect perfusion pressure and CBF. (Eq.2) Increased osmolarity reduces brain edema and ICP, which favorably affects CBF. (Eq.2) It is worthy to note that intravenous administration of almost all agents alters homeostasis due to various solvents which can affect hemodynamics and CBF as well.

2.5.1 Hematocrit Management

The normal hematocrit level is similar between human and rodents, ranging from 35 to 52% [196]. Hematocrit levels post resuscitation vary between different insults. Proper hematocrit level is critical to maintain perfusion pressure and oxygen delivery; however, lower hematocrit has been associated with higher CBF after resuscitation. Sakamoto *et al.* showed that piglets with 25 or 30% hematocrit by total blood infusion post-resuscitation had higher MAP but lower CBF compared with piglets with lower hematocrit (10 or 15%)[197]. This suggests that total blood infusion leads to increased CVR which could be attributed to higher blood viscosity or even formation of microthrombi during infusion. Halstead *et al.* also demonstrated in pigs that hematocrit of 31% by whole blood transfusion leads to ~20-40% lower CBF but superior outcome compared with hematocrit of 20% undergoing cardiopulmonary bypass [198]. Increased oxygen delivery could attribute to the better outcome observed in high hematocrit group. Since

hematocrit is inversely related to CBF, it is important to take both into consideration in the post-resuscitation phase.

2.5.2 Hemodilution Agents

Hemodilution leads to volume expansion which has been generally associated with higher CBF and improved microcirculatory flow in CA models [198, 199]. The potential mechanisms are reduced viscosity and increased perfusion pressure, assuming cardiac output increases to compensate expanded volume load. However, different substitute fluids affect CBF and metabolism after resuscitation. Liu, *et al.* found that Tris buffer and sodium bicarbonate enhanced CBF by ~50% without an effect on CPP or CePP in a 5 min VFCA piglet model compared with saline control[200]. Their result indicated that alkaline buffer infusion reduces CVR due to mitigation of cerebral acidosis, which is well-known to cause vasoconstriction[201]. Leonov, *et al.* pointed out that hemodilution with plasma substitute indeed increased CBF and generated homogeneous perfusion 1-4 hours after VFCA, however, the oxygen delivery remained unchanged, offset by the lower oxygen level[202]. This result suggests that hemodilution with oxygen carriers such as artificial hemoglobin can be promising. In fact, clinical study also suggests that higher hemoglobin levels were associated with better neurological outcome in out-of-hospital CA patients [203]. However, two animal studies infused hemoglobin or hemoglobin conjugates but found different results. In a swine VFCA model, infusing diaspirin cross-linked hemoglobin increased CePP [204], while the infusion of liposome-encapsulated hemoglobin did not increase hippocampal blood flow in rats after four-vessel occlusion [205]. Hemodilution can serve as a potential strategy to increase CBF,

especially with benefit in microcirculatory flow. However, the reduced oxygen level in the diluted plasma should be adjusted to prevent tissue hypoxia.

2.5.3 Osmolar Therapies

Brain edema is an inevitable consequence under ischemic conditions such as CA [206]. The mechanism of edema formation involves dysfunction of various ion channels, water channels and receptors on the blood-brain-barrier. Edema increases ICP which compromises CBF. Osmolar therapies are directed to resolve brain tissue edema, decrease ICP and increase CBF post-CA. Hypertonic solution with more concentrated NaCl and large molecules such as dextran or starch are often used to increase osmolarity. Hypertonic solution, either by infusion or single injection, increases CBF in both VF and asphyxial CA models [207-209]. In an 8 min VFCA model, pigs that received hypertonic-isooncotic saline (7.5% NaCl with 6% hydroxy ethyl starch) infusion during CPR had ~50% higher CBF and sustained for 240 min ROSC compared to pigs received normal saline[210]. The improved CBF was observed in multiple brain regions including cortex, basal ganglia, hippocampus and cerebellum. Noppens, *et al.* administered a single dose of hypertonic saline hydroxyethyl starch (7.2% NaCl, 6% hydroxyethyl starch) after 9 min asphyixal CA and found accentuated local CBF[208]. In addition, hypertonic solution also improves cerebral microcirculatory flow and reduces “no-reflow phenomenon”. Fischer and Hossmann stated that infusion of hypertonic hydroxyethyl starch solution (7.5% NaCl/6% hydroxyethyl starch) reduced no-reflow area from 28% to 15% in in the forebrain in a 15 min VFCA model [211]. Although the result of CBF improvement is promising, whether hypertonic solution improves neurological outcome or survival after CA remains to be demonstrated. It was proposed that hypertonic solution alone is not enough to reverse the severe brain injury post-CA.

Wallisch *et al.* demonstrated that aquaporin-4 inhibitor AER-271 ameliorated early cerebral edema and early neurological deficit in a pediatric asphyxial CA rat model [212]. Their results suggest aquaporin as a promising target post-CA. Combination therapy using hypertonic solution as a solvent is a promising strategy.

2.6 ANTIOXIDANT AND ANTI-INFLAMMATION THERAPIES

The ischemic and reperfusion injury underlies the pathophysiology of post-CA brain injury. The inflammatory factors, cytokines, superoxide and other reactive oxygen species (ROS) generated in this process further exacerbate the neuronal injury [211]. To alleviate the detrimental effects of these substances, various antioxidant and anti-inflammatory agents have been evaluated as approaches to improve outcome. Although increasing CBF is not the primary goal for these agents, secreted inflammatory factors could result in higher blood viscosity and compromise CBF. On the other hand, inflammatory factors and cytokines can also stimulate coagulation cascade, further blockade microcirculatory flow and decrease CBF.

Although a wide range of antioxidants have been used in global ischemia models, only a few of agents are investigated with CBF assessment. **N-acetylcysteine (NAC)** and **alpha-phenyl-tert -butyl nitrone (PBN)** are both free radical scavengers. Continuous infusion of NAC in a neonatal hypoxia-ischemia model was reported to improve cerebral perfusion with increased carotid flow and decreased vascular resistance [213]. Pre-treatment with PBN in a pediatric cardiopulmonary bypass model also restored global CBF to 78% of baseline compared with 52% in the vehicle group [214]. However, neither agents were assessed in CA models with CBF measurement. **Deferoxamine** and **U74006F** are both inhibitors for lipid peroxidation with

different effect on CBF. Deferoxamine administrated 5min prior to resuscitation increased cerebral perfusion in hippocampus, thalamus, hypothalamus, and amygdala, but not in cortex in rats undergoing prolonged CA induced by esmolol and vecuronium[215]. In a 12.5 min VFCA canine model, U74006F given after reperfusion showed no increase of cerebral perfusion in any brain region [216]. **Polynitroxyl albumin** (PNA) exerts antioxidant properties by decreasing oxidative and nitrative stress. When PNA was dosed in pediatric rats resuscitated from 9 min asphyxial CA, attenuated early hyperemia was observed using MRI but no effect was observed with hypoperfusion [183] Attenuation of hyperemia with PNA was associated with improved neurological outcomes, suggesting that hyperemia might be detrimental. There is no clear pattern to describe the effect of antioxidants on CBF after CA. More often, the mechanism of observed changes remains to be clarified.

Methylprednisolone is a glucocorticoid often used to suppress inflammatory responses. The effect of methylprednisolone on CBF is controversial. Langley, *et al.* reported that pretreatment with methylprednisolone increased global and regional CBF after hypothermic CA using radio-labelled microsphere [13]. Conflicting evidence is provided by Schubert, *et al.* who showed no protective effect of methylprednisolone pre-treatment in neither cerebral perfusion nor neuronal injury in a neonatal piglet model [217]. CBF change after other anti-inflammatory agents is still under investigation. Similar to antioxidants, there is no obvious pattern to characterize CBF alterations after anti-inflammatory therapies.

In most studies, both antioxidant and anti-inflammation therapies were used as pre-treatment. Although antioxidant and anti-inflammation therapies are mostly targeted on oxidative stress and neuronal injury which does not manifest until hours or days after resuscitation, these

therapies should be initiated in the early phase of post-resuscitation or in combination with other agents to mitigate oxidative stress.

2.7 COMBINATION THERAPIES

To synergize the effect of increasing CBF or alleviate the deleterious effect of a specific agent, combination therapy has been investigated in animal studies as a potential strategy. For example, Epi has been used in combination with vasopressin to improve CBF and outcome post-CA[103, 218]. Compared with Epi used alone, the combination therapy similarly restored spontaneous circulation and survival rate but with significantly less neurological deficit [103, 219]. Synergistic effects have also been reported when combining Epi and vasopressin with more sustained and higher cerebral perfusion [219-221], although lower cerebral perfusion was also reported[222, 223]. A more recent study by Halvorsen, *et al.* reported vasopressin dosed alone at resuscitation produced 36% higher cortical CBF but similar CPP compared with Epi and vasopressin[100]. Benefit was also reported with another combination with Epi, vasopressin and nitroglycerin with higher CBF and better neurological outcome compared with Epi alone [101, 103, 223]. To further establish the superior effect of these combinations, more detailed evaluation is needed to address benefit in long-term outcome.

Some studies combined antioxidants such as deferoxamine and superoxide dismutase and found restored CBF post-CA [101, 224]. Another study combined streptokinase and dextran and reported increased CBF in the grey matter and hippocampus [225]. In fact, agents such as isoflurane, heparin, methylprednisolone which could affect CBF are also used as part of the experiment protocol. It is very important to design appropriate control group to minimize

confounding variables such as anesthetics or thrombolytics. When interpreting results, it is equally important to take these factors into consideration and prevent overinterpretation.

2.8 DISCUSSION AND CONCLUSION

To provide a better understanding of therapeutic effect on CBF post-CA, we created a comprehensive search strategy for existing literature and categorized the pharmacological therapies into flow promotion, vasodilatory, thrombolytic, hemodynamic, antioxidant and anti-inflammatory therapies with their effect on CBF post-CA summarized in previous sections. Overall, we believe that flow promotion and vasodilatory therapies which directly targeted at CBF are promising agents to improve CBF post-CA. Future studies should further evaluate their detailed effect on cerebral microcirculation and the long-term outcome assessments. The effect of other therapies such as hemodynamic, antioxidant and anti-inflammatory therapies, is indirect and less potent on CBF improvement post-CA. These agents could serve as a part of combination therapy to maximize the effect of CBF restoration and off-set the potential adverse effects of other agents.

We identified several important research areas during literature review. The first research area is the heterogenous global ischemia models used in the literature. The CBF alterations after CA differs by species, insult type and duration and even animal ages. Although a classical early hyper-perfusion and secondary hypoperfusion was observed in most animal studies, several studies revealed the temporal and regional variations of CBF in different animal models [8, 190]. Given the different pathophysiology of CA, such as VF versus asphyixal, pediatric vs adult, the

different CBF patterns could deviate the interpretation of treatment effect. As a result, the same treatment could produce beneficial or detrimental effect depending on differences in the model selected. At the same time, there is a general need for both randomization and blinding of preclinical studies to increase the overall rigor for preclinical CA research. Future studies that focus on model specific mechanisms of CA alterations as they relate to known changes in patients will aid in both the identification of individualized therapeutic approaches and translatability of preclinical findings.

Another important area for future research is in the development and validation of novel methods for high resolution CBF assessment in both the preclinical and clinical setting. We noticed different methodologies utilized for CBF assessment (Appendix III). Each methodology has its own strengths and limitations as reviewed previously [7, 9]. The advanced resolution and depth of imaging provide more detailed assessments which is not captured previously.

Dose regimen is another significant area of research which is often underestimated in animal studies. Most pharmacological agents follow a positive dose-response relationship for efficacy as well as adverse effects. Higher or more frequent dose regimen often enhances its pharmacological efficacy but also magnifies unwanted adverse effects. Therefore, a thorough dose-finding study is necessary to optimize efficacy and avoid adverse effect. More importantly, the timing for dosing initiation and ending is critical to produce desired pharmacological effect. For example, Epi is the most extensively investigated agent in CA studies compared with others. The desired vasoconstriction mediated by α-ARs is essential for shorter resuscitation time, however, prolonged α-adrenergic effect will constrict cerebral artery and increase CVR. At the same time, β-adrenergic effect early is also beneficial by relaxation of trachea smooth muscle and enable better ventilation. Prolonged β-adrenergic effect will increase oxygen consumption in

the heart and exacerbate ischemia. The early flow over shooting can generate neuronal toxic ROS which hopefully could be reversed by antioxidant treatment. The vessel dilators especially dilator for small artery could mitigate or prevent hypoperfusion within a given concentration range. Taken together, we believe that a combination or sequential therapies might be beneficial to target multiple mechanisms of brain injury post-CA and offset each other's adverse effect (Figure 2.3). Detailed characterizations of individual agent, including the dose regimen and interval, should proceed the combination or sequential therapies.

Long-term outcome assessment is an essential piece of evidence but remains missing for some therapies. Post-CA brain injury is a complicated pathophysiology process. Although CBF alteration is critical to enable sufficient oxygen and nutrients delivery, it is also important to monitor other aspects such as brain metabolism to avoid deleterious effect. Most importantly, multiple outcome assessments should be performed to determine long-term efficacy.

Last but not least, the evaluation of cerebral microcirculatory is of great significance. Microcirculatory flow is the determinant of oxygen delivery and substances exchange. Apparently increased CBF cannot represent better microcirculation due to possible shunt flow. Recent studies also emphasize the significance of cerebral microcirculation in CBF regulation after ischemia [148, 226, 227]. The cerebral microcirculatory evaluation of different pharmacological agents will provide convincing evidence to support or against their effects on CBF and outcome post-CA. Novel mechanisms of neuroprotection could also be revealed for existing therapies.

In conclusion, we reviewed pharmacological agents in different categories targeted on CBF restoration after CA. Each category possesses a different mechanism while overlapping mechanisms are also suggested. Some agents such as flow promotion agents are better

characterized with the existence of conflicting evidences. Further studies are warranted to confirm the efficacy and avoid potential adverse effect on CBF and outcome after CA.

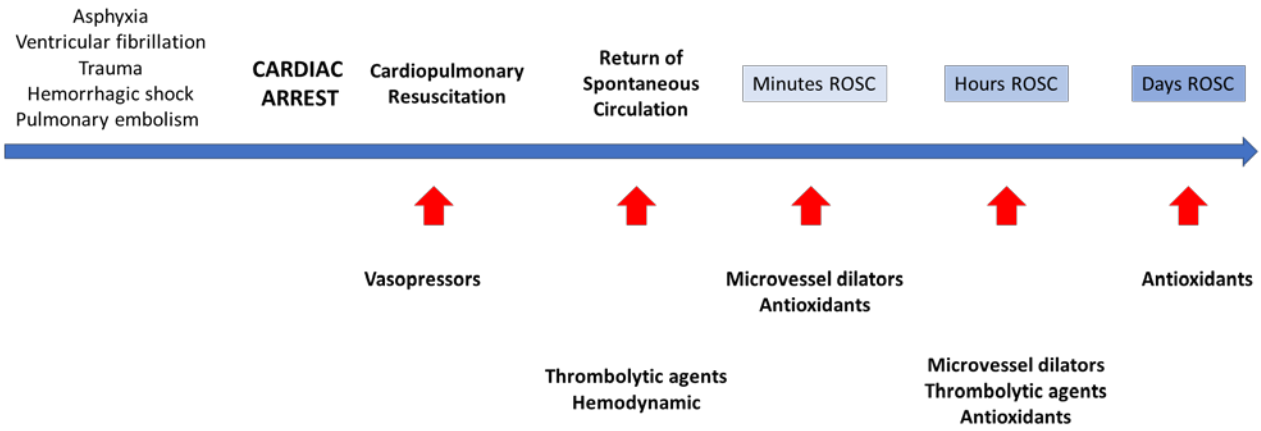

Figure 2.3 Proposed schematic sequential treatment to improve CBF post-CA

3.0 CHARACTERIZATION OF CEREBRAL MICROCIRCULATION AFTER PEDIATRIC ASPHYXIAL CARDIAC ARREST USING *IN VIVO* MICROSCOPY

[Li L, *et al. J Cereb Blood Flow Metab*.2017]

3.1 INTRODUCTION

CBF impairment have served as a therapeutic target for improvement of neurological function after CA, especially the cerebral hypoperfusion in the initial minutes to hours post-CA contributes to the overall ischemic injury, as described in animal models [8, 203]. However, the cerebral microcirculation post-CA *in vivo* remains to be characterized, especially the alterations of various types of vessels, the red blood cell (RBC) flow and plasma flow in the capillaries. In this section, we sought to establish a scaffold to assess microvascular disturbances after pediatric asphyixal CA.

3.1.1 Epidemiology of Pediatric CA

Cardiac arrest (CA) is a significant cause of mortality in the pediatric population. Approximately 16,000 pediatric patients suffer from CA every year in the United States, accounting for up to one quarter of all pediatric mortalities [228]. Thirty-five percent of the surviving patients at discharge have unfavorable neurological outcome [229]. To date, no pharmacological therapy has demonstrated neuroprotective benefit in the treatment of post-CA brain injury.

3.1.2 Previous Studies about CBF and Cerebral Microcirculation Post-CA

Cerebral hypoperfusion in the initial minutes to hours post-CA contributes to the overall ischemic injury, as described in animal models [8, 203]. Previously we established a clinically relevant pediatric asphyxial CA model in rats [230]. We noted marked regional and temporal variation in CBF characterized using arterial spin label magnetic resonance imaging (ASL-MRI) [8]. Cortical hypoperfusion was observed 30-120 min after resuscitation and prolonged cortical hypoperfusion was associated with poor long-term behavioral outcome. Subsequently, we reported cortical tissue hypoxia, using brain tissue oxygen (PbO2) monitoring, which regionally and temporally mimicked the CBF decrement [231]. While the presence of post-CA hypoperfusion is well established, the pathophysiological underpinnings of the cortical hypoperfusion post-CA have not been completely elucidated or detailed at the microcirculation level. A thorough understanding of the status of the cerebral microcirculation early after CA is essential for the development of CBF targeted therapies.

3.1.3 Role of Cerebral Microvasculature in Regulating CBF

Cerebral vasoconstriction represents an important microvascular disturbance postulated to cause post-ischemic hypoperfusion, as cerebral microvessels play a key role in regulating CBF and contribute significantly to cerebral vascular resistance [148, 232]. Various mediators of vasoconstriction such as thromboxane, calcium, endothelin (ET), or reactive oxygen species, have been targeted experimentally and improved post-resuscitation CBF [77, 233]. In our model, inhibition of 20-Hydroxyeicosatetraenoic acid (20-HETE) formation, a vascoconstrictor produced in the cerebral microcirculation, improved neurological outcome [27]. Ristagno et al.

suggested that microcirulatory disturbances post resuscitation after experimental CA in adult pigs contribute to cortical hypoxia, and suggested a possible contribution of epinephrine [47]. However, there is limited understanding of cerebral microcirculation and RBC flow post-CA, especially at the level of pial vessels, penetrating vessels, and capillaries.

3.1.4 No-reflow Phenomenon

The no-reflow phenomenon was first described histologically in a global ischemia model in 1968 [171]. Rabbits subjected to ischemia had incomplete capillary filling upon reperfusion and developed occlusive lesions at the particle size of red blood cells (RBCs) in the cerebrum. Subsequent studies questioned the existence of the no-reflow phenomenon—suggesting that it may have resulted from an artifact of inadequate perfusion pressure in the experimental system used [234, 235]. However, others suggested that it can develop, and may result from astrocyte swelling, platelet and leukocyte adherence, increased blood viscosity, and/or post-insult hypotension, among other mechanisms [236, 237]. The no-reflow phenomenon has yet to be characterized *in vivo* after CA.

3.1.5 Hypothesis and Objectives

Two major mechanisms have been identified to date that contribute to decreased CBF post-CA: intravascular stasis, also known as the no-reflow phenomenon, and vasoconstriction. These pathophysiological processes have been largely characterized ex vivo using histological methods or have been ascertained from experiments using pharmacological manipulations. Therefore, we

hypothesize that microvessel constriction and disturbances of capillary RBC flow lead to cortical hypoperfusion post-CA.

3.2 METHODS

3.2.1 Animals

This study was performed in accordance with Guide for the Care and Use of Laboratory Animals (8th Ed), published by National Research Council and approved by the Institutional Animal Care and Use Committee at the University of Pittsburgh. All experiments were reported according to the Animal Research: Reporting of *In Vivo* Experiments (ARRIVE) guidelines. Male Sprague-Dawley, post-natal day (PND) 16-18 rats (30-45 g) were used in this study. Four cohorts of rats were used for the measurement of microvascular diameter (n=8), assessment of capillary RBC flow (n=12), RBC velocity and density (n=8), and cortical plasma mean transit time (MTT) (Sham and CA group, n=5/group).

3.2.2 Surgical Preparation and Asphyxial CA

We utilized an established pediatric asphyxial CA rat model [230] with slight modifications for CBF assessment [8]. Rats were initially anesthetized via inhalation of 3% isoflurane in N_2O and oxygen (50:50), administered via a nasal cone. The trachea was then intubated, mechanical ventilation was initiated, and isoflurane was reduced to 2.5%. After the placement of femoral arterial and venous catheters, to reduce the effect of isoflurane on CBF, we discontinued the

isoflurane and administered fentanyl intravenously at a constant rate of 50 µg/kg/h for the entire duration of the experiment. Neuromuscular blockade using vecuronium was administered intravenously at a rate of 5 mg/kg/h. Body temperature was maintained at 37°C with a heating pad. The experiment settings are illustrated in Figure 3.1.

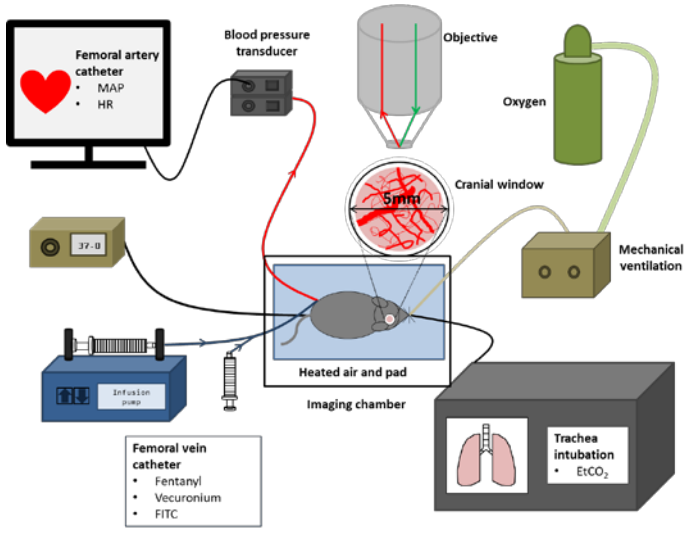

Figure 3.1 Experiment settings for *in-vivo* microscopy

To prepare for *in vivo* microscopy, the rat was placed prone on the surgical table and the head was stabilized in a stereotactic frame. The skull was then exposed through a midline scalp incision. A circular craniotomy of 3-4 mm was performed over the sensory-motor cortex. After removing the bone, an optical chamber was created. A solution of 1% agarose in normal saline was applied to the intact dura. A coverslip of 5 mm diameter was applied over the agarose and was secured with tissue glue and dental cement.

Rats were subjected to 9 min asphyxial CA, which produces cortical hypoperfusion as assessed by ASL-MRI [8]. The FiO2 was reduced to 0.21 (room air) for 1 min before asphyxia to prevent hyperoxygenation. CA was induced by disconnecting the tracheal tube from the ventilator for 9 min after neuromuscular blockade. Resuscitation was started by reconnecting the ventilator at a FiO2 of 1.0 and was followed by the administration of epinephrine (0.005 mg/kg, iv), sodium bicarbonate (1 mEq/kg, iv), and manual chest compressions until return of spontaneous circulation (ROSC). A FiO2 of 1.0 was maintained until the end of the experiment.

3.2.3 Cerebrovascular Imaging Using Multi-Photon Microscopy

To assess the microcirculation, we used *in vivo* multiphoton microscopy. A Nikon A1R MP microscope was configured with the Nikon Ni-E (Nikon Instruments; Tokyo, Japan) upright motorized system. The microscope was equipped with a Chameleon Laser Vision (Coherent, Inc; CA, USA), an APO LWD 25× water immersion objective with 1.1 NA, a high-speed (30 frames/second) resonant scanning mode and a galvano-mode scanning suitable for linescanning acquisitions. The Nano-Drive system was used to acquire fine high-speed control of z-plane selection. The fluorescence detection unit of the microscope consisted of four detectors (photo multiplying tubes). We used detector 2 for FITC 525 / 50 nm (green channel). The microscope components including the laser, stage, resonant scanning head, detectors and acquisition were controlled using NIS Elements software (Nikon).

To delineate the vasculature, we administered Fluorescein isothiocyanate–dextran (FITC; Sigma, wt 2,000,000) 3% (w/v) 0.1mL at baseline. Additional doses of FITC were given as needed to maintain adequate delineation of the microvasculature. The specific sequence of FITC administration for the MTT experiment is detailed below. Post-acquisition image processing

was achieved using NIS Elements and MATLAB (R2015a, The MathWorks, Inc. Natick, Massachusetts USA). The microscope stage was enclosed in a temperature controlled black plexiglass chamber, which prevented interference by the ambient light. We used an excitation wavelength of 850 nm and a laser power of 1-2%.

3.2.4 Assessment of Cerebral Microvessel Diameter

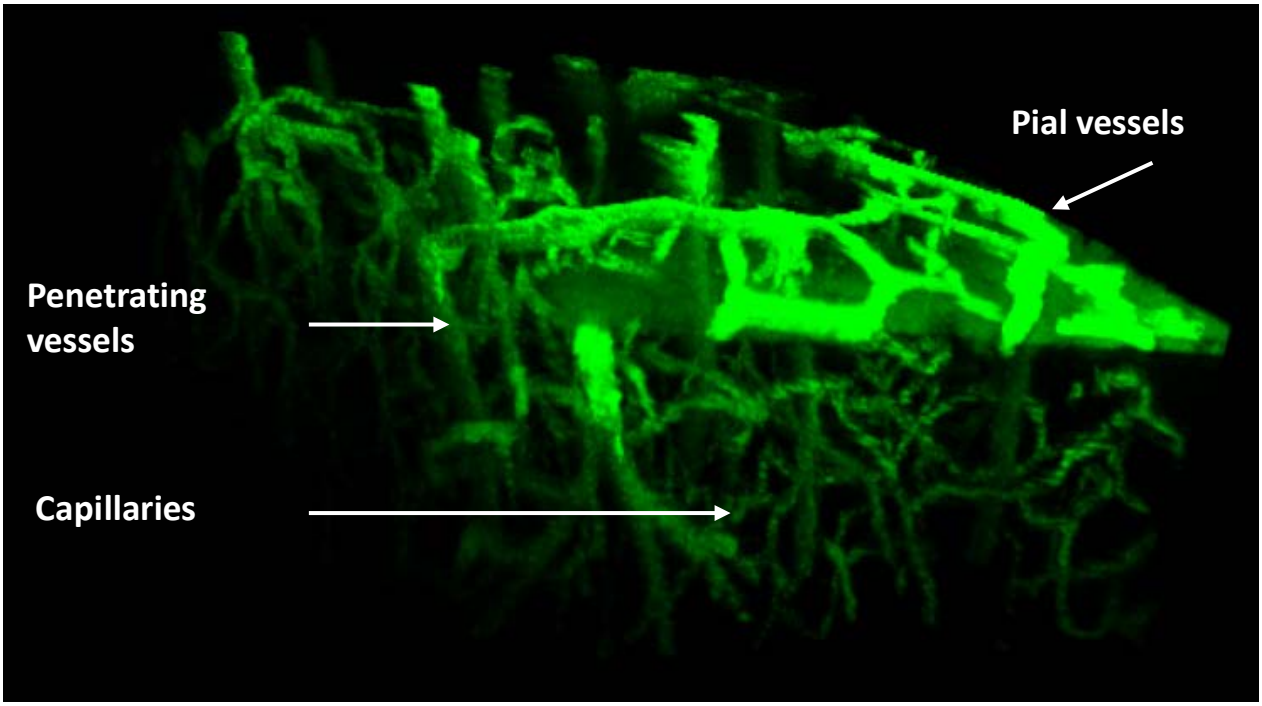

Figure 3.2 A representative 3D image stack of the cortical microvasculature. The z depth is about 250 µm.

Image stacks were acquired at baseline, and at 5, 30 and 60 min post-CA in 8 rats. The following parameters were used: field view of 512×512 pixels at a resolution of 1µm/ pixel using resonant mode, 16 times average. Cortical microvessels were categorized by size and morphology into five types. Data were collected from 8 rats and 39 pial arterioles, 134 pial venules, 16 penetrating arterioles, 42 penetrating venules, and 75 capillaries. Pial arterioles

were identified by their location on the pial layer, and morphologically by their relatively straight appearance and fewer branches. Pial venules were identified as vessels also located on the pia surface but with tortuous contours and more branches than the arterioles. Penetrating arterioles and penetrating venules were identified as vessels branching from the parent pial arterioles and draining into pial venules, respectively, and perpendicular to the pia. Capillaries were identified as microvessels located in the parenchyma and with diameter of less than 10 μm at baseline (Figure 3.2). For each animal, 3-5 locations with adequate contrast resolution were identified within the imaging window at baseline. The image stacks reached to a depth ranging from 250-400 μm from the pia. All the locations were saved in the software such that the system was able to automatically obtain imaging stacks at the same location post-CA. At each location, the baseline imaging stacks were set as reference stacks to which post-CA stacks (5, 30 and 60 min post-CA) were overlaid in the x-y-z dimensions (Figure 3.3). The vessel diameters at each time point were then quantified from a single location per segment from the maximum projection of the aligned image stacks using the Annotation and Measurement function in NIS Element. The accuracy of the measured shape is subject to the point-spread function of the system which is roughly 0.29 μm in-plane. Simulations at this resolution show that under noiseless conditions, vessel diameter can be estimated with sub-pixel precision with error <10% for vessels >3um, error <7% for vessels >4um, and error <4% for vessels >5um. Only the vessels with acquired data at all four-time points were included.

3.2.5 Assessment of Capillary RBC flow (No-reflow Phenomenon)

The live time-series at baseline and post-CA were acquired to assess the presence of RBC flow vs. stasis in the capillaries, defined as microvessels in the parenchyma with diameter of less than

10 μm. With FITC delineating the plasma, RBCs appear as oval negative signals and a size of 3-6 μm. The time-series were acquired at the speed of 30 frames/s with resonant mode. To capture the movement of RBCs, 2-3 time-series were identified per animal at baseline and 1-3 capillaries with adequate contrast were included in each time-series. The locations for each time-series were recorded so that the same capillaries could be repeatedly assessed post-CA. All capillaries captured at baseline had continuous RBC flow. Absent RBC flow was defined as no RBC flow during the time series (15-30 s). Some capillaries were observed to have stagnant RBCs that appeared fixed in place in the vessel, while others did not have any RBCs or RBC flow visualized, such that only plasma filled vessels were seen. A total of 59 capillaries from 12 rats were evaluated.

3.2.6 Assessment of Capillary RBC Velocity and Density

To quantify the capillary RBC velocity and density, the linescan method was applied, as previously described [238]. Briefly, a straight section of a capillary with adequate contrast was identified at baseline. The scan path was then placed along the capillary lumen. In linescan mode, the movement of RBCs is detected as an angled streak. For a known scan speed, the velocity of the RBC movement is proportional to the slope of the streak. Linescans were collected at a speed of 1000 lines/s for 10-15s on capillaries at baseline and post-CA. To quantify and compare the effect of CA on RBC velocity, only capillaries with both baseline and post-CA reliable measurements were included. Capillaries with stagnant RBCs flow were not included due to unreliable linescan reading. The RBC velocity was quantified by analyzing the angle of RBC streaks in contiguous 150-250 lines using MATLAB. In total, we measured the RBC velocity and density in 39 capillaries from 8 rats at baseline and post-CA. To assess the

effect of anesthesia over time in our preparation on RBC velocity, we also collected measurements from 33 capillaries of 4 sham operated rats and found no change in either RBC velocity or density during the 60 min measurements (data not shown).

3.2.7 Assessment of Mean Transit Time of Plasma Through the Cortical Microcirculation

The MTT was assessed to describe the time required for plasma to traverse the cortical microcirculation. A pial artery and adjacent pial vein supply regional cortical blood flow, therefore the plasma transit time from the pial artery to the pial vein indicates the plasma flow that traverses the cortical capillary bed. A longer MTT indicates slower capillary plasma flow which suggests capillary flow disturbances. MTT was assessed at baseline and at 30 and 60 min after CA or sham surgery (n=5/group) using a previously described method [239, 240]. Briefly, a pial artery and an adjacent pial vein were identified in the imaging field (512×512 μm) at baseline. Time-series were recorded at the speed of 30 frames/ second with resonant mode during a bolus of FITC dextran (3% w/v, 0.03mL) iv injection at baseline, 30 and 60 min post-CA. The time-series were fitted with a median filter and smooth function to reduce the motion artifact. Two regions of interests (ROIs), one on a pial arteriole and the other on a pial venule were identified (Figure 3.5B). The intensity of the fluorescent tracer in the selected ROIs were then plotted over time using NIS Element software. The standard γ function was fit to the intensity-time curves in MATLAB (Figure 3.5C). Time-to-peak (TTP) was defined as the time required for intensity change from baseline to the peak in the fit curves for the artery and vein. MTT was defined as the difference of TTP between the pial artery and the pial venule ROIs (Figure 3.5 C) at each time point. In addition, to evaluate the MTT for the entire pial vessel

network within the imaging field, the TTP for each pixel in the time-series was calculated and normalized to the TTP of the arterial ROI. Image processing was implemented in MATLAB. All the post-measurements were normalized to the corresponding baseline values.

3.2.8 Statistical Analysis

Descriptive statistics were tabulated to summarize the measurements. Means and standard error of the means (SEM) were presented for the continuous variables. Data were analyzed by using SPSS (IBM Corp. IBM SPSS Statistics for Windows, Version 24.0. Armonk, NY: IBM Corp.) and figures were generated using Graphpad Prism 6 (GraphPad Software, Inc. La Jolla, CA, USA). Physiological parameters were tested for time effect within each experiment using repeated measurement ANOVA followed by Dunnett' post-hoc comparison. For the MTT experiments, physiological data were analyzed using repeated measure ANOVA. Microvessel diameters were log transformed to normalize the distribution. In each type of vessel, we analyzed the diameter measurements in a mixed linear model. In this statistical model, repeated measurements for each vessel were nested within vessel number, and vessel numbers were nested in each animal. Similarly, RBC velocity and density were also log transformed and analyzed in a mixed linear model. MTT measurements were normalized to the baseline value for each rat and analyzed using two-way ANOVA. For all tests, $p\text{-value}<0.05$ was considered statistically significant.

3.3 RESULTS

3.3.1 Physiological Parameter Summary

Physiological parameters, including mean arterial pressure (MAP), end-tidal (Et) CO_2 and temperature, were recorded throughout the experiment. All physiologic parameters were within normal limits at baseline. All animals included in the study were successfully resuscitated from CA and had return of systemic circulation for at least 60 min post-CA. The physiologic parameters for each experimental group are summarized in Table 3.1. As expected, rats subjected to CA had a modest temperature reduction at 5 min post-CA compared to baseline as normothermia was not actively maintained during the no-flow period—to mimic clinical CA. Also as anticipated, given the resuscitation, for the group in which capillary RBC flow was assessed, $EtCO_2$ was lower at 5 and 30 min post-CA, and MAP higher at 5 min post-CA compared with baseline. Similarly, for the group in which MTT was assessed, the CA group had lower $EtCO_2$ compared with shams. No other significant differences were observed in the physiological data.

3.3.2 Assessment of Microvessel Diameter

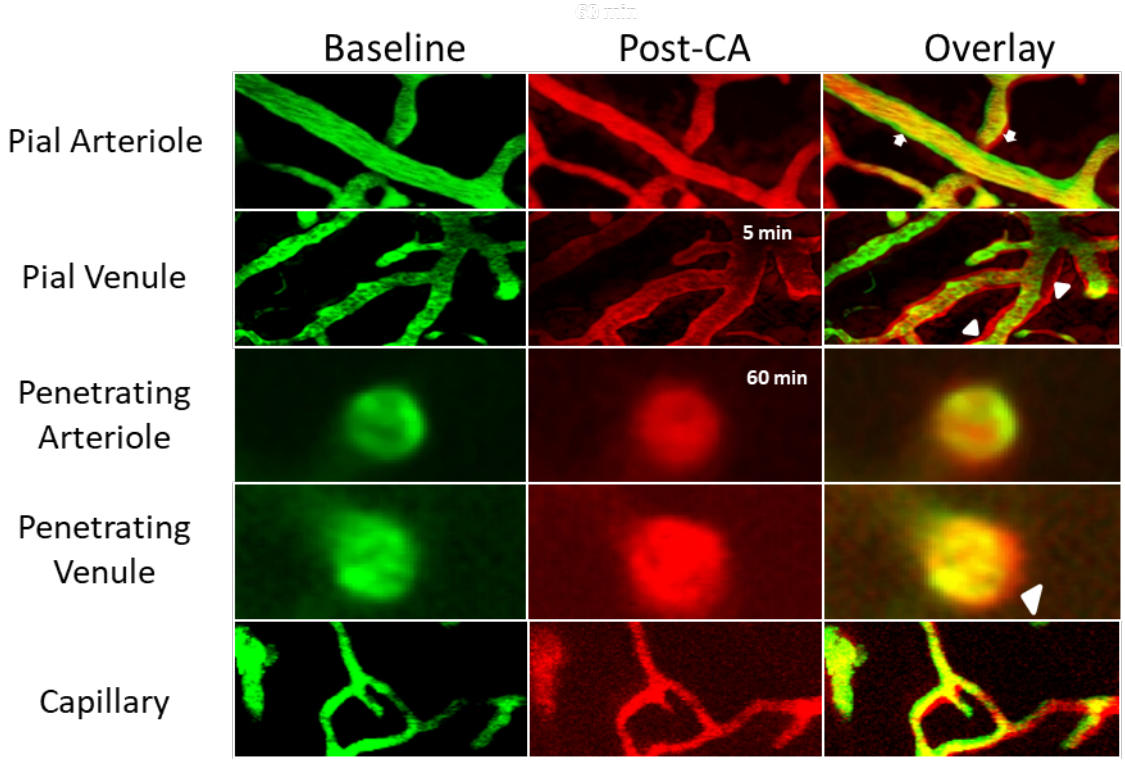

Figure 3.3 Representative images of a pial arteriole, pial venule, penetrating arteriole, penetrating venule, and cortical capillary at baseline and post-CA coded with pseudo colors.

We observed pial arteriolar constriction at 60 min post-CA compared with baseline, indicated by white arrows. The pial and penetrating venule and capillary dilations are visualized at 5 min post-CA and indicated by white triangles.

Figure 3.2 illustrates images of microvessels from one representative rat at baseline. The diameter change post-CA for representative microvessels is illustrated in Figure 3.3. Vascular dynamics post-CA were different in different types of vessels. The diameter of pial arterioles was similar to baseline at 5 min post-CA and decreased at 30 and 60 min post-CA (19.6±1.3, 19.3±1.2 vs 22.0±1.2μm, 30, 60 min post-CA vs baseline, respectively, $p<0.05$) (Figure 3.4 A). No difference was found in the diameter of penetrating arterioles after CA vs baseline (Figure 3.4 B). Capillaries had increased diameter early post-CA at 5 min and returned to baseline value

at 30, 60 min post-CA (5.5±0.2 vs 5.0±0.2µm, 5 min post-CA vs baseline, $p<0.05$) (Figure 3.4 C). Penetrating venules had increased diameter at 5 min post-CA and returned to baseline value at 30 and 60 min post-CA (20.6±1.2 vs 18.0±1.1µm, 5 min post-CA vs baseline, respectively, $p<0.001$) (Figure 3.4 D). Similarly, the diameter of pial venules increased at 5 min post-CA and returned to baseline at 30 and 60 min post-CA (20.0 ± 1.0 vs 17.2±0.8µm, 5 min post-CA vs baseline, $p<0.001$) (Figure 3.4 E).

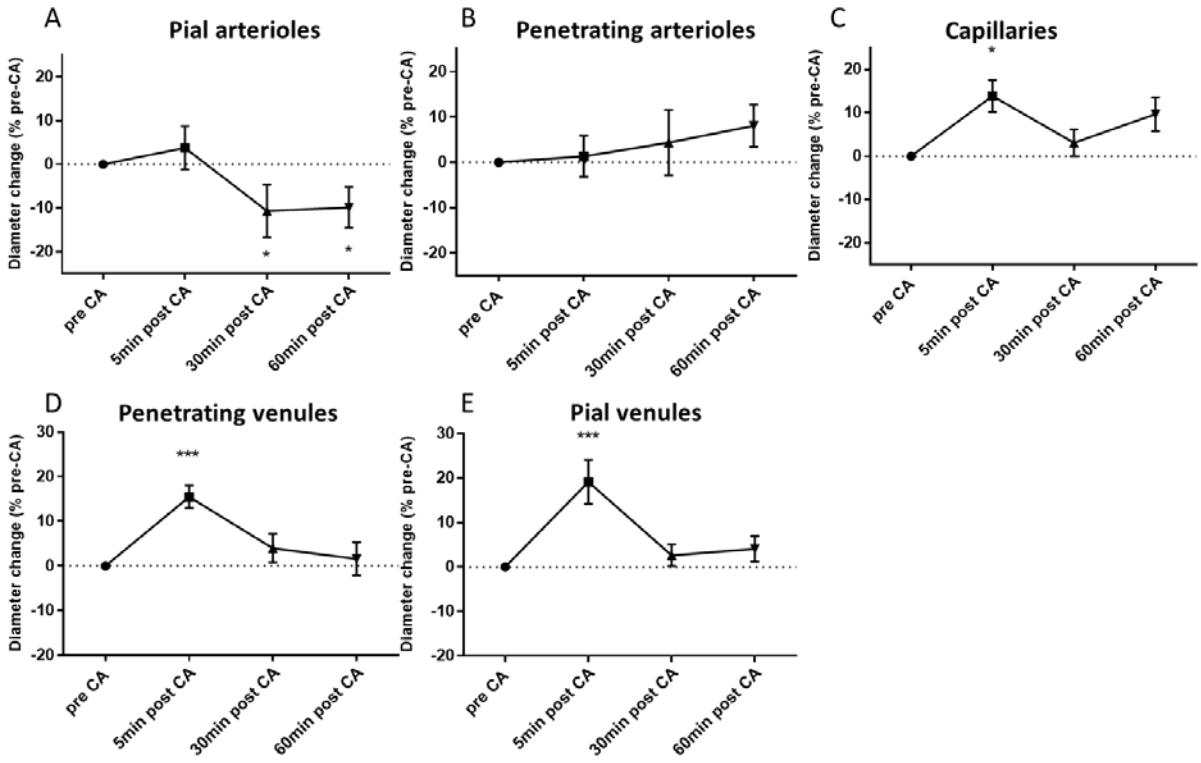

Figure 3.4 Mircovascular diameter changes post-CA.

Diameter changes for pial arterioles (A), penetrating arterioles (B), capillaries (C), penetrating venules (D) and pial venules (E). Post-CA values are normalized to pre-CA values for each vessel. Data were collected from eight post-natal day 16-18 rats at baseline and post CA. The diameters of pial arterioles decreased at 30 and 60 min post CA vs. baseline (* $p<0.05$). The diameters of capillaries increased at 5 min post CA compared with bassline ($p<0.05$). The diameters of the pial and penetrating venules increased at 5 minutes post-CA (*** $p<0.001$).

3.3.3 RBC Flow (No-reflow Phenomenon)

We assessed the continuity of RBC flow in the cortical capillaries at baseline and post-CA. At baseline, RBC flow was continuous in all capillary branches (Supplementary video V1). In capillaries, stagnant RBCs were seen early as 5 min post-CA (Figure 3.5 A and supplementary video V2). Stagnant RBCs were observed in several bifurcated branches of a capillary loop (Figure 3.5 A), or more often stagnant flow was observed in only one of the branches, while in the other branches RBC flow remained continuous (Figure 3.5 B). Stagnant RBCs appeared to be attached to the capillary wall (Supplementary video V2 and V3).

Among 59 capillary branches from 12 rats with continuous RBC flow at baseline, 25.4% of capillaries (15/59) were observed to have no RBC flow at 30 min post CA. At 60 min post-CA 13.5% capillaries (8/59) were found with no RBC flow. Out of the 8 capillaries with no RBC flow at 60 min post-CA, 7 capillaries had no RBC flow at 30 min post-CA.

Overall, no-reflow was captured in 7 out of 12 rats at 30 or 60 min after CA. In four rats the no-reflow was observed at 30 min and was not observed at 60 min in the capillaries studies. In two rats no-reflow was observed at both time points, and in one rat it was observed only at 60 min post-CA.

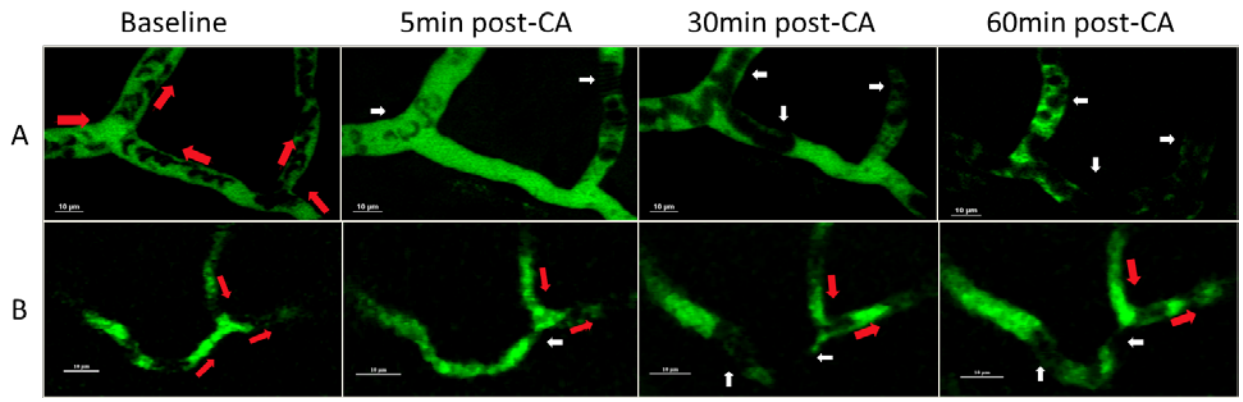

Figure 3.5 Capillary RBC flow after CA.

Upper panel: Illustration of RBC stasis (no-reflow phenomenon) in representative capillaries *in vivo*. Panels A and B represent two individual capillaries with stagnant RBCs post-CA from two rats. Both capillaries were continuously perfused with red blood cells (RBCs) prior to CA. Red arrows indicate the flow direction in every capillary branch. White arrows indicate stagnant RBCs. In panel A, RBC flow was stagnant in all branches at 5, 30 and 60 min post-CA. In panel B, RBC flow in the left branch was stagnant at 5, 30 and 60 min post-CA, while the RBC flow in the other two branches was continuous.

3.3.4 Assessment of capillary RBC velocity and density

To quantify the movement of RBCs in the capillaries with continuous RBC flow post-CA, we examined the RBC velocity and density using linescan. Capillaries with stagnant RBCs were not included in this evaluation due to the unreliable linescan quantification. Capillary RBC flow was highly heterogeneous at both baseline and post-CA (Figure 3.6 A and B). No change was seen in the capillary RBC velocity at baseline and post-CA (0.62±0.08 and 0.67±0.07 mm/s, p=0.195). RBC density increased post-CA in the perfused capillaries (7.57±0.37 vs 6.50±0.46 RBC/s, post-CA vs baseline, $p<0.05$).

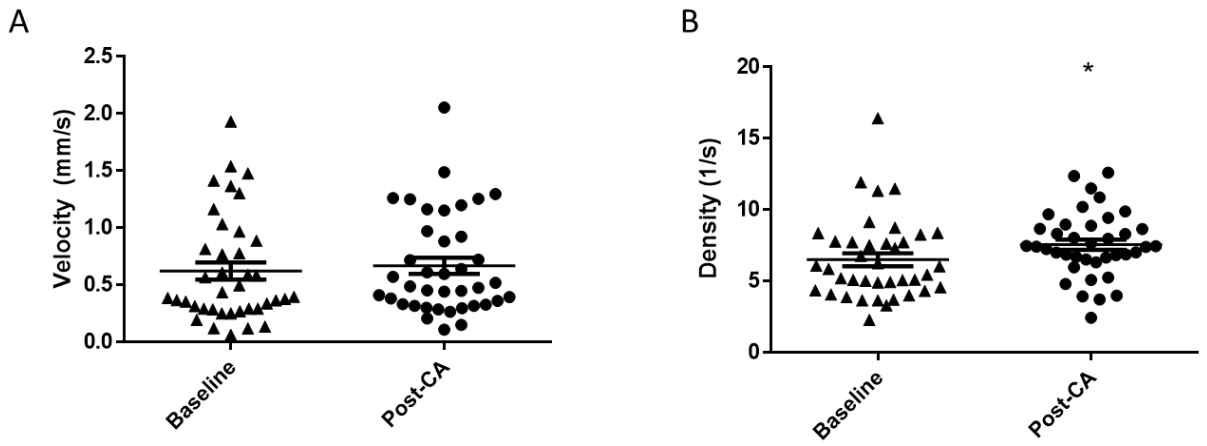

Figure 3.6 RBC velocity and density in patent capillaries.

RBCs velocity (A) and density (B) were calculated from capillaries with continuous flow at baseline and post-CA (39 capillaries from 8 CA rats). RBC density was increased post-CA compared with baseline. Each symbol represents a single vessel. *p<0.05.

3.3.5 Assessment of Capillary Mean Transit Time of Plasma Through the Cortical Microcirculation

Overall MTT increased post-CA compared with sham (200.6±29.2 vs 90.0±9.1%, post-CA vs post-sham, $p<0.05$). At 30 min post-CA, MTT increased compared to baseline ($p<0.001$) while at 60 min post-CA, MTT showed a non-significant trend towards increase compared to baseline ($p=0.08$) (Figure 3.7 A). No change in MTT for sham rats was observed at any time points.

Figure 3.7 B shows the pial vascular network in a representative rat with pial artery and pial vein ROIs (white and yellow squares, respectively). Figure 3.7 C presents intensity-time curves at baseline, 30, and 60 min post-CA.

Prolonged MTT was also observed when the entire pial network was evaluated (Figure 3.7 D). In the representative example illustrated, brighter color indicates relatively longer

latency compared with arterioles, and the brightness appeared in almost all the branches of pial venules. The most prolonged MTT appeared at 30 min post-CA, and partially recovered at 60 min post-CA.

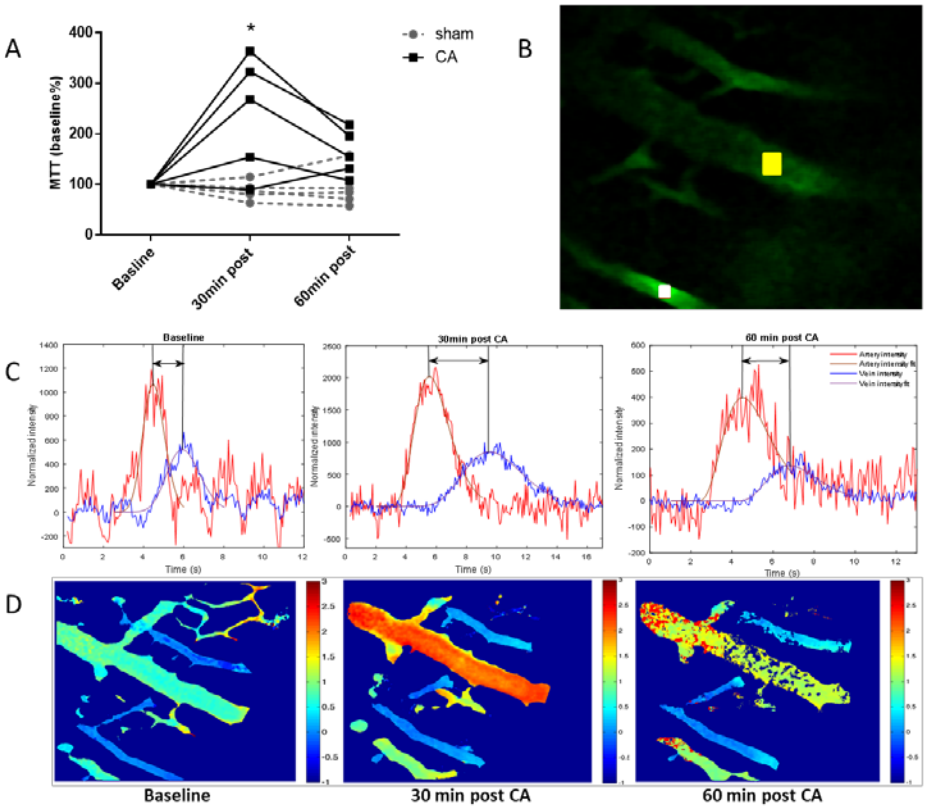

Figure 3.7 Mean transit time of plasma through cortical microcirculation.

A. MTT increased post-CA at 30 and 60 min vs. sham (* $p<0.05$). Each line represents an individual rat, n= 5/group. B. The cortical pial vasculature of a representative rat: the yellow square represents a region of interest (ROI) on a pial vein, while the white square represents a ROI on a pial artery. The intensity of the fluorescent tracer was repeatedly measured in the same ROIs at baseline, and at 30 and 60 min post-CA. C: Intensity-time curves and γ fit curves at baseline, 30, 60 min post-CA (left to right). MTT increased at 30 and 60min post-CA, indicated by the black arrows. D: The time-to-peak (TPP) for each pixel on the pia layer was calculated and normalized to mean arterial TPP. Increased MTT was observed at 30, 60min post-CA in most of the pial veins, indicated by brighter color.

Table 3.1. Physiology parameters for each group of rats.

Experiment groups		Temperature (℃)				EtCO2 (mmHg)				MAP (mmHg)			
	N	baseline	5min	30min	60min	baseline	5min	30min	60min	baseline	5min	30min	60min
Diameter	8	37.3±0.3	36.2±0.2#	37.3±0.4	36.8±0.2	35.7±1.9	31.5±1.1	29.7±3.1	27.0±2.4	56.4±3.2	66.1±6.4	52.57±3.5	55.0±3.8
RBC flow	12	37.1±0.3	35.6±0.2#	36.9±0.3	37.1±0.2	36.3±1.1	30.9±1.2#	28.3±2.0#	29.5±2.1	54.5±3.0	68.5±4.4#	50.7±3.7	51.5±3.7
RBC velocity	8	37.2±0.4	35.7±0.2#	36.4±0.3	37.2±0.3	36.1±1.0	36.3±2.9	30.1±2.0	32.6±1.6	56.4±4.0	59.0±4.5	55.0±3.2	50.0±4.1
MTT (CA)	5	37.9±0.4	35.6±0.3*#	36.7±0.4	37.2±0.5	33.6±2.6*	32.0±2.1*	32.0±3.4*	30.3±2.3*	65.0±2.2	61.0±2.4	59.6±4.8	57.0±9.4
MTT (Sham)	5	37.6±0.5	37.2±0.4	37.6±0.2	37.4±0.1	36.1±1.6	38.7±2.1	36.4±1.7	37.0±3.7	59.2±1.9	56.3±3.8	56.3±2.4	55.0±4.6

*$p<0.05$ vs. sham, #$p<0.05$ vs. baseline

3.4 DISCUSSION

Using *in vivo* microscopy, we characterized cortical microcirculatory disturbances during the first 60 min after CA in a pediatric rat model of CA and resuscitation. Immediately after resuscitation, brief transient dilation of capillaries and venules is followed by prolonged pial arteriolar constriction. At the capillary level, the microcirculatory disturbances are heterogeneous; a no-reflow phenomenon is present in a quarter of capillary branches post-CA, while the RBC velocity is maintained in the patent capillary branches, there is a higher density of RBCs. Overall, the time required for plasma to travel from the pial arterioles through capillaries and into the pial venules is increased after CA (Figure 3.8). Our results detail the cortical microvascular alterations post-CA in the developing rat brain, and should serve as a platform to assess both the impact of standard of care interventions and novel vascular-targeted therapies on perfusion after CA.

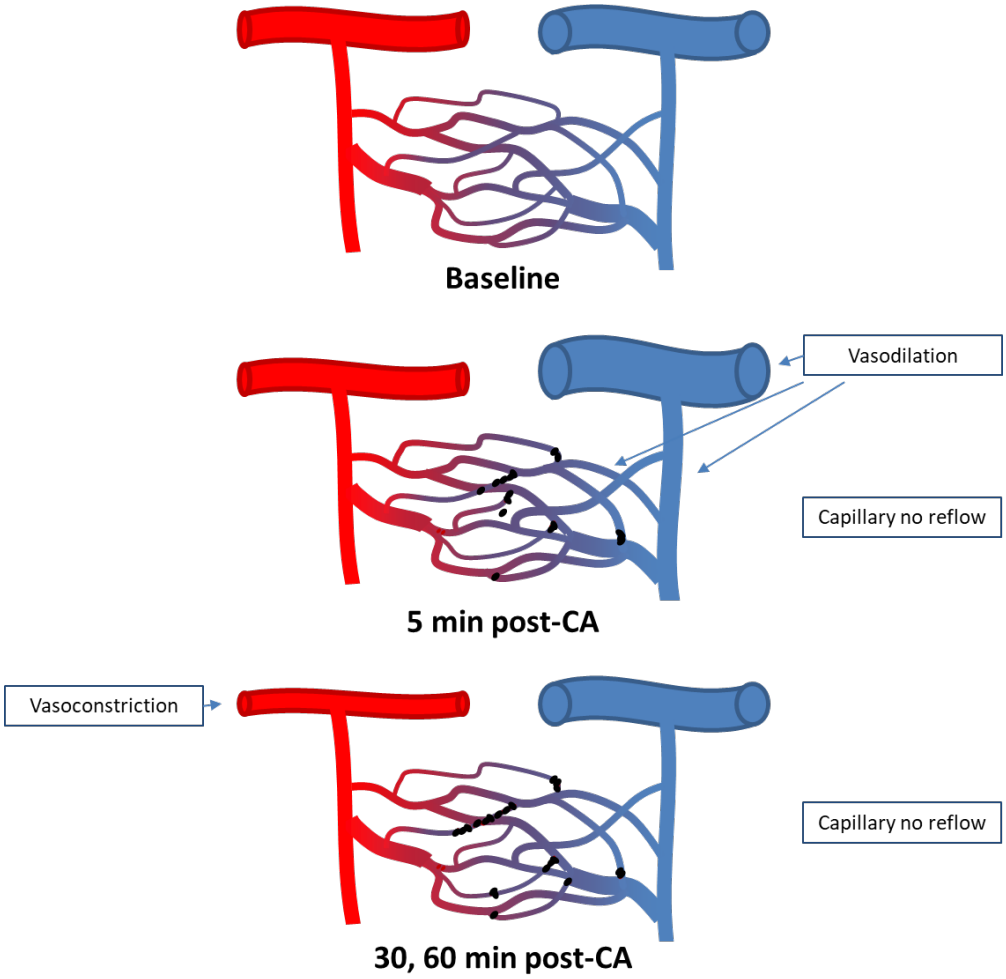

Figure 3.8 A schematic summary of our finding.

The capillaries are perfused with RBC flow at baseline. At 5 min post-CA, capillary no-reflow is present in some capillaries, and pial venules and penetrating venules are dilated. At 30, 60 min post-CA, pial arterioles are constricted while the diameter of venules returned to baseline level. No-reflow is present in a fourth of capillaries at 30 min post-CA.

3.4.1 Pial Arteriolar Constriction

We observed constriction at the level of the pial arterioles and not penetrating arterioles at 30 and 60 min after resuscitation, suggesting that pial arterioles are responsible in part for the decreased cortical CBF after CA. Arteriolar smooth muscle plays an important role in regulating local CBF

and maintaining blood pressure autoregulation [232, 241]. Under physiological conditions, pial arterioles on the surface of the brain are regarded as the major site of flow control, especially during functional hyperemia when upstream pial arteriolar dilation was observed away from the site of brain activity [242]. According to the Poiseuille's equation, arterial constriction of 10% is expected to produce a CBF reduction of ~36%. The arteriolar constriction observed thus correlates with the 30-50% decreased in cortical CBF assessed using ASL-MRI in our model in a prior report [8]. Our results are also consistent with previous reports of arteriolar constriction in gerbils after bilateral carotid artery occlusion and reperfusion [239]. The pathophysiological mechanisms governing post-ischemic arteriolar vasoconstriction are not fully elucidated. It has been suggested that disturbances in the balance of vasoconstrictors and vasodilators are responsible for arteriolar vasoconstriction post-CA. Vasoconstrictive mediators such as ET, reactive oxygen species, and some products of arachidonic acid metabolism are increased after global or focal ischemia [27, 77]. Vasodilator mediators such as nitric oxide or selected metabolites of arachidonic acid are decreased after ischemia and might facilitate vasoconstriction [27, 243]. Our observations further support the potential benefit of therapies promoting vasodilatation to optimize CBF after CA [244]. Indeed, several vasodilator strategies such as use of the calcium channel blockers [127], or thromboxane inhibitors [245] proved beneficial in improving CBF and in some instances outcome after CA in preclinical models. In our model, inhibiting the vasoconstrictive eicosanoid 20-HETE improved CBF early after CA, and decreased neuronal degeneration and neurological deficits [27]. Similarly, in other models, the ET(A) receptor antagonist BQ123 improved functional outcome and CO_2 reactivity after CA [77] and administration of the vasodilator nitrite improved neurological outcome and was accompanied with reduced reactive oxygen species production [243]. A more complete

characterization of the effects of therapies targeting arteriolar vasodilation in cortex is warranted and supported by our findings. The impact of these interventions on the observed derangements in the microcirculation could provide additional insight to conventional CBF assessments.

3.4.2 Early Capillary and Venular Dilation

Capillary and venular dilation was observed at 5 min after resuscitation. At this early time some of the capillaries had evidence of RBC stasis, despite a lack of pial and penetrating arteriolar constriction. The role of capillaries in regulating CBF is controversial. The dilatation of capillaries could represent either a passive compensatory mechanism to accommodate blood flow in patent capillaries, or an active process in response to tissue acidosis and/or hypoxia, and merits further study. Hall, et al. suggest that 84% of CBF regulation occurs at the capillary level, and the capillaries responded to whisker-pad stimulation earlier than the arterioles [148]. Conversely, other studies suggest that arterioles rather than capillaries are responsible for CBF regulation [232]. Similarly, we found that the capillary diameter increased only transiently at 5 min post-CA and returned to baseline afterwards. At 5 min post-CA, the increased MAP in the absence of arteriolar constriction may have produced increased hemodynamic pressure in the capillaries and venules, leading to capillary dilation. The increased MAP could be secondary to a transient increase in cardiac output and the hypertensive effect of epinephrine post-resuscitation if autoregulation is impaired [246], or may be due to a transient increase of blood volume secondary to the osmolar effect of bicarbonate administrated at resuscitation. At 30 and 60 min post-CA we observed constriction of the pial arterioles with concomitant return of MAP to baseline, which could explain the return diameter of capillaries and venules to baseline levels.

3.4.3 RBC stasis and No-reflow phenomenon

We observed RBC stasis in a fourth of the capillary branches. This observation, referred to as the no-reflow phenomenon, was previously described *ex-vivo* and was suggested as a mechanism underlying cerebral hypoperfusion after global ischemia [247]. In a model of CA, the no-reflow phenomenon was observed post-CA in 30% of brain regions [173]. Our *in-vivo* evaluation provides specific morphological data regarding the no-reflow phenomenon, supporting its existence and further defining its appearance at the microcirculatory level. Our data suggest that individual capillary branches are affected, and flow is diverged from the affected branches towards the surrounding capillaries. Some branches with no RBC flow regain perfusion by 60 min after CA. Thrombocyte and leukocyte aggregation, as well as decreased RBC deformability post-CA may play a role in the no-reflow phenomenon [248]. Thrombolytic therapy using plasminogen activator and heparin reduced the no-reflow post-CA [180] and blood flow promotion therapy with hypertension and hemodilution instituted upon resuscitation from CA normalized post-resuscitation CBF and improved neurological outcome in dogs [203]. Pentoxifylline, a hemorheological agent which can reduce RBC deformability, has been shown to ameliorate the hypoperfusion post CA [249]. Similarly, we qualitatively observed that RBCs appeared to be less deformable after CA. Given that decreased in RBC deformability has been associated with acidosis [250], the change in RBC membrane elasticity in the acidotic milieu post-CA might contribute to the RBC stasis. Additionally, arteriolar constriction may exacerbate the no-reflow phenomenon, as arteriolar constriction in a model of focal ischemia was thought to contribute to hypoperfusion, thrombosis and distal microvascular occlusions [232].

3.4.4 Increased RBC density post-CA

We observed increased RBC density in the patent capillaries after CA. The increased density of RBC could represent their passive redistribution diverted from the blocked capillaries towards patent capillaries, or active recruitment of oxygen carrying RBCs to areas affected by the no-reflow via an alternative capillary route. In patent capillaries, RBC velocity was similar to baseline. Obstruction of ~25% of capillaries without an increase in RBC velocity in the capillaries that remain patent contributes to the increased plasma MTT.

3.4.5 Plasma Mean Transit Time post-CA

The transit time of plasma in the cortex provides an overall assessment of microvascular dynamics after CA and integrates the microcirculatory components assessed, including vascular diameter, capillary patency, and velocity. Similar to our data, Crumrine and LaManna calculated MTT based on measurements of CBF and cerebral blood volume (CBV) and reported a four-fold increased transit time at 30 and 60 min after CA [251]. The peak increase in MTT in our study was observed at 30 min post-CA, coinciding with the peak of the capillary obstruction, suggesting that the longer duration required for plasma to traverse the capillary bed is secondary to the capillary obstructions. Pial arterial vasoconstriction, along with stasis at the level of capillaries likely contribute to increased MTT and together represent the underlying vascular mechanism for cortical hypoperfusion observed in our model.

3.4.6 Limitations

We assessed alterations in cerebral microcirculation in a pediatric model of CA in immature rats. In pediatric CA asphyxia is the predominant mechanism, in contrast to adult CA where most cases are resulted from ventricular fibrillation (VF) [228]. In comparison with VF CA, the unique pathophysiology of asphyxial CA includes hypoxia, bradycardia, hypovolemia, arrhythmia, acidosis leads to different CBF disturbances post-CA [252], and most likely, distinct alterations in cerebral microcirculation. Indeed, the CBF alterations observed in our model using ASL-MRI differ from the adult model of CA, especially at early time points after resuscitation, where cortical hyperemia is observed after adult CA [252]. The alterations observed in our study might be specific to the pediatric brain, especially in light of recent data that unveiled that the vascular response to neuronal stimulation was different in neonatal vs. adult rats, specifically functional hyperemia was uncoupled from neuronal activity in developing rats from 7 to 13 days postnatally [253]. This difference in the vascular response in pediatric vs. adult brain may be explained by myriad processes occurring at the neurovascular unit in the developing brain, such as angiogenesis, vascular pruning, and gradual maturation of astrocytes until PND 21 [254]. The vast majority of studies of microcirculation in global cerebral ischemia or CA used adult models [47], and thus the current characterization of microcirculatory changes in a pediatric model is important for the understanding of pediatric specific post-CA pathophysiology and ultimately for the development of pediatric specific therapies.

We observed a modest decrease of temperature at 5 min post-CA compared to baseline due to spontaneous cooling during CA. Clinically the same extent of cooling may not develop during CA in humans, due to significantly different body surface area and metabolism rates. This is a limitation of the rodent model that may affect vascular changes at early time points (5

min). Sodium bicarbonate was given in this experiment to correct the acidosis post-CA. This could potentially limit the translational significance of the current study. Post-CA hypocarbia may also contribute to the reduced CBF post-CA. We used male rats in our study, and although PND 16-18 is a pre-pubertal age, innate sex differences have been reported: cytotoxicity and programmed cell death [255, 256]. Further experiments using female rats are warranted.

3.5 CONCLUSION

In conclusion, we characterized *in vivo* the dynamic changes of the cortical microcirculation in an established pediatric CA model that produces cortical hypoperfusion and tissue hypoxia in rats. Our study identifies several vascular-specific targets in the microcirculation to mitigate these derangements. Characterization of the effects of both standard post-resuscitation therapies along with novel approaches on the microcirculation after pediatric CA could optimize post-resuscitation perfusion and ultimately improve neurological outcome.

4.0 20-HETE FORMATION INHIBITION INDUCES CEREBRAL ARTERIOLAR DILATION AFTER ASPHYXIAL CARDIAC ARREST IN PEDIATRIC RATS

[Li L, *et al. J Cereb Blood Flow Metab.* Submitted]

4.1 INTRODUCTION

4.1.1 Arachidonic Acid Metabolism Pathway by Cytochrome P450 Enzyme

Metabolites of arachidonic acid (AA) have long been recognized to play a pivotal role in multiple pathophysiologic processes [257, 258]. The bioactivation of AA by cytochrome P450 to hydroxylated and epoxygenated metabolites has been implicated in inflammation, hypertension, cancer, and neurological disorders [146, 259, 260]. Under pathophysiological conditions, AA is released from phospholipids and quickly metabolized by cytochrome P450 enzymes into hydroxyeicosatetraenoic acids and epoxyeicosatrienoic acids, which are vasoactive fatty acids that regulate blood flow in the renal, cerebral, coronary and pulmonary circulations [261-263].

4.1.2 20-hydroxyeicosatetraenoic acid (20-HETE) Inhibition Serves as a Promising Target for Neurovascular Diseases

Terminal hydroxylation of AA by CYP4A/4F subfamilies produces 20-hydroxyeicosatetraenoic acid (20-HETE) which is a potent vasoconstrictor and also involved in apoptosis, neuroinflammation and superoxide production pathways [154-156]. In neurological conditions, increased 20-HETE was observed after CA, traumatic brain injury (TBI), intracerebral hemorrhage and ischemic stroke [27, 264, 265]. Inhibitors of the CYP4A/4F enzymes reduce

20-HETE synthesis and have been shown to be neuroprotective both *in vitro* and *in vivo*. N-Hydroxy-N'-(4-n-butyl-2-methylphenyl) formamidine (HET0016), a potent CYP4A/4F inhibitor, increased cerebral perfusion and improved short-term neurological outcome in an experimental pediatric cardiac arrest (CA) model [27]. More recently, direct neuroprotectant effects of 20-HETE inhibition were described both *in vivo* and in vitro. HET0016 treatment was shown to exert protective effects on cultured neurons, astrocytes and also hippocampal slices exposed to oxygen-glucose deprivation [155, 266, 267]. Neuroprotection after HET0016 treatment was also observed in a model of pediatric asphyxial CA in piglets, albeit without a measurable effect on cerebral perfusion evaluated by laser doppler [268]. Therefore, 20-HETE formation inhibition serves as a potential therapeutic strategy to improve neurological outcome in hypoxic and ischemic conditions through dual neuronal- and vascular effects. The precise mechanism of 20-HETE action at the level of cerebral microvasculature has not been detailed *in vivo*.

3.1.3

The mechanism of 20-HETE induced vasoconstriction involves the depolarization of vascular smooth muscle membrane secondary to blocking the large-conductance Ca^{2+}-activated K^{+}-channels [150-152] and stimulation of the L-type Ca^{2+} channel [90, 153]. Exogenous addition of 20-HETE constricted pressurized cat pial arteries in a concentration-dependent manner [150]. More recently, 20-HETE was also reported to have an important role in constricting small cerebral arterioles and capillaries [148].

Cerebral microvessels play a critical role in regulating cerebral blood flow (CBF) by significant contributing to the cerebral vascular resistance [148, 232]. By constricting cerebral microvessels, pathological 20-HETE production very likely contributes to cerebral hypoperfusion and leads to the secondary ischemia observed in multiple neurovascular diseases

animal models [8, 203]. We have previously shown that inhibition of 20-HETE formation by HET0016 improved cortical perfusion, brain edema, neuronal survival and neurological outcome in a pediatric asphyixal CA model in developing rats [27]. In this established CA model, the cortical hypoperfusion and hypoxia are well documented [8, 77, 230]. Moreover, a recent study by our group reported the heterogenous flow disturbances post-CA in the cortical microcirculation in the same model [269]. Using *in vivo* multiphoton microscopy, we observed post-CA arterial vasoconstriction and intravascular stasis, also known as the no-reflow phenomenon.

4.1.3 Hypothesis and Objectives

To investigate the effect of inhibition of 20-HETE formation on the cerebral microcirculation post-CA, we assessed the effect of HET0016 administration at resuscitation using *in vivo* multiphoton microscopy in a clinically relevant pediatric CA model. We hypothesize that intravenous HET0016 administration post-CA alleviates microvascular constriction, therefore reduce CBF disturbances post-CA. In HET0016 treated rats we observed penetrating arteriolar dilation. Prolonged plasma MTT was attenuated after HET0016 treatment. No significant effect of HET0016 was observed on the no-reflow phenomenon compared with vehicle. Our findings suggest that 20-HETE inhibition by HET0016 has a vasodilator effect on cerebral arterioles but has no effect on reducing the no-reflow phenomenon. Combination treatments with multiple targets should be evaluated to further improve cerebral microcirculatory disturbances post-CA.

4.2 METHODS

4.2.1 Animals

This study was performed in accordance with the Guide for the Care and Use of Laboratory Animals (8th Ed), published by National Research Council and approved by the Institutional Animal Care and Use Committee at the University of Pittsburgh. Male Sprague-Dawley, post-natal day (PND) 16-18 rats (30-45 g) were used in this study (HET0016 vs vehicle, n=5-6/group).

4.2.2 N-hydroxy-N'-(4-n-butyl-2-methylphenyl) Formamidine (HET0016) Formulation and Dosage

N-hydroxy-N'-(4-n-butyl-2-methylphenyl) Formamidine (HET0016) was purchased from Maybridge, Cambridge, UK. A water-soluble formulation of HET0016 was prepared for intravenous administration as previously described [270]. Briefly, HET0016 was added into 15% of (2-Hydroxypropyl)-β-cyclodextrin (HPβCD) (Sigma-Aldrich, Inc. US) with a final concentration of 0.15 mg/mL and agitated for 48 hours at room temperature on a Titer Plate Shaker (Lab-Line Instruments, Inc. US). The HET0016 solution was then lyophilized to complete dryness with a FreeZone 6 Lyopholizer (Labconco, Inc.). The lyophilized powder was reconstituted with phosphate-buffered saline (MP Biomedicals, LLC. US) before administration. Rats randomized to HET0016 treatment were dosed with 1 mg/kg HET0016 at 1 min after resuscitation from CA. Rats randomized to vehicle treatment received the same volume of 15% of HPβCD. Treatment was randomized using random number generator before

the experiment started. The surgical personnel were blinded to treatment until all data was collected.

4.2.3 Surgical Preparation and Asphyxial CA

An established pediatric asphyxial CA rat model [230] was used with slight modifications for *in vivo* microscopy [269]. Rats were initially anesthetized with isoflurane, orally intubated and mechanical ventilated. After the placement of femoral arterial and venous catheters, we discontinued the isoflurane and administered fentanyl intravenously at a constant rate of 50 μg/kg/h to avoid the vasodilator effect of isoflurane on blood flow. Vecuronium as neuromuscular blockade was infused intravenously at a rate of 5 mg/kg/h. A heating pad was used to maintain the body temperature at 37℃. An imaging window was created on the skull over the parietal area as previously described [269]. The experiment settings are illustrated in Figure 4.1A. Rats were subjected to 12 min asphyxial CA, which produces cortical hypoperfusion as previously described using ASL-MRI [8]. The induction of asphyxia and resuscitation were conducted as described previously, by stopping mechanical ventilation after neuromuscular blockade [269]. Rats were resuscitated in a clinically relevant fashion with, bicarbonate (1 mEq/kg iv), epinephrine (0.005 mg/kg iv) and chest compressions until return of systemic circulation (ROSC). HET0016 of 1 mg/kg or the same volume of vehicle were injected iv at 1 min after return of systemic circulation (ROSC). Physiological parameters were recorded throughout the experiment, including mean arterial pressure (MAP), end-tidal (Et) CO_2 and temperature.

4.2.4 Cerebrovascular Imaging Using Multi-Photon Microscopy

The multiphoton microscopy was performed as previously described [269]. Briefly, a Nikon A1R MP microscope together with the Nikon Ni-E (Nikon Instruments; Tokyo, Japan) upright motorized system were used in the current study. The microscope was equipped with a Chameleon Laser Vision (Coherent, Inc; CA, USA), an APO LWD 25× water immersion objective with 1.1 NA, a high-speed (30 frames/second) resonant scanning mode. We used the fluorescence detector 2 for FITC 525 / 50 nm (green channel), an excitation wavelength of 850 nm and a laser power of 1-2% during the experiment. All microscope components including the laser, stage, resonant scanning head, detectors and acquisition were controlled through the NIS Elements software (Nikon). Post-acquisition image processing was achieved using NIS Elements and MATLAB (R2015a, The MathWorks, Inc. US). The intravenous dye Fluorescein isothiocyanate–dextran (FITC; Sigma, wt 2,000,000) 3% (w/v) 0.1mL was administered at baseline to delineate the vasculature (Figure 4.1B). Additional doses of FITC were given as needed to maintain adequate contrast.

4.2.5 Assessment of Cerebral Microvascular Diameter

To measure the microvascular diameters, image stacks at a resolution of 1µm/ pixel using resonant mode were acquired at baseline, and at 5, 30 and 60 min post-CA in 5-6 rats. The cortical microvessels were characterized as previously described [269] into five types: pial arterioles, penetrating arterioles, capillaries, penetrating venules, and pial venules, as shown in Figure 4.1B. Micro vascular diameters for the vehicle group were collected from 5 rats and 21

pial arterioles, 180 pial venules, 12 penetrating arterioles, 104 penetrating venules, and 440 capillaries. The diameters of microvessels in HET0016 group were acquired from 6 rats and 25 pial arterioles, 163 pial venules, 16 penetrating arterioles, 88 penetrating venules, and 383 capillaries. For each animal, 2-5 locations with adequate contrast resolution were identified within the imaging window at baseline. The z-depth of the image stacks reached to a depth ranging from 250-400 μm from the pia. The post-CA stacks (5, 30 and 60 min post-CA) were overlaid with the baseline stacks in the x-y-z dimensions in each location. The vessel diameters at each time point were then quantified from a single location per segment from the maximum projection of the aligned image stacks using the Annotation and Measurement function in NIS Element. Only the vessels with data acquired at all four-time points were included.

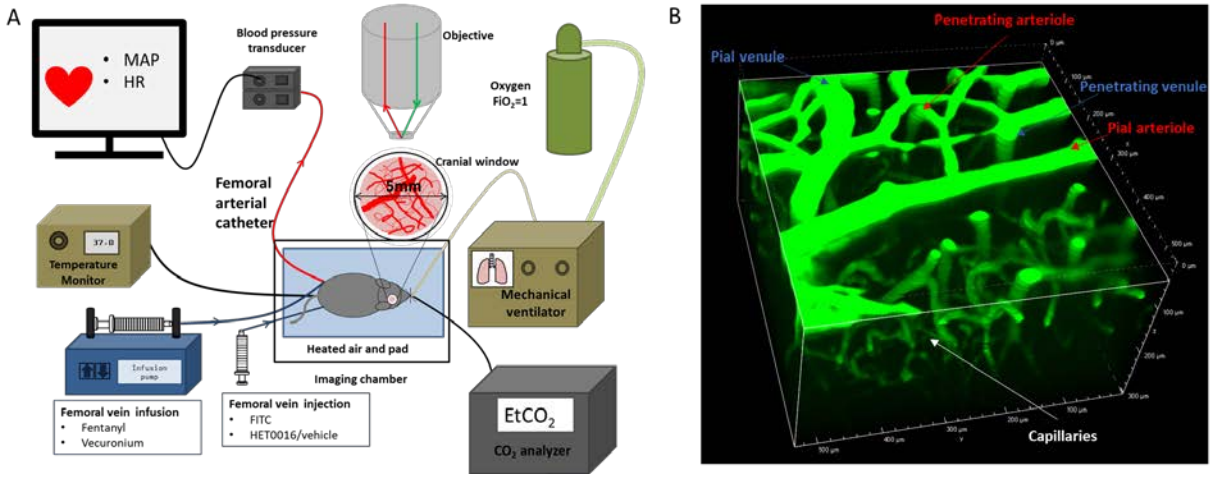

Figure 4.1 Surgical setting (A) and a representative image of the microvasculature (B)

A. The surgical and imaging settings of our experiments. B. A representative 3D image of the cortical microvasculature, delineated with green pseudo color. The *z* depth is about 300 μm. Different types of micro vessels and their relative locations are identified.

4.2.6 Assessment of Capillary Red Blood Cell (RBC) Flow (No-reflow Phenomenon)

The assessment of the capillary RBC flow was conducted as previously described [269]. The time-series at baseline and post-CA were acquired at the speed of 30 frames/s with resonant mode to assess the presence of RBC flow vs. stasis in the capillaries, which were defined as small vessels in parenchyma with diameters of less than 10 μm. RBCs appeared as oval negative signals and a size of 3-6 μm in the bright plasma delineated with FITC (Video 1 A&B). The capillary branches were randomly selected at baseline and were followed to 60 min post-CA. Time-series of the same capillaries were repeatedly assessed post-CA at 30 and 60 min. Absent RBC flow was defined as no RBC flow during the time series (15-30 s). In vehicle group, 82 capillaries from 6 rats were evaluated while in HET0016 group 65 capillaries from 6 rats were assessed.

4.2.7 Assessment of Mean Transit Time (MTT) of Plasma

MTT was assessed at baseline and at 30 and 60 min after CA in HET0016 or vehicle group (n=6/group) using a previously described method [239, 269]. Briefly, two regions of interests (ROIs), one on a pial arteriole and the other on an adjacent pial venule were identified. Time-series were recorded at a speed of 30 frames/s with resonant mode during a bolus of FITC dextran (3% w/v, 0.03mL) iv injection at baseline, 30 and 60 min post-CA. The standard γ function was fit to the intensity-time curves in MATLAB. Time-to-peak (TTP) was defined as the time required for the intensity change from baseline to the peak in the fit curves for the artery

and vein. MTT was defined as the difference of TTP between the pial artery and the pial venule ROIs at each time point.

4.2.8 Statistical Analysis

Means and standard error of the means (SEM) were presented for the continuous variables. Data were analyzed by using SPSS (IBM Corp. IBM SPSS Statistics for Windows, Version 24.0. Armonk, NY: IBM Corp.) and figures were generated using Graphpad Prism 6 (GraphPad Software, Inc. La Jolla, CA, USA). Physiological parameters were tested for time effect within each experiment using repeated measurement ANOVA followed by Dunnett' post-hoc comparison. Microvessel diameters were log transformed and analyzed using a mixed linear model with vessels from the same subject nested within each animal. Dunnett' post-hoc comparisons were conducted within each fixed effect. In the quantification of capillary RBC flow, the number of capillaries with RBC stasis were recorded and fit in a logistic mixed effect model with treatment effect as well as time effect using SPSS. MTT measurements were analyzed using two-way ANOVA with Dunnett' post-hoc comparison. For all tests, $p < 0.05$ was considered statistically significant. The researchers performing the surgical preparation and data analysis were blinded to the treatment groups. The blinding code was broken after data analysis was finished and before the statistical analysis was performed.

4.3 RESULTS

4.3.1 Physiological Parameters Summary

All animals included in the study were successfully resuscitated from CA and had ROSC for at least 90 min post-CA. The physiological parameters recorded for both groups are summarized in Table 4.1. At baseline all physiologic parameters were within normal limits. Rats had a modest temperature reduction post-CA compared to baseline, similar in the vehicle and HET0016 group. No differences were observed in $ETCO_2$ or MAP for each group vs. baseline and between groups.

Table 4.1 Temperature, $EtCO_2$, and Mean arterial pressure (MAP) at baseline and post-CA.

	Temperature (°C)				EtCO2 (mmHg)				Mean Arterial Pressure (mmHg)			
Group	baseline	5min post	30min post	60min post	baseline	5min post	30min post	60min post	baseline	5min post	30min post	60min post
Vehicle	37.2±0.5	35.3±0.8*	36.1±0.4*	36.6±0.5*	38.0±6.2	40.8±17.2	36.4±15.0	41.8±16.4	58.3±4.1	65.5±13.8	51.7±16.9	55.8±8.0
HET0016	37.2±0.3	34.3±1.3*	36.3±1.1*	36.6±0.5*	35.8±6.5	29.7±3.4	35.0±8.7	31.3±4.9	62.5±7.6	69.2±16.9	51.3±10.8	49.2±12.0

*$p<0.05$ compared to baseline

4.3.2 Assessment of Cerebral Microvessel Diameter

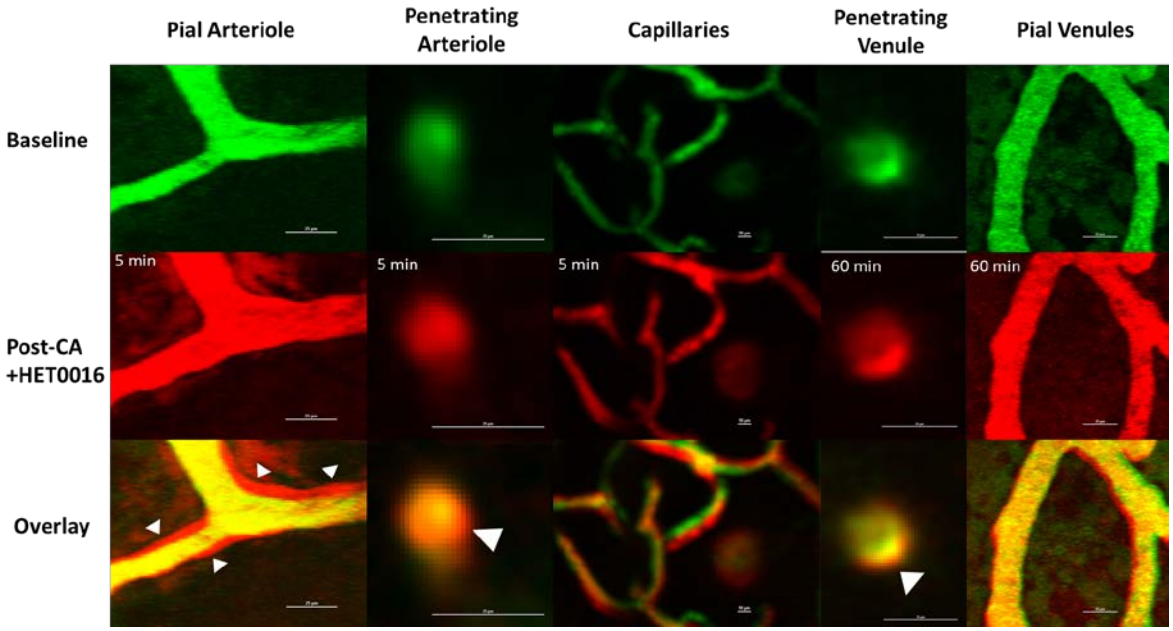

Figure 4.2 Representative images of a pial arteriole, pial venule, penetrating arteriole, penetrating venule, and cortical capillary at baseline and post-CA from a rat treated with HET0016.

Pial and penetrating arteriolar dilation at 5 min post-CA is indicated by white triangles. The penetrating venule dilations are also visualized at 60 min post-CA and indicated by white triangles.

The diameter of pial arterioles in rats treated with vehicle was similar to baseline after 12 min of asphyxia (31.0±2.6, 33.0±2.4 and 32.0±2.6 vs. 29.8±2.3 µm, 5, 30 and 60 min post-CA vs. baseline, p= 0.96, 0.25 and 0.67, at 5, 30, and 60 min vs. baseline, respectively) (Figure 4.3 A). The diameter of pial arterioles in rats treated with HET0016 were also similar to baseline (42.1±8.4, 40.7± 8.1, 40.7±8.1 vs 37.1± 7.4µm, 5, 30 and 60 min post-CA vs. baseline, p= 0.08, 0.35 and 0.70, at 5, 30, and 60 min vs. baseline, respectively) (Figure 4.3 A). Rats treated with HET0016 had increased pial arteriolar diameters compared with vehicle-treated rats at 5 min post-CA (42.1±8.4 vs 31.0±2.6 µm, $p<0.05$, HET0016 vs vehicle) (Figure 4.2, 4.3A).

The diameters of penetrating arterioles in rats treated with vehicle were similar post-CA compared with baseline (27.9±3.5, 28.2±4.0, and 32.1±4.0 vs 28.9± 3.4 µm, 5, 30 and 60 min post-CA vs. baseline, p=0.96, 0.92 and 0.61, at 5, 30, and 60 min vs. baseline, respectively) (Figure 4.3 B). Penetrating arterioles post-CA in rats treated with HET0016 had increased diameter compared with baseline (34.3±2.3, 32.8±2.6 and 37.3±3.0 vs 28.7±2.1 µm, 5, 30 and 60 min post-CA vs. baseline, respectively, $p<0.05$ at 5, 30, and 60 min vs. baseline) (Figure 4.2, 4.3B). HET0016 treatment showed a trend towards increased penetrating arteriolar diameter at 5 min post-CA compared with vehicle group (34.3±2.3 vs 27.9±3.5µm, p=0.051) (Figure 4.3 B). There was no difference between treatment groups in the diameters of penetrating arterioles at 30 and 60 min post-CA (p=0.175,0.197, respectively).

Capillaries in rats treated with vehicle had increased diameter at 5 and 60 min post-CA compared with baseline (5.9±0.1, 6.1±0.1 vs. 5.5±0.1µm, 5, 60 min post-CA vs baseline, $p<0.05$) (Figure 4.3 C). The diameters of capillaries in rats treated with HET0016 remained similar with baseline (6.0±0.1, 5.9±0.1, and 6.3±0.2 vs 5.9±0.2 µm, 5, 30 and 60 min post-CA vs. baseline, p=0.82, 0.97 and 0.13, respectively) (Figure 4.2, 4.3 C). There was no difference between treatment groups in the diameters of capillaries post-CA.

Penetrating venules in rats treated with vehicle had increased diameter at only 60 min post-CA compared with baseline (21.8±2.1 vs 19.2±1.9µm, 60min post-CA vs baseline, $p<0.05$). The diameter of penetrating venules in rats treated with HET0016 increased at 5 and 60 min post-CA compared to baseline (22.8±1.2, 23.9±1.1 vs 21.1±1.2µm, 5, 60min post-CA vs baseline, $p<0.05$) (Figure 4.2, 4.3 D). The diameters of penetrating venules in rats treated with HET0016 were similar to the ones treated with vehicle post-CA.

Pial venules in rats treated with vehicle had increased diameter at 60 min post-CA compared with baseline (19.5 ± 0.7 vs 17.7±0.7µm, 60 min post-CA vs baseline, p<0.05) (Figure 4.2, 4.3 E). Pial venules in rats treated with HET0016 remained similar to baseline (19.8±0.9, 19.1±0.9, and 19.2±0.9 vs 18.8±0.9 µm, 5, 30 and 60min post-CA vs baseline, p=0.09, 0.89, and 0.92, respectively). There was no difference between treatment groups in the diameters of pial venules post-CA.

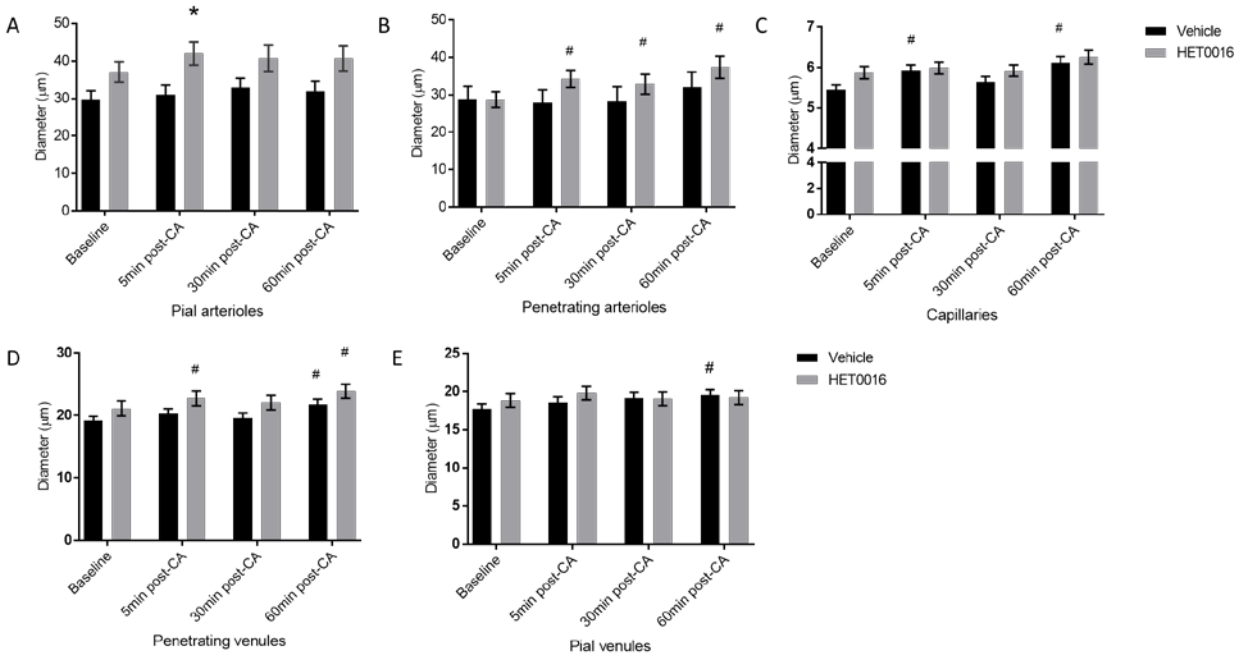

Figure 4.3 Microvascular diameter changes post-CA.

Diameter changes for pial arterioles (A), penetrating arterioles (B), capillaries (C), penetrating venules (D) and pial venules (E). Data were collected from 6 post-natal day 16-18 rats at baseline and post CA from each group. In the HET0016 group, the diameters of pial arterioles increased at 5 min post CA vs. vehicle (* p<0.05). The penetrating arterioles dilated post-CA vs. baseline (# p<0.05). In the vehicle group, the diameters of capillaries increased at 5 and 60 min post CA compared with bassline (# p<0.05). The penetrating venules dilated at 5 and 60 min in the HET0016 group post-CA vs. baseline (# p<0.05). In the vehicle group the diameters of the pial and penetrating venules increased at 60 minutes post-CA vs. baseline (# p<0.05)

4.3.3 Assessment of Capillary RBC Flow (No-reflow Phenomenon)

We assessed the continuity of RBC flow in the cortical capillaries at baseline and post-CA in both vehicle and HET0016 groups. At baseline, all capillary branches had continuous RBC flow (Supplementary video V1). After CA, stagnant RBCs were seen in capillaries in all rats (Figure 4.4, Supplementary video V2). Absence of RBC flow was observed most often in one of the capillary branches of a capillary network, while in the other branches RBC flow remained continuous (Supplementary video V3). In some capillaries, the stasis of RBCs resolved at later time points (Supplementary video V4), while in other capillaries the RBC stasis persisted to the end of the observation period (Figure 4.4).

Stagnant RBCs were present in all the rats at least at one time point in both vehicle and HET0016 group. Overall, in the vehicle group, 26.4% of capillary branches had no-reflow at 30 min post-CA. This phenomenon gradually recovered and11.7% capillaries with no-reflow were present at 60 post-CA (Figure 4.4). Similar trends were observed with HET0016 treatment with absence of RBC flow observed in 28.9% and 12.3% capillary branches at 30 and 60 min post-CA, respectively (Figure 4.4). There was no difference between treatment groups in the proportion of capillaries with no-reflow post-CA.

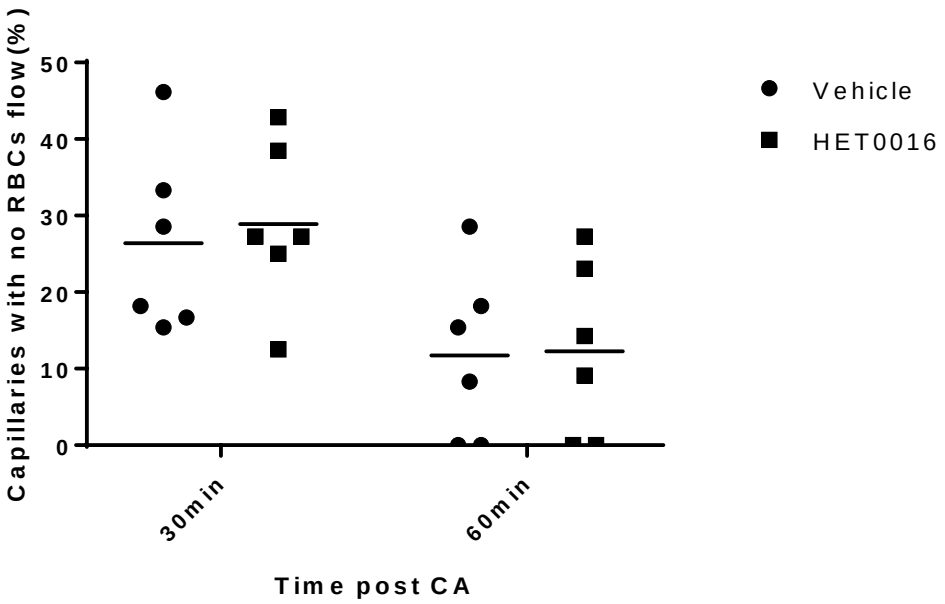

Figure 4.4 Capillary RBC flow after CA.

Representation of percent of capillaries in each rat with absence of RBC flow post-CA for the HET0016 and vehicle groups. Each dot of the scatterplot represents an independent animal.

4.3.4 Assessment of Mean Transit Time (MTT) of Plasma

Figure 4.5 illustrates MTT of representative rats from the vehicle group (5A) and from HET0016 group (5B). MTT in the vehicle group was similar at 30 min post-CA compared with baseline (2.0 ± 0.3s vs 1.6 ±0.3s, p=0.35) but increased 60 min post-CA compared with baseline (2.7±0.7s vs 1.6 ±0.3s, p<0.05) (Figure 4.5C). MTT post-CA in HET0016 group was similar to baseline (1.9 ± 0.2s and 1.8 ±0.2s vs 1.3 ±0.1s, 30min and 60 min post-CA vs baseline, p= 0.09 and 0.16, respectively). No difference was observed in MTT between two treatment groups.

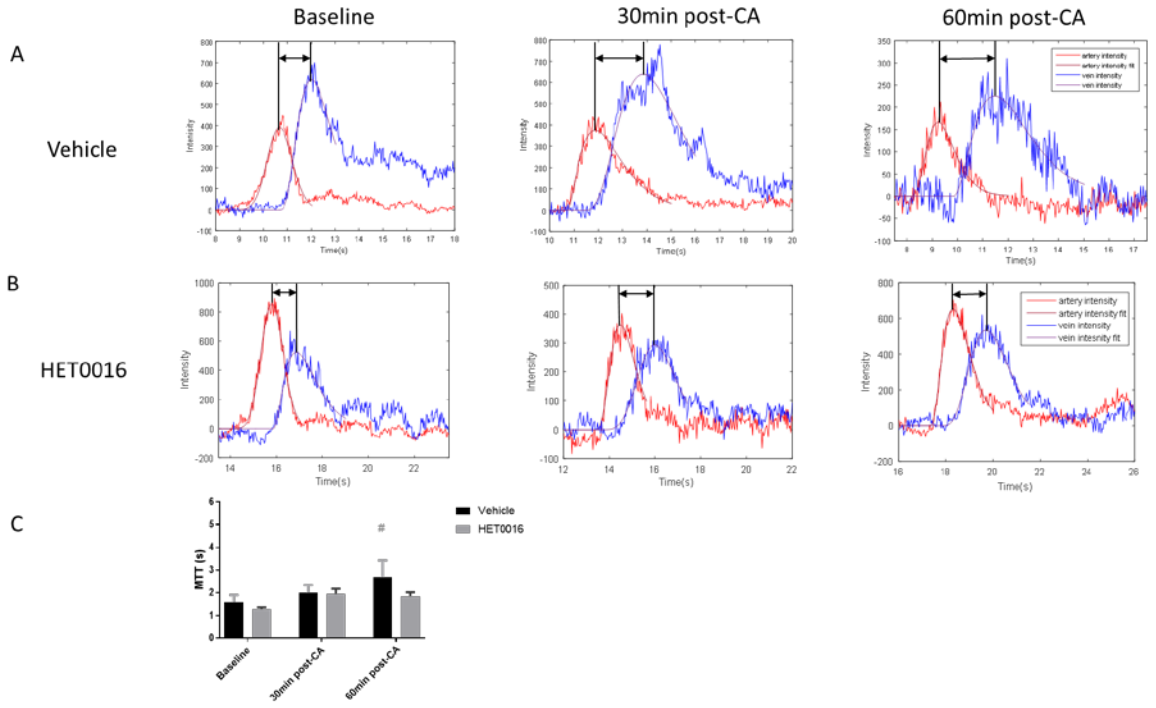

Figure 4.5 Mean transit time of plasma through the cortical microcirculation.

Representative intensity-time curves and γ fit curves at baseline, 30, 60 min post-CA (left to right) from HET0016 (A) and vehicle group (B). MTT increased post-CA, indicated by the black arrows. C. MTT increased post-CA at 60 min vs. baseline in the vehicle group (# $p<0.05$) (n= 6/group).

4.4 DISCUSSION

To our knowledge this is the first study assessing the direct vasodilatory effect of 20-HETE inhibition after CA. We have recently shown in our pediatric asphyxial CA model that 20-HETE levels are increased in the cortex at 5 min after resuscitation, and 20-HETE inhibition with HET0016 reduced the 20-HETE level in cortical homogenates [27]. Treatment with HET0016 improved cortical perfusion as assessed by Laser Speckle and improved neurological outcome and neurodegeneration in this model [27]. As 20-HETE has dual neuronal and vascular effects

[148, 155, 266, 268], our previous *in-vivo* studies did not allow to directly assess the direct vascular contribution of 20-HETE inhibition. In our current work we directly assessed the cortical microcirculation *in vivo* using multi-photon microscopy. Inhibition of 20-HETE formation had a trend towards early and transient pial arteriolar dilation, produced sustained dilation of the penetrating arterioles, reduced the transit time of plasma in the cortex, and had no effect on the capillary no-reflow. Our results suggest that inhibition of 20-HETE formation by HET0016 exerts its main vascular effects on the penetrating arterioles.

HET0016 treatment produced dilation of penetrating arterioles compared with baseline. Compared with vehicle, HET0016 transiently dilated pial arterioles immediately after ROSC, and had a trend towards dilation of penetrating arterioles. Cerebral microvascular flow is arranged such that an abundant lattice of surface pial microvessels gives raise to much fewer penetrating arterioles. Distinct cortical territories are supplied by a single penetrating arteriole, and thus penetrating arterioles can considerably limit the blood flow influx to large cortical area that extend up to 350 μm in radius [271]. Pial and penetrating arterioles contribute to a significant portion of the resistance, as regulation of the cortical microcirculation system is dependent on the regulation of arteriolar flow [272, 273]. The vasodilator effect observed at the level of penetrating arterioles is physiologically important as cortical perfusion is inversely related to the cerebral vascular resistance by the 4^{th} power of vessel diameter [272, 274]. According to Poiseuille's equation, an arterial constriction of 10% is expected to produce a CBF reduction of ~36%. In the current study, we observed ~20% arteriolar dilation at 5 min post-CA which could lead to dramatic change in flow as well as the perfusion pressure downstream.

We also observed the unchanged plasma MTT after HET0016 treatment in contrast to increased MTT post-CA in rats treated with vehicle. The improvement of cortical transit time of

plasma could be a downstream effect of arteriolar dilation and reduced flow resistance. MTT is directly proportional to cerebral blood volume (CBV) and inversely related to CBF. Since cerebral capillaries and venules serve as a reservoir for CBV, capillary and venular dilation in both HET0016 and vehicle groups indicates increased CBV for both groups. In the context of increased CBV, unchanged MTT suggests increased CBF, consistent with the effect of arteriolar dilation in the absence of an effect of HET016 on capillary flow.

Capillary no-reflow was not affected by the HET0016 treatment. As a downstream effect of arteriolar dilation post-CA in HET0016 treated rats, the perfusion pressure gradient may decrease, and therefore, RBCs stasis in the capillary bed may not be affected. Worth noting is that this is the first report of *in vivo* no-reflow phenomenon in a prolonged duration of CA. We have recently reported capillary no-reflow in a less severe albeit significant CA of 9 min and observed no-reflow in 60% of rats studied. Importantly, after 12 min CA no-reflow is observed in all rats. The observation of increased no-reflow with increased insult duration is similar to the original ex vivo description of the no-reflow phenomenon by Ames [171].

The vehicle used in the study is HPβCD, necessary to reconstitute HET0016. It is possible that the compound HPβCD has vasodilator properties via stimulation of NO release, which could reduce the net effect of HET0016 vasodilation observed here. A recent study reported that HPβCD induced angiogenesis in cultured endothelial cells, effect mediated by the endothelial nitric oxide synthase (eNOS)/NO pathway [275]. Furthermore, one important mechanism proposed of NO vasodilation is via inhibition of 20-HETE synthesis [148], which could also explain the absence of arteriolar constriction post-CA in the vehicle group and the apparent lack of observed difference between vehicle and HET0016 groups.

Our study underlines two important factors in optimizing perfusion to decrease secondary insults after cerebral ischemic events. First, in evaluating CBF-directed therapies, direct *in vivo* observation of microcirculatory flow is important to optimize perfusion. In this model, a vasodilator therapy produced arteriolar vasodilation, however did not affect the nutrient blood flow at the capillary level. Consequently, therapies that affect vasomotor tone ought the be combined with therapies promoting capillary flow for maximal cerebral perfusion benefit to decrease secondary insults. Combinations of vascular-targeted therapies have been proposed and some achieved long-term outcome improvement after CA. Studies by Safar, *et al.* applied flow promotion (norepinephrine), hypervolemic hemodilution and heparinization at resuscitation of CA. Mitigation of both no-reflow and delayed hypoperfusion were achieved post-CA [203, 276]. Nitroglycerin has also been proposed to use in addition to vasopressors to improve outcome [277]. Superoxide dismutase and deferoxamine were combined for better recovery of cerebral blood flow post-CA [26]. Synergic effect of hypothermia and 20-HETE were also evaluated in hypoxia-ischemia piglet model [278]. Utilizing therapies with complementary mechanisms, and optimizing the compound structures, dosage and intervals will be necessary to identify optimal therapeutic combination aimed at improving outcome after CA.

We also recognize that we did not assess cerebral metabolic rate (either glucose or oxygen utilization) after resuscitation in our model and specifically the impact of HET0016 on cerebral metabolism and/or brain tissue partial pressure of oxygen (PbO_2). In prior work, we have reported that PbO_2 is critically reduced in the cortex for several hours after resuscitation in this model,[279] and thus future studies assessing the impact of HET0016 on tissue hypoxia are warranted.

In conclusion, 20-HETE formation inhibition by HET0016 has arteriolar vasodilator effect *in vivo*, attenuates increased cortical transit time of plasma post-CA, and does not affect RBC stasis post-CA in a 12 min asphyxial CA model in developing rats. Therapies targeting the capillary no-reflow are needed in addition to arteriolar dilators to improve blood flow post-CA.

5.0 PRELIMINARY CLINICAL STUDY OF 20-HETE AND CO_2 REACTIVITY AS TWO BIOMARKERS IN ANEURYSMAL SUBARACHNOID HEMORRHAGE PATIENTS

5.1 INTRODUCTION

Subarachnoid Hemorrhage (SAH) is a devastating neurovascular disease which accounts for 5% of stroke with high fatality [280]. Delayed cerebral ischemia (DCI) is a major contributing factor of poor neurological outcome and morbidity [280]. Despite similar severities on presentation, patients develop a widely disparate range of outcomes in days after aneurysm repair. Current hypertensive therapy treatment is uniformly applied to patients to prevent vasospasm regardless of the assessment of their vascular reactivity. The validity of hypertensive therapy assumes that constricted vessels due to vasospasm can be re-opened under hypertension. However, if cerebral vessels in certain patients are not responsive to any stimuli, these patients would not benefit from hypertensive therapy. Instead, they could be subjected to unnecessary complications such as secondary hemorrhage or brain edema, which could further worsen the outcome. Previous clinical study suggests 20-hydroxyeicosatetraenoic acid (20-HETE), a potent vasoconstrictor for small vessels as a biomarker for aSAH patients [281]. In this chapter, we will further discuss the role of 20-HETE in aSAH patients as a biomarker and establish the association of 20-HETE and vascular reactivity in aSAH patients.

5.1.1 Epidemiology of SAH

SAH is a form of hemorrhagic stroke which affects 30,000 patients in the United States annually [282]. Aneurysmal SAH (aSAH) is the major type in 85% SAH patients and occurs at a fairly young age. Half of the patients are aged less than 55 at the time of the hemorrhage [283]. Given the advances in early repair of ruptured aneurysms and postoperative management, SAH remains to be a devastating disease due to high mortality rate (~50%) and low functional

independence in survivors (<60%) [282]. Current treatments include endovascular obliteration by platinum spirals and neurosurgical clipping, as well as prophylactic administration of nimodipine. Hypertension and hypervolemia are induced to prevent cerebral vasospasm uniformly in aSAH patients, while the efficacy is questioned by multiple complications such as cerebral hemorrhage, and cerebral edema [284]. Patients who survive the initial hemorrhage often suffer from permanent neurological, cognitive, or functional deficits. It is estimated that the cost to the society of SAH is greater than that of ischemic stroke [285].

5.1.2 Neurological Deterioration and Delayed Cerebral Ischemia (DCI)

More than 40% of SAH patients develop neurological deterioration in 3-14 days after aneurysm repair regardless of injury severity [280]. Neurological worsening which cannot be attributed to intracranial or systemic complications is attributed to DCI [280, 286]. DCI is attributed to poor outcome or even death in 30% SAH patients [286, 287], however, the diagnosis of DCI is poorly defined or even missing in clinical studies [280, 288].

The mechanism of neurological deterioration remains unclear but multiple factors are thought to be involved in the pathogenesis, including angiographic vasospasm, cortical spreading ischemia, micro thrombosis and microcirculation constriction [286]. Angiographic vasospasm, for example, is found in two-thirds of aSAH but only half of these patients developed DCI [289, 290]. Therapies targeted at large vessels such as endothelin receptor antagonists have shown benefits in vasospasm but not in DCI [291, 292]. Recent evidence suggests microvascular dysfunction and complex neuronal-glial interactions play an important role in the development of DCI and neurological deterioration [227, 291].

5.1.3 Cerebrovascular Reactivity in aSAH Patients

Cerebrovascular reactivity describes the change of CBF in response to a certain vasoactive stimulus. The utilization of CO_2 inhalation to map cerebrovascular reactivity has gained application in recent literature due to its potency in vasodilation, good safety profile and fast onset as well as cessation [293]. Intact cerebrovascular reactivity enables normal autoregulation therefore serves as the premise for multiple vasodilatory therapies. Impaired CO_2 reactivity has been documented in the literature for animal studies as well as aSAH patients [294-297]. However the utilization of CO_2 reactivity to predict patient outcome has not been fully validated. Hassler *et al*. demonstrated a weak hypercapnic response in vasospastic aSAH patients [298]. A study by Fierstra and colleagues reported lower reactivity in the early phase of 18 aSAH patients but did not predict vasospasm or functional outcome [297]. Currently, CO_2 reactivity is not routinely monitored as standard of care for aSAH patients. However, profiles of cerebrovascular reactivity could provide useful insights to identify vulnerable or responsive subpopulations and to tailor vasoactive therapies for aSAH patients.

5.1.4 20-HETE as a Biomarker in aSAH

20-HETE is a potent microvascular vasoconstrictor in renal, mesenteric, and cerebral vascular beds and plays an important role in determining cerebral vascular tone and autoregulation [299]. Previous pre-clinical and clinical studies have demonstrated that 20-HETE may contribute to DCI in aSAH [281, 300-302]. Donnelly *et al.* reported moderate to high level of CSF 20-HETE was associated with 3-fold higher mortality and worse outcome in aSAH patients [281]. Similar association was replicated by another group [300]. However, the utilization of CSF samples

limited the access to aSAH patients without CSF drainage and the generalizability of the conclusion in other neurovascular diseases. Therefore, the correlation of plasma and CSF 20-HETE concentrations is needed to increase the generalizability of current data.

5.1.5 Hypothesis and Objectives

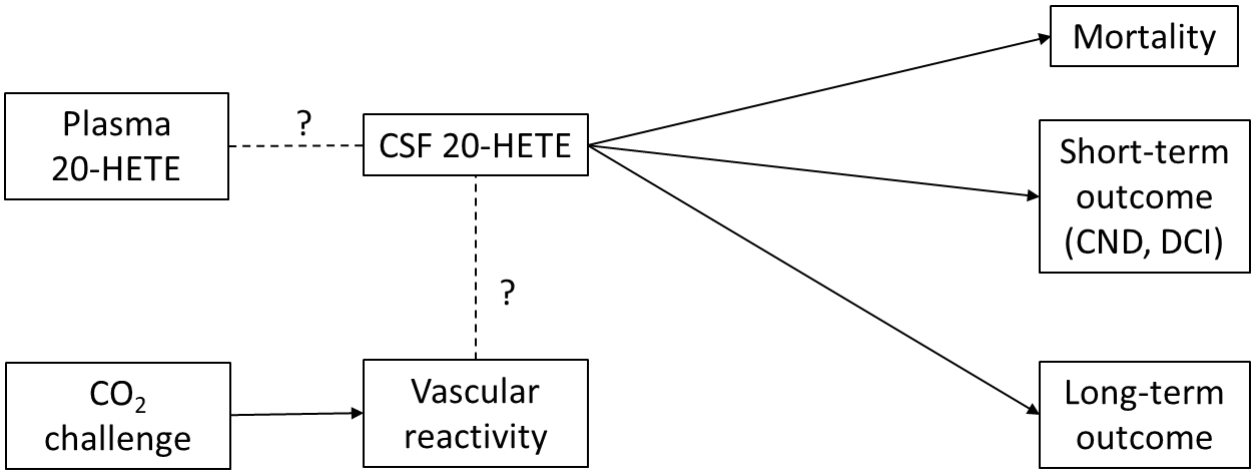

Figure 5.1 Schematic presentation of the hypothesis

The current gap in knowledge is to determine the role of 20-HETE in cerebral vascular reactivity and to determine if these indices can be used as a basis for individualized care to improve poor outcomes in aSAH patients. We hypothesize that plasma 20-HETE concentration is correlated with CSF therefore could potentially serve as a prognosis biomarker for aSAH patients. We also hypothesize that CO_2 reactivity serves as a prognosis biomarker for aSAH patients which could predict mortality, and short- and long-term outcome (Figure 5.1). To test these hypothesizes, first we need to establish the association between plasma and CSF 20-HETE

concentration in aSAH patients. Second, we need to assess CO_2 reactivity in SAH patients and establish the correlation between CSF 20-HETE level and CO_2 reactivity.

5.2 METHOD

5.2.1 Study Design and Sample Collection

5.2.1.1 Study to Assess Plasma and CSF 20-HETE Correlation

Plasma and CSF samples were previously obtained from aSAH patients who were recruited in the University of Pittsburgh Medical Center (UPMC) neurovascular intensive care unit between October 2000 and August 2010 [303]. The Institutional Review Board of the University of Pittsburgh approved the protocol and informed consent was obtained from the patient or their proxy prior to sample collection (IRB Protocol number: PRO 021039). Patients included in this study were adults aged 18–75 years, diagnosed with aSAH via cerebral angiogram or head computed tomography (CT). Criteria for enrollment also included Fisher grade >1 and CSF access (ventriculostomy or lumbar drain). The exclusion criteria are a history of debilitating neurological disease or SAH from trauma, mycotic aneurysm or arteriovenous malformation.

CSF and plasma were withdrawn by registered nurses directly from the CSF tubing and venous catheter each morning (8am+/−1 hour) and evening (7pm+/−1 hour) through 14 days after initial hemorrhage (contingent on CSF access). All specimens were frozen and stored at −80 degrees for batch analysis.

To establish the correlation of 20-HETE levels in the plasma and CSF, 35 aSAH patients were selected based on their CSF levels previously measured by Mark Donnelly [281] and

categorized into three groups: high (maximum CSF 20-HETE>1ng/mL, 11 subjects), medium (maximum CSF 20-HETE between 0.1-1 ng/mL, 12 subjects) and low (maximum CSF 20-HETE <0.1 ng/mL, 12 subjects).

5.2.1.2 A Pilot Feasibility Study to Assess CO_2 Reactivity Following SAH

This is a prospective, interventional clinical study in adult aSAH patients (IRB Protocol number: PRO16030073) at UPMC neurovascular intensive care unit. The Institutional Review Board of the University of Pittsburgh approved the protocol (Appendix III). The study design is depicted in Figure 5.2.

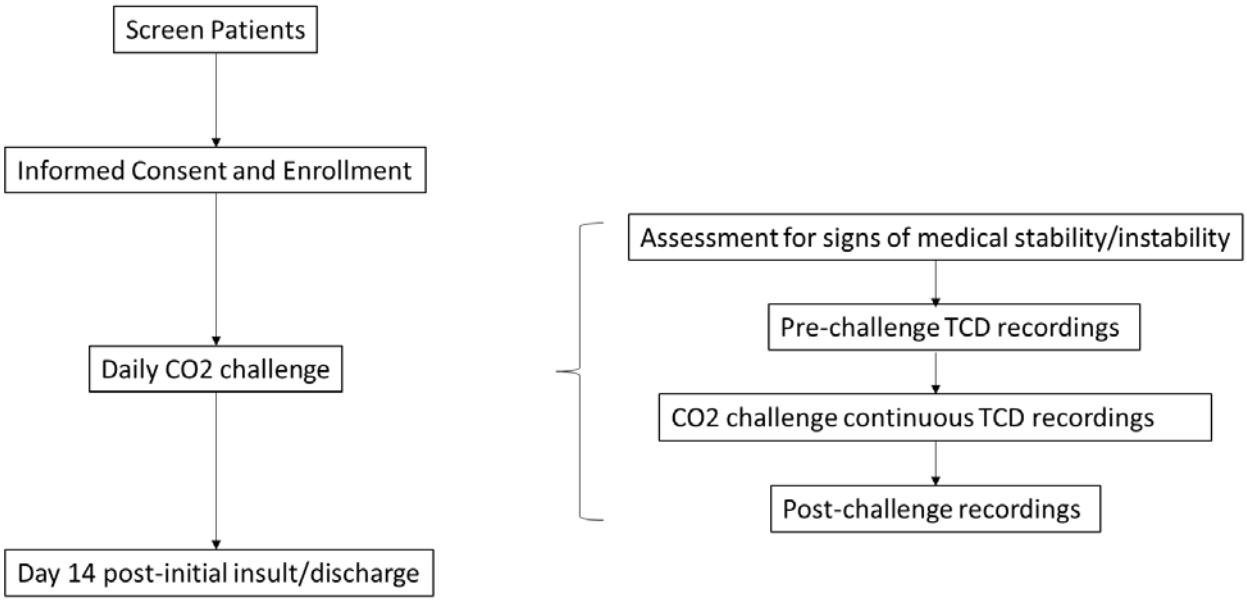

Figure 5.2 Study design for CO_2 reactivity in aSAH patients

Medical stability assessment is based on vital signs (heart rate, blood pressure, ICP, CPP, respiratory rate, SpO_2). If the patient had high intracranial pressures (ICP > 30) or respiratory distress - SaO2 < 92%, RR > 30, no challenge study would be attempted. Pre-challenge recordings included stable mean blood flow velocity (mBFV) of bilateral middle cerebral artery (MCA) and internal carotid artery (ICA) measured by transcranial Doppler (TCD) (Natus Neurology, Middleton, WI) and end-tidal CO_2 ($EtCO_2$). $EtCO_2$ level was continuously monitored by a capnograph connected to a face mask in non-intubated patients or the ventilator circuit in intubated patients. The CO_2 challenge was done by inhalation of 5% CO_2 (Matheson Tri-Gas, Inc. Montgomeryville, PA) until a 6 mm Hg absolute increase in $EtCO_2$ level was achieved. After this level was reached, the tubing was disconnected in in non-intubated patients or ventilator settings were reset to pre-testing values in intubated patients. CO_2 levels and TCD values continued to be measured until they reach pre-challenge levels.

Inclusion criteria: 1) Newly (within 5 days) SAH diagnosis verified via CT and cerebral angiogram and Fisher grade >2: Degree of hemorrhage that increases complication risk; 2) Over 21 years; able to read/ speak English; and 3) No history of previous neurological disorders; 4) Patients who have consented IRB 021039 for plasma and CSF collection.

Exclusion criteria: 1) Women who were pregnant; 2) Patients with unstable respiratory failure as indicated by FiO_2 need > 80%, SaO_2 < 92%; PEEP > 10. 3) Patients with unstable ICP as indicated by ICP > 30.

Prior to the CO_2 challenge in aSAH patients, 8 healthy volunteers (4 men and 4 women) participated and validate the CO_2 challenge under current settings. Oral consent was obtained from these volunteers. Five aSAH patients were recruited into current study and only 4 patients

had CSF collection. CO2 reactivity was calculated as percentage change of MCA velocity divided by absolute change in $EtCO_2$ [304].

5.2.2 Outcome Assessment

Hunt & Hess grade (HH), vasospasm and modified Rankin Scale score (mRS) at discharge and 3 months later were assessed in all 5 patients recruited as previously described [281]. Briefly, HH and mRS were assessed at discharge by experienced medical personnel. Cerebral vasospasm was evaluated by angiography and graded from 0 to 5 based on severity by neurology surgeons. The mRS score was also obtained after 3 months of discharge during a face-to-face interview or phone call with the patient or their surrogate.

5.2.3 Sample Analysis

CSF and plasma concentrations of 20-HETE were determined using a modified and validated assay previously described [305]. Both samples were processed using solid phase extraction. Briefly, CSF sample volumes of 2.0-3.0 mL (or plasma sample volumes of 0.5 mL) were loaded onto 3cc (or 1cc) Oasis HLB-SPE cartridges (Waters, Milford, MA, USA). Columns were washed and eluted with 3 mL (or 1 mL) of 5% methanol and 100% methanol, respectively. Samples were reconstituted in 50 μL or 125 μL of 80:20 methanol:water. Quantification of 20-HETE was performed by UPLC-MS/MS with minor modifications [305]. Concentrations of 20-HETE were determined from the standard curve of peak area ratio utilizing 20-HETE-*d6* as an internal standard. For measurements below the limit of quantification, value of half limit of quantification was assigned.

5.2.4 Data Analysis and Statistics

Descriptive statistics were used to summarize the measurements. Means and standard deviation were presented for the continuous variables. Correlation analysis was performed to evaluate the correlation of 20-HETE levels in CSF and plasma samples from aSAH patients in GraphPad Prism 7 (GraphPad Software, Inc. La Jolla, CA, USA). Pearson correlation coefficient was calculated to estimate the correlation. Hierarchical cluster analysis was performed to explore the subgroups within all the samples collected in SPSS (IBM Corp. IBM SPSS Statistics for Windows, Version 24.0. Armonk, NY: IBM Corp). Paired t-test was performed to assess the change of $EtCO_2$ and MCA velocity in healthy volunteers at baseline and during CO_2 challenge. For all the test, p-value<0.05 was considered statistically significant.

5.3 RESULTS

5.3.1 Temporal Alteration in CSF and Plasma 20-HETE Levels

To evaluate if the plasma 20-HETE levels reflect the temporal variation of CSF 20-HETE concentration, 20-HETE levels were plotted for individual patient from all groups (Figure 5.3). In almost all patients plotted, the pattern of plasma 20-HETE level did not show consistency with CSF 20-HETE fluctuations within patients. In high CSF 20-HETE group, most 20-HETE levels are higher than plasma levels. In low CSF 20-HETE group, 20-HETE levels in the plasma overshot the ones in the CSF. While in the medium CSF group, 20-HETE levels in the plasma

are either higher or lower than those in the CSF. The peak concentrations of 20-HETE concentration in the CSF was not followed by plasma levels.

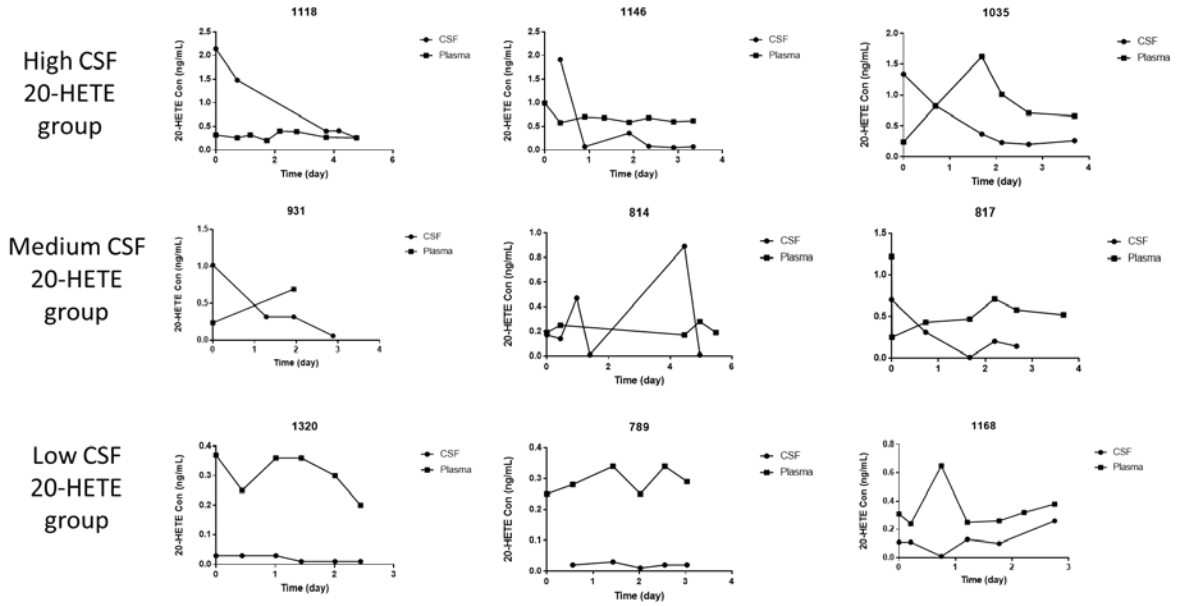

Figure 5.3 Temporal variation of CSF and plasma 20-HETE concentrations in individual aSAH patient

5.3.2 Correlation of 20-HETE Levels in CSF and Plasma

Since the number of samples pulled from each patient varies, we assessed the maximum 20-HETE CSF level and the corresponding plasma level as presented in figure 5.4. There is no correlation between plasma and maximum CSF 20-HETE concentrations in aSAH patients.

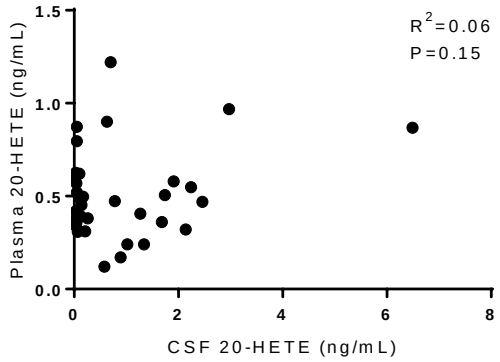

Figure 5.4 Maximum CSF level and corresponding plasma levels from 35 aSAH patients

A total of 123 plasma samples from 35 patients were pulled from the biobank freezer for analysis. As presented in figure 5.5, there was a trend toward correlation between plasma and CSF 20-HETE levels, however, it is not statistically significant. The correlation coefficient is 0.176 for all the samples.

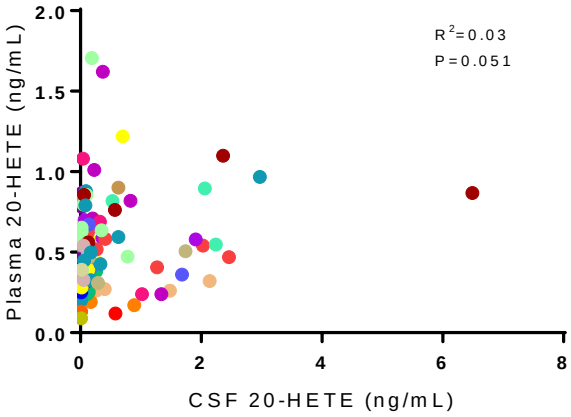

Figure 5.5 Plasma and CSF 20-HETE levels from 35 aSAH patients. Each color represents an individual patient

A trend of separation was noticed in figure 5.5, therefore cluster analysis was performed using Hierarchical cluster analysis and two subgroups were identified as depicted in figure 5.6.

Correlation between CSF and plasma 20-HETE concentrations was significant within each subgroup. Correlation coefficient also improved in both subgroups.

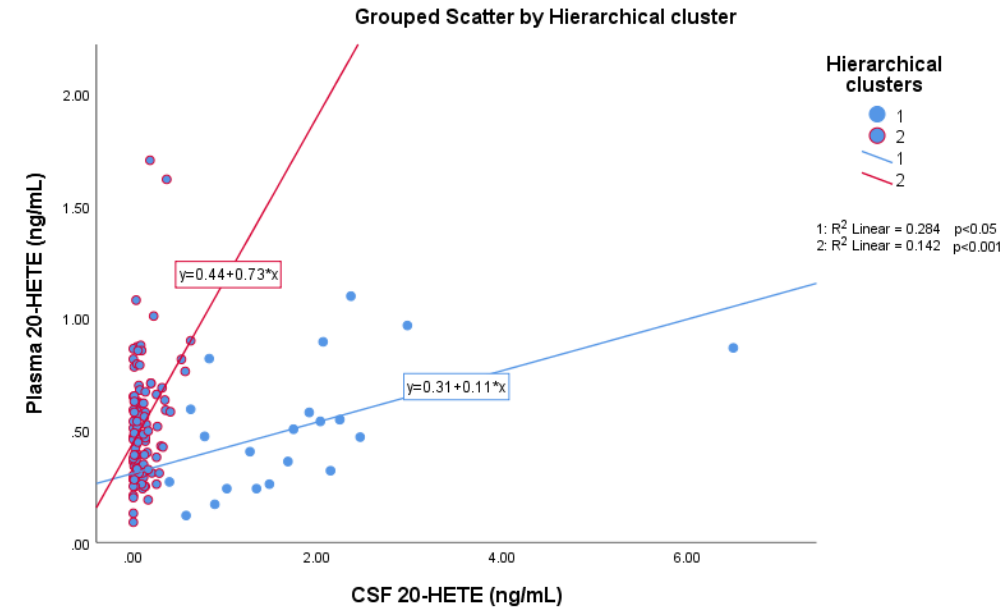

Figure 5.6 Samples groups by Hierarchical cluster number

5.3.3 CO_2 Reactivity in aSAH Patients

Prior to the measurement of CO_2 reactivity in aSAH patients, the CO_2 challenge was validated in 8 volunteers under current clinical settings. Each test was finished within 10 minutes and volunteers did not express any discomfort during the test. As expected, MCA velocity increased during the challenge compared to baseline, as $EtCO_2$ increased during the challenge (Data not shown).

A total of 5 aSAH patients were recruited in the study so far (Table 5.1). Inhalation of CO_2 resulted in increased $EtCO_2$. MCA velocity increased in left and right MCA velocity in most measurements. However, heterogeneous MCA velocity change was observed in aSAH

patients. The MCA velocity increased or decreased within the same patient at different days post injury. The left and right MCA velocity was not always associated on the same day for the same patients.

Table 5.1 Summary of MCA velocity change and 20-HETE levels in aSAH patients

Patient ID	days post injury	baseline $EtCO_2$	challenge CO_2	Left MCA change%	left CO_2 reactivity	Right MCA change%	right CO_s reactivity	20-HETE Con(ng/mL)
1962	3	23	29	24.69	4.12	35	5.83	0.01
1962	4	20	27	94	13.43	6.33	0.9	0.01
1962	5	29	35	-9.64	-1.61	38.81	6.47	0.01
1962	7	34	40	9.91	1.65	17.48	2.91	0.01
1981	6	24	32	6.52	0.82	3	0.38	0.03
1982	7	24	31	33.33	4.76	27.78	3.97	NA
1982	8	23	29	17.24	2.87	56.14	9.36	0.01
1982	9	23	30	6.9	0.99	10	1.43	0.01
1983	4	24	33	NA	NA	4.76	0.53	0.01
1985	5	23	29	20.63	3.44	21.88	3.65	0.01
1985	6	24	32	87.72	10.96	18.42	2.3	0.01

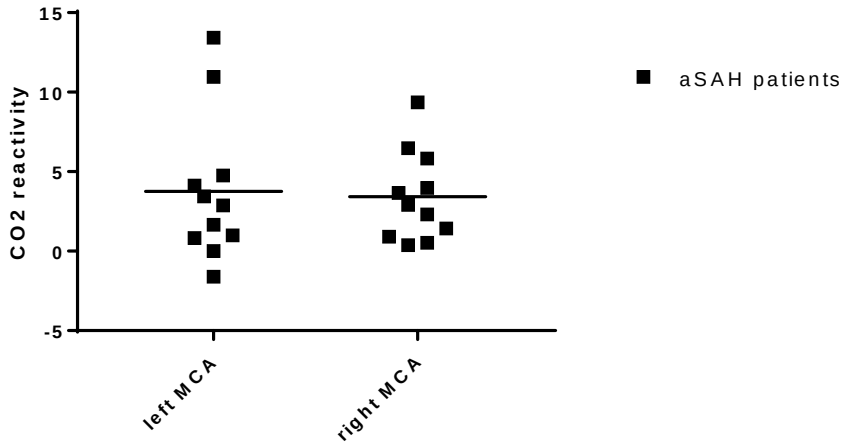

Figure 5.7 CO_2 reactivity for aSAH patients

CO_2 reactivity was calculated for aSAH patients (Figure 5.7) and aSAH patients displayed a wide range of CO_2 reactivity. Within the same patient (1962), CO_2 reactivity varied at different days post injury. The left and right CO_2 reactivity were not always correlated on the same day for the same patient.

5.3.4 CSF 20-HETE Levels in aSAH Patients

As depicted in Table 5.1, CSF was collected and analyzed in 4 aSAH patients. Most patients had very low 20-HETE levels in the CSF. Patient 1981 had a relative higher level of 20-HETE at the time of the CO_2 reactivity assessment.

5.3.5 Patient Outcome Assessment

Outcome assessment results were summarized in Table 5.2 for all patients recruited. Only patient 1985 had vasospasm during hospitalization and relatively worse outcome compared with other patients at discharge and after 3 months. Patient 1981 also had poor outcome at discharge despite of no vasospasm presented.

Table 5.2 Outcome assessment for aSAH patients

Patient ID	HH score	Vasospasm	mRS score at discharge	3 months mRS score
1962	3	0	4	2
1981	4	0	5	3
1982	2	0	1	0
1983	2	0	1	0
1985	5	3	5	4

5.4 DISCUSSION AND CONCLUSION

This is a pilot clinical study to explore the potential of utilizing CO_2 reactivity and 20-HETE levels as two biomarkers in aSAH patients. In the retrospective study, poor correlation was found between plasma and CSF 20-HETE levels either within the same patient or in all aSAH

patients. The correlation improved in subgroups after cluster analysis, suggesting different mechanisms of 20-HETE production and accumulation in certain portion of the patients. In the prospective interventional study, we validated the CO_2 reactivity measurement under current clinical setting in both healthy volunteers and aSAH patients with well-tolerated safety profile. aSAH patients displayed a widely disparate range of CO_2 reactivity with temporal variations and no signs of symmetry. A larger sample size of aSAH patients is needed to establish the association between 20-HETE levels and CO_2 reactivity.

As a potent vasoconstrictor, 20-HETE is produced by cytochrome P450 4A and 4F subfamilies localized in vascular smooth muscle cells, endothelial cells, neurons and astrocytes in the brain [150, 155, 299, 306]. The expression of CYP 4A has been found higher in small arterioles and an inversely proportional correlation was found in 20-HETE production and vessel diameter [307, 308]. 20-HETE as a fatty acid should be freely diffusible across membranes and blood-brain-barrier, and plasma 20-HETE has been associated with neurological deterioration acute minor ischemic stroke [309]. In current aSAH population, the correlation of plasma 20-HETE and CSF 20-HETE levels is weak for all samples but improved in subgroup analysis. This might suggest a burst local production of 20-HETE in the brain override the plasma levels in some patients at certain time points and contribute to the pathogenesis of worse outcome. In other patients whose plasma 20-HETE levels are comparable or higher than CSF levels, local production of 20-HETE is not predominant. Precautions should be taken when interpreting systemic levels for paracrine biomarkers. An important limitation in current study is the possible selection bias when picking samples from high, medium and low CSF 20-HETE groups. This could limit the generalizability of the conclusion to a different population. To further elucidate the pathogenesis of 20-HETE production, pre-clinical models and clinical studies with large

sample size should be conducted. It is possible that plasma 20-HETE could still serve as a biomarker independently from CSF levels. To further explore the potential of plasma 20-HETE as a biomarker for aSAH patients, multiple covariates such as injury severity (Fisher score), gender, age, vasospasm, etc. could be incorporated to test whether plasma 20-HETE is a significant predictor of patient outcome or mortality.

The CO_2 reactivity in aSAH patients displayed a wide range of variation compared with healthy volunteers. Such temporal and regional heterogeneity delineates the impaired cerebrovascular reactivity in current patient population. Similar findings are observed in the literature [296, 297]. Due to limited sample size, no correlation could be attempt between 20-HETE levels and CO_2 reactivity or patient outcome. The heterogeneous profile observed in these 5 patients complicates the categorization of patients since "non-intact" reactivity is insufficient to describe patient CO_2 reactivity. The same patient may exert impaired reactivity in only a day or two with one hemisphere but normal reactivity in other days. However, hypertensive therapy given when cerebrovascular reactivity is poor could do harm than good to the patient. This is because hypertensive therapy assumes that constricted vessels could be dilated or re-opened if perfusion pressure is increased. However, in patients with non-intact cerebrovascular reactivity, cerebral vessels would not respond to increased pressure. These patients would not benefit from hypertensive therapy; instead, they would unnecessarily suffer from complication due to hypertensive therapy. Also it is necessary to establish an algorithm to describe the extent of impaired reactivity in aSAH patients and tailor treatment based on the extent. Previous publication used normalized autoregulatory response (NAR) as an index to describe patient cerebrovascular reactivity, however, the definition of NAR is variable across studies and no threshold was consistently accepted to distinguish impaired NAR versus normal

values [296, 310-312]. It is also difficult to use NAR as an appropriate index since duration is not included in the calculation. A more comprehensive measurement should be established to better capture the dynamic change of cerebrovascular reactivity. Continuous or periodic monitoring of CO_2 reactivity is necessary to characterize the profile with more aSAH patients. Once the dynamic profile of CO_2 reactivity is characterized, other clinical covariates, such as gender, age, injury severity, days post injury, brain edema scores could be incorporated to systemically assess whether CO_2 reactivity is a significant predictor of aSAH patient outcome and/or mortality.

In conclusion, we conducted a pilot clinical study to explore the potential of 20-HETE plasma concentration and CO_2 reactivity as two biomarkers for aSAH patients. Both biomarkers are potentially useful in providing insights to understanding the pathogenesis of neurological deterioration in aSAH patients. Further studies with large sample size are required to establish the association between each biomarker with patient outcome.

6.0 CONCLUSIONS AND FUTURE DIRECTIONS

6.1 SUMMARY

The aim of this dissertation is to explore and describe the role of cerebral microvascular alterations in both clinically relevant animal model and clinical patients who are subjected to neurovascular diseases, including CA and SAH. Three approaches were adopted to fulfill this aim. In Chapter 2, an extensive systematic review was conducted to summarize the current understanding of pharmacological therapies used for CA and global ischemia, with emphasis on cerebral microcirculation. In Chapter 3 and 4, an *in-vivo* multiphoton microscopy platform was established for a pediatric CA model to better evaluate the pathophysiology and pharmacology for cerebral microcirculation in CA. Lastly in Chapter 5, the role of a vessel constrictive fatty acid, 20-HETE was explored for its potential as a biomarker in the plasma from aSAH patients, together with cerebrovascular reactivity.

6.1.1 Systematic Review on Pharmacological Therapies after CA

In this review, we summarized the current understanding of pharmacological therapies with their effect on CBF after CA and global ischemia. Five categories of therapies were identified based on mechanism of reaction: flow promotion, vessel dilatory, thrombolytic, hemodynamic, and antioxidant therapies. Each category targets on different determinants of CBF. For example, flow promotion therapies mostly increase perfusion pressure at resuscitation therefore improve CBF while vessel dilatory therapies are expected to decrease vascular resistance and improve CBF.

Early studies focused on cerebral macrovasulcar alterations, probably due to limited CBF measurement methods. Recent advances in methodology such as MRI enable more detailed temporal, regional and dimensional characterizations of CBF, emphasizing cerebral microcirculation as an important target. At the same time, questions rise to the traditional therapies, such as epinephrine and heparin, regarding to their effects on cerebral microcirculation. Epinephrine, for example, has been used as a standard of care for CA resuscitation over 40 years. Recently, detrimental effect of epinephrine was reported to decrease microcirculatory perfusion in CA model [46]. Different temporal and dimensional CBF profile post-CA in addition to the pharmacology profile of each therapy, suggests that sequential or combination therapies might be beneficial.

After a thorough review of the literature, we identified three knowledge gaps. First, the understanding of temporal and regional alterations of cerebral microcirculation post-CA is lacking, especially for different types of small vessels such as small arterioles and capillaries. This is very important because the alterations in different types of vessels suggest potential therapeutic targets therefore direct to specific treatments. Second, a systemic evaluation of different therapies on cerebral microcirculation after CA is missing *in-vivo*. Given the dynamic variation of CBF post-CA, the understanding of mechanism for each category of therapy is critical to optimize the therapeutic effect on cerebral microcirculation. Last but not least, the translation of therapeutic effect on cerebral microcirculation from pre-clinical models to clinical studies is warranted. Multiple pharmacological agents such as Ca^{2+} channel blockers failed in clinical trials which suggests that the interpretation and application of animal studies should be cautious. Deeper understanding of cerebral microcirculation, in both pre-clinical and clinical studies, will bridge the translation of various treatment effect.

6.1.2 Pre-clinical Approach to Evaluate Cerebral Microcirculation *in-vivo*

In Chapter 3, we established a platform to characterize cerebral microcirculation alterations post-CA *in-vivo* using multi-photon microscopy. To better capture the disturbances, static measurements (vessel diameter) and dynamic measurements (RBC and plasma flow) were collected in pediatric rats subjected to 9 min asphxial CA. Two major targets were identified in this model: small arterial constriction and RBC stasis in the capillaries- "no-reflow phenomenon". The finding provides rationales for microvessel dilatory as well as hemodynamic agents and paves the way for the evaluation of these therapies.

In Chapter 4, assessment of a vessel dilator HET0016 was performed in the same model and dilatory effect on small arterioles was confirmed *in-vivo*. HET0016 had no effect on RBC stasis but provided benefit in plasma transit time, indicating dual mechanisms for the two targets identified previously. The results also support the potential of combined treatments to synergize their effects and improve cerebral microcirculation post-CA.

We recognized that we did not assess microcirculatory metabolism in these two chapters. This is a major limitation we hope to address in the future studies. It is possible that flow "shunting" is taking place after the resuscitation which could be indicated by shortened MTT. In this case the apparently attenuated MTT could confound the interpretation of the result. On the other hand, even if the microcirculatory flow is restored, it is still possible that vascular units are severely damaged from the injury and no efficient oxygen exchanges are allowed. Therefore it is ultimately important to monitor brain tissue oxygenation when we are assessing microcirculatory flow alterations.

6.1.3 Clinical Approach to Explore Vasoactive 20-HETE as a Biomarker in aSAH Patients

In Chapter 5, we aimed to explore the potential roles of plasma 20-HETE and cerebrovascular reactivity as two biomarkers for aSAH patients. Previously CSF 20-HETE has been associated with higher mortality rate and worse outcome in aSAH patients. It is straightforward to assess the correlation between plasma and CSF 20-HETE given the easier access and better generalizability of the results. However, we did not find a correlation between plasma and CSF 20-HETE. In subgroup analysis, correlation greatly improved, indicating the involvement of local 20-HETE production in the brain and may serve as a new mechanism to predict patient outcome. To reveal the underlying mechanism, pre-clinical models are required to test the hypothesis.

In the interventional, prospective clinical study where we aim to establish the association of cerebrovascular reactivity and CSF 20-HETE concentration, we observed different CO_2 reactivity profile in aSAH patients. We test the clinical feasibility of CO_2 reactivity in these patients. To depict the profile of cerebrovascular reactivity, more aSAH patients are needed. To validate the profile, modeling simulation would be informative to simulate patient population and establish the association.

6.2 FUTURE DIRECTION

6.2.1 Pre-clinical Inferences

Multiphoton microscopy serves as an ideal platform to unmask the physiological or pathophysiological change in real-time and at the cell level. In our pediatric CA model where we observed the "no-reflow phenomenon", the underlying mechanism remains to be illustrated. One possible hypothesis is platelet aggregation and neutrophil infiltration, which can be tested under current experimental setting. By labeling platelet and neutrophils with corresponding antibody, their role in "no-reflow phenomenon" could be described. It is worth noting that appropriate control is necessary to distinguish the artificial labeling effect from the actual pathophysiological process.

This tool of multiphoton imaging can also provide evidence for therapeutic mechanism because of its high sensitivity and resolution. The tracking of small molecular drugs *in-vivo* might be limited, because tagging the fluorophore would very likely change the pharmacokinetic and pharmacodynamic behavior of the original compound. However, utilization of this tool to reveal the mechanism of big molecules, such as antibodies, long-chain fatty acids and polymers is rather promising. For example, drag-reducing polymer (DRP), a long-chain rheological agent with molecular weight over 100kDa, could be evaluated using multiphoton microscopy. Previously it has been reported that DRP can improve microcirculatory blood flow and oxygenation in a rat model of TBI [313]. The benefit of DRP in our pediatric CA model has also been evaluated in the preliminary study. However, the mechanism of DRP, especially the location where the drag-reducing effect takes place, has not been characterized *in-vivo*. By tagging a fluorophore at the end of each DRP and injecting intravenously, evidence of this

polymer could be provided to illuminate its mechanism of reaction. Another potential use of this tool is immunotherapy (eg. Bevacizumab) in CNS tumors, where traditional pharmacokinetic and pharmacodynamic models are not good enough. Multiphoton imaging could detail the spatial and temporal information of antibody on the tumor site, which enables better application of the therapy.

Besides the microcirculatory flow, the characterization of metabolism in microcirculation is also very important. Earlier studies suggest a mismatch between flow and metabolism post-CA [314]. This means that an apparent increase in flow might be a waste and certain brain region might still suffer hypoxia. To address this issue, flow shunting vessels could be quantified post-CA and studied with different therapies. Nemoto, et al. demonstrated the feasibility of quantifying shunted microvessel when ICP increased [315]. The autofluorescence of NADH/NADPH has also been suggested as a metabolism marker [315]. At wavelength around 700-750 nm, NADPH can be excited. By quantifying autofluorescence pre- and post-CA can provide useful information about neuronal activity and metabolism post-CA.

Limitations of multiphoton microscopy do exist. Besides the expensive cost of the instrument and theoretical limitations such as high phototoxicity and certain imaging depth, one limitation is the high inter-individual variability. To prepare an animal for multiphoton imaging is delicate and time-consuming. The imaging locations are limited by the prepared window. The observations could be affected by the specific location and sampling strategy. Repeated observations and subjects are essential to overcome the inter-individual variability with appropriate statistical methods. Another limitation is the relative descriptive and qualitative evidence compared with quantitative methodology. The spatial resolution in current experiment setting is 1 μm while the diameter of small capillary is 3~5 μm. The quantification of these

capillaries should be cautiously and consistently done with appropriate blindness. Therefore, multiphoton imaging is more descriptive method to reveal the mechanism in a process, rather than a quantitative method to distinguish different effects.

6.2.2 Clinical Inferences

Although multiphoton microscopy could not be used in clinical studies at this moment, our results from chapter 3 and 4 proposed novel therapeutic targets with underlying mechanism which has translational significance. We utilized a clinically relevant rat model in our assessment and the physiology changes are well-documented and close to patients as much as possible. The resuscitation protocol used in this study is also adjusted to follow clinical practice. The two targets we identified in animal model could apply to patients and provide supportive evidence to microvessel dilators and hemodynamic agents. More importantly, we observed the arteriolar dilatory effect of HET0016 *in-vivo* post-CA. This further supports the rationale of developing microvessel dilators, especially targeted on 20-HETE pathways for clinical use.

Besides new compound development, another clinical strategy to assess 20-HETE as a biomarker in neurovascular diseases. Based on sample availability, we applied this strategy in aSAH patients. Despite the lack of correlation between plasma and CSF 20-HETE levels in all samples collected, the improved correlation identified in subgroup analysis suggested a burst 20-HETE local production in certain aSAH patients. In this situation, sampling plasma 20-HETE cannot represent the true level in the brain and mislead the interpretation. Cautions are also warranted for other paraendocrine molecules. If there is a burst production of 20-HETE and contributes to worse outcome, genetic or epigenetic factors could be used to identify these

patients. It also provides information for future development of treatment targeted on 20-HETE pathway: quick distribution, great brain penetration and prophylactic dosing strategy.

We observed a spread range of cerebrovascular reactivity in only 5 aSAH patients in the prospective clinical study. Although no pattern could be identified, we saw temporal and asymmetric variations even within the same patient. This is very informative since previously proposed parameters such as Normalized Autoregulatory Response or Vasomotor Reactivity is not able to describe patient profile. Without an appropriate measurement of vascular reactivity, no plausible prediction or correlation could be established between reactivity and patient outcome. Therefore, there is an urgent need to establish a new measurement to fully capture patient cerebrovascular reactivity profile, taking duration of lack of reactivity, either/both sides lack of reactivity, the extent of lack reactivity and super reactivity into account. This is a necessary step to validate cerebrovascular reactivity as a clinical biomarker to tailor treatment or predict patient outcome.

To conclude, the cerebral microcirculation serves as a key player in neurovascular diseases such as CA and SAH. Alterations identified in cerebral microcirculation using multiphoton microcopy indicates new therapeutic targets and can be further explored using pre-clinical and clinical approaches. Biomarkers in cerebral microcirculation provides new insights in identifying vulnerable patient population and personalize treatment.

A.1 APPENDIX I

Comprehensive literature search strategy generated for systemic review. This strategy generated 1063 items in PubMed.

((("Heart Arrest"[Mesh] OR Asystole[tw] OR “cardiac arrest”[tw] OR Cardiopulmonary arrest*[tw] OR Cardiovascular arrest*[tw] OR “circulatory arrest”[tw] OR “heart arrest”[tw] OR “Postcardiac arrest”[tw] OR “Post-cardiac arrest”[tw] OR postresuscitation[tw] OR ROSC[tw] OR "four-vessel occlusion"[tw] OR "4-vessel occlusion"[tw] OR “neck tourniquet”[tw])) AND ((("Brain/blood supply"[Mesh] OR "Brain/metabolism"[Mesh] OR "Cerebrovascular Circulation"[Mesh] OR "Cerebral Cortex/blood supply"[Mesh] OR "Cerebral Cortex/metabolism"[Mesh] OR "Hypoxia, Brain"[Mesh] OR "Neurons/blood supply"[Mesh] OR "brain oxygen"[tw] OR "brain oxygenation"[tw] OR "Cardiocerebral resuscitation" [tw] OR "cerebral blood flow" [tw] OR "cerebral microcirculatory perfusion" [tw] OR "cerebral oxygen" [tw] OR "cerebral oxygenation" [tw] OR "cerebral oximeter" [tw] OR "Cerebral oximetry"[tw] OR "cerebral perfusion" [tw] OR "cerebral protection" [tw] OR "Cerebral resuscitation"[tw] OR "Cerebral saturation" [tw] OR "Cerebrovascular circulation"[tw] OR Ischemic Encephalopath*[tw] OR "J Cereb Blood Flow Metab"[jour])) OR ("Regional Blood Flow"[Mesh] AND ("brain"[MeSH Terms] OR "brain"[All Fields])))) AND ("Acetylcysteine"[Mesh] OR "Acid-Base Equilibrium"[Mesh] OR "Acidosis/drug therapy"[Mesh] OR "Adenosine"[Mesh] OR "Amiloride"[Mesh] OR "Angiotensin II"[Mesh] OR "Antioxidants"[Mesh] OR "Antithrombins"[Mesh] OR "Argon"[Mesh] OR "Blood Substitutes"[Mesh] OR "Blood Viscosity"[Mesh] OR "Blood Volume"[Mesh] OR

"Buffers"[Mesh] OR "Carbonates"[Mesh:NoExp] OR "Deferoxamine"[Mesh] OR "Diltiazem"[Mesh] OR "Dopamine"[Mesh] OR "Endothelins"[Mesh] OR "Epinephrine"[Mesh] OR "Fibrinolytic Agents" [Pharmacological Action] OR "Fibrinolytic Agents"[Mesh] OR "Flunarizine"[Mesh] OR "Hematocrit"[Mesh] OR "Hemodilution"[Mesh] OR "Heparin"[Mesh] OR "Hydrogen/therapeutic use"[Mesh] OR "Hydrogen-Ion Concentration"[Mesh] OR "Hydroxyeicosatetraenoic Acids/antagonists and inhibitors"[Mesh] OR "Hyperbaric Oxygenation"[Mesh] OR "Hypertonic Solutions/administration and dosage"[Mesh] OR "Hypertonic Solutions/therapeutic use"[Mesh] OR "Methoxamine"[Mesh] OR "N-acetylcysteine lysinate" [Supplementary Concept] OR "Neuroprotective Agents"[Mesh] OR “Neuroprotective Agents" [Pharmacological Action] OR "Nitrates"[MeSH Terms] OR "Nitrites"[MeSH Terms] OR "Nitric Oxide"[Mesh] OR "Nitroglycerin"[Mesh] OR "Nitroprusside"[Mesh] OR "Norepinephrine"[Mesh] OR "Pentoxifylline"[Mesh] OR "Plasma Substitutes"[Mesh] OR "Phenylephrine"[Mesh] OR "Phenytoin"[Mesh] OR "Plasminogen Activators"[Mesh] OR "Poly(ADP-ribose) Polymerases/deficiency"[Mesh] OR "Poly(ADP-ribose) Polymerases/metabolism"[Mesh] OR "Pyruvates"[Mesh] OR "Saline Solution, Hypertonic"[Mesh] OR "simendan" [Supplementary Concept] OR "Sodium Bicarbonate"[Mesh] OR "Streptokinase"[Mesh] OR "Superoxide Dismutase"[Mesh] OR "Sympathomimetics"[Mesh] OR "tempol" [Supplementary Concept] OR "Thiopental"[Mesh] OR "Thrombolytic Therapy"[Mesh] OR "tirilazad" [Supplementary Concept] OR "Urokinase-Type Plasminogen Activator"[Mesh] OR "Vasodilator Agents"[Mesh] OR "Vasopressins"[Mesh] OR "Xenon"[Mesh] OR Adrenaline[tw] OR “alkaline buffer”[tw] OR Anistreplase[tw] OR Antioxida*[tw] OR Buffer[ti] OR Cardizem[tw] OR Epinephrine[tw] OR Freedox[tw] OR HET0016[tw] OR “20-HETE”[tw] OR Levophed[tw] OR Levosimendan[tw] OR “Methyl

isobutyl amiloride”[tw] OR “N-Acetylcysteine”[tw] OR Neo Synephrine[tw] OR Neuroprotection[tw] OR neuroprotective[tw] OR Nitroglycerin[tw] OR Nitropress[tw] OR Nitrostat[tw] OR Noradrenaline[tw] OR “PARP-2 deletion”[tw] OR “Sodium Nitroprusside”[tw] OR Streptodornase[tw] OR Streptokinase[tw] OR “Tissue Plasminogen Activator”[tw] OR “Urokinase-Type Plasminogen Activator”[tw] OR Vasopressin[tw] OR Vasopressor*[tw]) AND English[lang].

A.2 APPENDIX II

Summary of Therapy Categories with Mechanism of Action and Effect on CBF

Therapy categories	Agents	Mechanism of action	Species	Methodology	CA type	Effect on CBF post-CA	References
Flow promotion therapies	Epinephrine	α-1, α-2, β1, β2agonist	pig, dog, cat	microspheres, MRI, laser Doppler flowmetry, calculated, orthogonal polarization spectral imaging	VF, asphyixal, hemorrhagic, calculated	increase CBF, decreased microcirculatory blood flow	[39-48, 64, 66, 101, 219, 221, 223, 316-322]
	Norepinephrine	α-1, α-2, β1agonist	pig	microspheres	VF	increase CBF	[48, 221, 323]
	Phenylephrine	α-1 agonist	pig	microspheres	VF	increase CBF	[40, 316]
	Methoxamine	α-1 agonist	dog	microspheres	VF	increase CBF	[42]
	Dexmedetomidine	α-2 agonist	dog	microscopy	VF	no effect on microcirculation	[50]

	Dopamine	DA1 and DA2 receptors	pig	calculated	VF	increase CPP	[51]
	Vasopressin	V1 receptor mediated peripheral vasoconstriction	pig	microspheres, laser-Doppler flowmetry, orthogonal polarization spectral imaging	VF, asphyxial, hemorrhagic	increase CBF, improved microcirculatory blood flow	[46, 64, 66, 101, 219-221, 223, 318, 324, 325]
	Endothelin-1	increase calcium concentration in smooth muscle cells	pig	microspheres	VF	increase CBF	[72, 73, 326]
	Phosphoramidon	inhibits endothelin converting enzyme	pig	microspheres	cardiopulmonary bypass	no effect on CBF	[185]
	Angiotensin II	AT1 receptors mediated vasoconstriction	pig	microspheres	VF	increase CBF	[82]
Vasodilatory therapies	Nitric Oxide	vasodilation through increasing cGMP	mouse	MRI	KCl	no effect on CBF	[92]
	L-arginine	NOS substrate	pig, rat	microspheres, laser-Doppler	cardiopulmonar	increase CBF	[94, 327]

				flowmetry, two-photon microscopy	y bypass, asphyxial		
	Sodium nitroprusside	NO donor	pig, rat	laser Doppler flowmetry, two-photon microscopy	asphyxial	increase CBF	[95]
	Nitroglycerin	vasodilation mediated by releasing NO, usually combined with epinephrine or vasopressin	pig	microspheres	VF	combined with epi or vasopressin increase CBF	[101]
	N(G)-nitro-L-arginine methyl ester hydrochloride(L-NAME)	non-selective NOS inhibitor	pig	laser Doppler flowmetry	cardiopulmonary bypass	decrease CBF	[93, 107]
	Methylene blue	reduced nitrite/nitrate content	pig	laser Doppler flowmetry	VF	increase CBF	[110]
	7-nitroindazole(7-NI)	nNOS inhibitor	rat	laser Doppler flowmetry	4-vessel occlusion	no effect on CBF	[113, 114]

	L-N(5)-(1-iminoethyl)ornithine (L-NIO)	eNOS inhibitor	pig	laser Doppler flowmetry	4-vessel occlusion	no effect on CBF	[114]
	Adenosine	modulate adenylate cyclase activity	rat	calculated	KCl	increase CBF	[118]
	Nimodipine	Calcium-channel blockers	pig	microsphere	VF	increase CBF	[126]
	Diltiazem	Calcium-channel blockers	pig	microsphere	asphyixal	increase CBF	[128]
	Flunarizine	Calcium antagonist	dog	thermal method	VF	increase CBF	[129, 130]
	Levosimendan	Calcium sensitizer	rat	laser Doppler flowmetry	asphyxial	increase CBF	[132]
	MK-801	NMDA receptor antagonist	pig	microsphere	cardiopulmonary bypass	depressed CBF	[144]
	NBQX	AMPA receptor blockade	pig	microsphere	cardiopulmonary bypass	depressed CBF	[144]
	Indomethacin	nonselective COX inhibitor	pig	microspheres	VF	attenuate hyperperfusion	[157]
	Celecoxib	COX-2 inhibitor	pig	microspheres	VF	attenuate hyperperfusion	[157]
	HET0016	CYP4A/4F	rat	laser Doppler flowmetry	asphyxial	increase CBF	[27]

		inhibitor					
	Bupivacaine	Sodium channel blocker	rat	laser Doppler flowmetry	4-vessel occlusion	attenuate early hyperperfusion and hypoperfusion	[161]
	Thiopental	activate GABA channel	monkey	133Xe activity	neck tourniquet	increase CBF	[28]
	Desflurane	activate GABA channel	pig	laser Doppler flowmetry	low-flow cardiopulmonary bypass	no effect on CBF	[168]
	Methyl isobutyl amiloride	inhibition of the Na+/H+ antiporter	rat	radio tracer	KCl	decrease CBF	[170]
Thrombolytic therapies	Heparin	activate antithrombin III	cat, baboon	Xenon-133, fluorescence microscopy	cardiopulmonary bypass, VF	increase CBF	[328]
	Enoxaparin	activate antithrombin	rat	laser Doppler flowmetry	four-vessel occlusion	increase CBF	[189]
	Antithrombin	inhibit coagulation factors	pig	laser Doppler flowmetry	VF	no effect on cortical CBF	[182]
	Recombinant human activated protein	anticoagulant and anti-inflammatory	rat	laser-Doppler flowmetry	bilateral clip occlusion of the common carotid	no effect on CBF	[183]

					arteries		
	Aspirin	Thromboxane A2	rat	laser Doppler flowmetry	four-vessel occlusion	increase CBF	[181]
	Vapiprost	Thromboxane A2-receptor antagonist	pig	microspheres	cardiopulmonary bypass	increase CBF	[185]
	Pentoxifylline	antagonist of adenosine 2 receptor and increase	cat	photoelectric method	VF	increase CBF	[187]
	Urokinase	activator of plasminogen	rabbit	Dual-slice spiral CT	asphyxial, KCl	increase CBF	[189]
	Recombinant tissue type plasminogen activator (rt-PA)	activate plasminogen	cat	fluorescence microscopy	VF	increase CBF	[180]
	Aprotinin	antifibrinolytic by inhibition of serine proteases	pig	microspheres, electromagnetic flowmeter	cardiopulmonary bypass	increase CBF	[192]
	Streptokinase	activate plasminogen	dog, pig		VF	increase CBF	[190, 191, 329]

Antioxidant and antiinflammation therapies	N-acetyl-l-cysteine (NAC)	free radical scavenger	pig	transit-time ultrasonic probe	neonatal hypoxia-reoxygenation	increased carotid flow	[214]
	Alpha-phenyl-tert-butyl nitrone (PBN)	free radical spin trap	pig		cardiopulmonary bypass	increase CBF	[215]
	U74006F	lipid peroxidation inhibitor	dog	xenon CT	VF	no effect on CBF	[330]
	Deferoxamine	lipid peroxidation inhibitor	rat	MRI	asphyxial	increase CBF	[26, 216, 225]
	Polynitroxyl albumin (PNA)	Anti-inflammatory	rat	arterial spin-labeled magnetic resonance imaging	asphyxial	attenuate hyperemia	[13]
	Methylprednisolone	anti-inflammatory	pig	microspheres	cardiopulmonary bypass	increase/no effect on CBF	[217, 218]
Hemodynamic therapies	Whole blood		pig	microspheres	cardiopulmonary bypass	decrease CBF	[199]
	Diaspirin cross-linked hemoglobin		pig	microspheres	VF	increase CBF	[205]
	Liposome-encapsulated		rat	laser Doppler flowmetry	four-vessel occlusion	no effect on CBF	[206]

	hemoglobin						
	Hemodilution		pig, dog, cat	microspheres, Xenon CT	cardiopulmonary bypass, VF	increase CBF and capillary flow	[145, 198, 200, 201, 203, 211]
	Hypertonic saline		pig, rat, cat	microsphere, laser Doppler flowmetry	VF, cardiopulmonary bypass, asphyxial	increase CBF	[208-210, 331, 332]

A.3 APPENDIX III

IRB approval letter and the most recent renewal letter

University of Pittsburgh

Institutional Review Board

3500 Fifth Avenue
Pittsburgh, PA 15213
(412) 383-1480
(412) 383-1508 (fax)
http://www.irb.pitt.edu

Memorandum

To:	Paula Sherwood , RN, PhD
From:	Sue Beers PhD, Vice Chair
Date:	6/20/2016
IRB#:	PRO16030073
Subject:	Assessing Cerebrovascular Reactivity after SAH

At its full board meeting on 5/5/2016, the University of Pittsburgh Institutional Review Board, Committee D, reviewed the above referenced research study and

approved it pending minor modifications. Your responses to these comments have been reviewed and the research submission, in its currently modified form, adequately addresses the concerns of the IRB and is therefore approved.

Please note the following information:

The risk level designation is Greater Than Minimal Risk.

Approval Date: 6/20/2016

Expiration Date: 5/4/2017

The following documents were approved by the IRB:

Consent form

For studies being conducted in UPMC facilities, no clinical activities can be undertaken by investigators until they have received approval from the UPMC Fiscal Review Office.

Please note that it is the investigator's responsibility to report to the IRB any unanticipated problems involving risks to subjects or others [see 45 CFR 46.103(b)(5) and 21 CFR 56.108(b)]. Refer to the IRB Policy and Procedure Manual regarding the reporting requirements for unanticipated problems which include, but are not limited to, adverse events. If you have any questions about this process, please contact the Adverse Events Coordinator at 412-383-1480.

The protocol and consent forms, along with a brief progress report must be resubmitted at least one month prior to the renewal date noted above as required by FWA00006790 (University of Pittsburgh), FWA00006735 (University of Pittsburgh Medical Center), FWA00000600 (Children's Hospital of Pittsburgh), FWA00003567 (Magee-Womens Health Corporation), FWA00003338 (University of Pittsburgh Medical Center Cancer Institute).

Please be advised that your research study may be audited periodically by the University of Pittsburgh Research Conduct and Compliance Office.

University of Pittsburgh

Institutional Review Board

3500 Fifth Avenue
Pittsburgh, PA 15213
(412) 383-1480
(412) 383-1508 (fax)
http://www.irb.pitt.edu

Memorandum

To: Paula Sherwood, RN, PhD

From: Judith Martin MD, Vice Chair

Date: 5/17/2018

IRB#: REN18050039 / PRO16030073

Subject: Assessing Cerebrovascular Reactivity after SAH

The Renewal for the above referenced research study was reviewed and approved by the Institutional Review Board, Committee C, which met on 5/15/2018.

Please note the following information:

The risk level designation is Greater Than Minimal.

Approval Date: 5/15/2018

Expiration Date: 5/14/2019

Please note that it is the investigator's responsibility to report to the IRB any unanticipated problems involving risks to subjects or others [see 45 CFR 46.103(b)(5) and 21 CFR 56.108(b)]. Refer to the IRB Policy and Procedure Manual regarding the reporting requirements for unanticipated problems which include, but are not limited to, adverse events. If you have any questions about this process, please contact the Adverse Events Coordinator at 412-383-1480.

The protocol and consent forms, along with a brief progress report must be resubmitted at least **one month** prior to the renewal date noted above as required by FWA00006790 (University of Pittsburgh), FWA00006735 (University of Pittsburgh

Medical Center), FWA00000600 (Children's Hospital of Pittsburgh), FWA00003567 (Magee-Womens Health Corporation), FWA00003338 (University of Pittsburgh Medical Center Cancer Institute).

Please be advised that your research study may be audited periodically by the University of Pittsburgh Research Conduct and Compliance Office.

BIBLIOGRAPHY

1. Berger, S., *Survival From Out-of-Hospital Cardiac Arrest: Are We Beginning to See Progress?* J Am Heart Assoc, 2017. **6**(9).
2. Reynolds, J.C. and B.J. Lawner, *Management of the post-cardiac arrest syndrome.* J Emerg Med, 2012. **42**(4): p. 440-9.
3. Laver, S., et al., *Mode of death after admission to an intensive care unit following cardiac arrest.* Intensive Care Med, 2004. **30**(11): p. 2126-8.
4. Edgren, E., et al., *The presenting ECG pattern in survivors of cardiac arrest and its relation to the subsequent long-term survival. Brain Resuscitation Clinical Trial I Study Group.* Acta Anaesthesiol Scand, 1989. **33**(4): p. 265-71.
5. Geocadin, R.G., et al., *Management of brain injury after resuscitation from cardiac arrest.* Neurol Clin, 2008. **26**(2): p. 487-506, ix.
6. Iordanova, B., et al., *Alterations in Cerebral Blood Flow after Resuscitation from Cardiac Arrest.* Frontiers in Pediatrics, 2017. **5**.
7. Iordanova, B., et al., *Alterations in Cerebral Blood Flow after Resuscitation from Cardiac Arrest.* Front Pediatr, 2017. **5**: p. 174.
8. Manole, M.D., et al., *Magnetic resonance imaging assessment of regional cerebral blood flow after asphyxial cardiac arrest in immature rats.* J Cereb Blood Flow Metab, 2009. **29**(1): p. 197-205.
9. Drabek, T., et al., *Global and regional differences in cerebral blood flow after asphyxial versus ventricular fibrillation cardiac arrest in rats using ASL-MRI.* Resuscitation, 2014. **85**(7): p. 964-971.
10. Poiseuille, J.L., *Recherches expérimentales sur le mouvement des liquides dans les tubes de très-petits diamètres*. 1844: Imprimerie Royale.
11. Link, M.S., et al., *Part 7: Adult Advanced Cardiovascular Life Support: 2015 American Heart Association Guidelines Update for Cardiopulmonary Resuscitation and Emergency Cardiovascular Care.* Circulation, 2015. **132**(18 Suppl 2): p. S444-64.
12. Jackson, D.L., et al., *Total cerebral ischemia: application of a new model system to studies of cerebral microcirculation.* Stroke, 1981. **12**(1): p. 66-72.
13. Manole, M.D., et al., *Polynitroxyl albumin and albumin therapy after pediatric asphyxial cardiac arrest: effects on cerebral blood flow and neurologic outcome.* J Cereb Blood Flow Metab, 2012. **32**(3): p. 560-9.
14. Yager, J.Y., M.A. Christensen, and R.C. Vannucci, *Regional cerebral blood flow following hypothermic circulatory arrest in newborn dogs.* Brain Res, 1993. **620**(1): p. 122-6.
15. Vognsen, M., et al., *Contemporary animal models of cardiac arrest: A systematic review.* Resuscitation, 2017. **113**: p. 115-123.

16. Weigl, M., et al., *A systematic review of currently available pharmacological neuroprotective agents as a sole intervention before anticipated or induced cardiac arrest.* Resuscitation, 2005. **65**(1): p. 21-39.
17. Kroppenstedt, S.N., et al., *Effects of early and late intravenous norepinephrine infusion on cerebral perfusion, microcirculation, brain-tissue oxygenation, and edema formation in brain-injured rats.* Crit Care Med, 2003. **31**(8): p. 2211-21.
18. Junyun, H., et al., *Real-time monitoring of cerebral blood flow by laser speckle contrast imaging after cardiac arrest in rat.* Conf Proc IEEE Eng Med Biol Soc, 2015. **2015**: p. 6971-4.
19. Ristagno, G., et al., *Cerebral cortical microvascular flow during and following cardiopulmonary resuscitation after short duration of cardiac arrest.* Resuscitation, 2008. **77**(2): p. 229-34.
20. Taylor, R.B., et al., *A model for regional blood flow measurements during cardiopulmonary resuscitation in a swine model.* Resuscitation, 1988. **16**(2): p. 107-18.
21. Li, L., et al., *Cerebral microcirculatory alterations and the no-reflow phenomenon in vivo after experimental pediatric cardiac arrest.* J Cereb Blood Flow Metab, 2017: p. 271678X17744717.
22. Verlhac, S., *Transcranial Doppler in children.* Pediatr Radiol, 2011. **41 Suppl 1**: p. S153-65.
23. Jarnum, H., et al., *Diffusion and perfusion MRI of the brain in comatose patients treated with mild hypothermia after cardiac arrest: a prospective observational study.* Resuscitation, 2009. **80**(4): p. 425-30.
24. Inoue, Y., et al., *Acute cerebral blood flow variations after human cardiac arrest assessed by stable xenon enhanced computed tomography.* Curr Neurovasc Res, 2007. **4**(1): p. 49-54.
25. Lee, J.K., et al., *A pilot study of cerebrovascular reactivity autoregulation after pediatric cardiac arrest.* Resuscitation, 2014. **85**(10): p. 1387-93.
26. Cerchiari, E.L., et al., *Protective effects of combined superoxide dismutase and deferoxamine on recovery of cerebral blood flow and function after cardiac arrest in dogs.* Stroke, 1987. **18**(5): p. 869-78.
27. Shaik, J.S., et al., *20-Hydroxyeicosatetraenoic Acid Inhibition by HET0016 Offers Neuroprotection, Decreases Edema, and Increases Cortical Cerebral Blood Flow in a Pediatric Asphyxial Cardiac Arrest Model in Rats.* J Cereb Blood Flow Metab, 2015. **35**(11): p. 1757-63.
28. Kofke, W.A., et al., *Brain blood flow and metabolism after global ischemia and post-insult thiopental therapy in monkeys.* Stroke, 1979. **10**(5): p. 554-60.
29. Schneider, A., B.W. Bottiger, and E. Popp, *Cerebral resuscitation after cardiocirculatory arrest.* Anesth Analg, 2009. **108**(3): p. 971-9.
30. Tank, A.W. and D. Lee Wong, *Peripheral and central effects of circulating catecholamines.* Compr Physiol, 2015. **5**(1): p. 1-15.
31. Cotecchia, S., *The α1-adrenergic receptors: diversity of signaling networks and regulation.* Journal of receptor and signal transduction research, 2010. **30**(6): p. 410-419.
32. Westfall, T.C. and D.P. Westfall, *Neurotransmission: the autonomic and somatic motor nervous system.* Goodman and Gilman's The Pharmacological Basis of Therapeutics, 12th ed. Edited by L Bruton. New York: McGraw Hill, 2011: p. 171-218.

33. Brown, C.G. and H.A. Werman, *Adrenergic agonists during cardiopulmonary resuscitation.* Resuscitation, 1990. **19**(1): p. 1-16.
34. Cao, L., et al., *Vasopressor agents for cardiopulmonary resuscitation.* J Cardiovasc Pharmacol Ther, 2003. **8**(2): p. 115-21.
35. Huang, L. and W. Tang, *Vasopressor agents: old and new components.* Curr Opin Crit Care, 2004. **10**(3): p. 183-7.
36. Carveth, S., *Standards for cardiopulmonary resuscitation and emergency cardiac care.* JAMA, 1974. **227**(7): p. 796-797.
37. Paradis, N.A., et al., *Coronary perfusion pressure and the return of spontaneous circulation in human cardiopulmonary resuscitation.* Jama, 1990. **263**(8): p. 1106-13.
38. Kern, K.B., et al., *Myocardial perfusion pressure: a predictor of 24-hour survival during prolonged cardiac arrest in dogs.* Resuscitation, 1988. **16**(4): p. 241-50.
39. Lindner, K.H., F.W. Ahnefeld, and I.M. Bowdler, *Comparison of different doses of epinephrine on myocardial perfusion and resuscitation success during cardiopulmonary resuscitation in a pig model.* Am J Emerg Med, 1991. **9**(1): p. 27-31.
40. Brown, C.G., et al., *Comparative effect of graded doses of epinephrine on regional brain blood flow during CPR in a swine model.* Ann Emerg Med, 1986. **15**(10): p. 1138-44.
41. Schleien, C.L., et al., *Effect of epinephrine on cerebral and myocardial perfusion in an infant animal preparation of cardiopulmonary resuscitation.* Circulation, 1986. **73**(4): p. 809-17.
42. Brown, C.G., et al., *Methoxamine versus epinephrine on regional cerebral blood flow during cardiopulmonary resuscitation.* Crit Care Med, 1987. **15**(7): p. 682-6.
43. Schmitz, B., et al., *Resuscitation from cardiac arrest in cats: influence of epinephrine dosage on brain recovery.* Resuscitation, 1995. **30**(3): p. 251-62.
44. Nozari, A., S. Rubertsson, and L. Wiklund, *Intra-aortic administration of epinephrine above an aortic balloon occlusion during experimental CPR does not further improve cerebral blood flow and oxygenation.* Resuscitation, 2000. **44**(2): p. 119-27.
45. Johansson, J., et al., *Increased cortical cerebral blood flow by continuous infusion of adrenaline (epinephrine) during experimental cardiopulmonary resuscitation.* Resuscitation, 2003. **57**(3): p. 299-307.
46. Ristagno, G., et al., *Effects of epinephrine and vasopressin on cerebral microcirculatory flows during and after cardiopulmonary resuscitation.* Crit Care Med, 2007. **35**(9): p. 2145-9.
47. Ristagno, G., et al., *Epinephrine reduces cerebral perfusion during cardiopulmonary resuscitation.* Crit Care Med, 2009. **37**(4): p. 1408-15.
48. Lindner, K.H., et al., *Effects of epinephrine and norepinephrine on cerebral oxygen delivery and consumption during open-chest CPR.* Ann Emerg Med, 1990. **19**(3): p. 249-54.
49. Brown, C.G., et al., *The comparative effects of epinephrine versus phenylephrine on regional cerebral blood flow during cardiopulmonary resuscitation.* Resuscitation, 1986. **14**(3): p. 171-83.
50. Iida, H., et al., *Effects of dexmedetomidine on cerebral circulation and systemic hemodynamics after cardiopulmonary resuscitation in dogs.* J Anesth, 2006. **20**(3): p. 202-7.

51. Liu, Z., et al., *The impact of dopamine on hemodynamics, oxygen metabolism, and cerebral resuscitation after restoration of spontaneous circulation in pigs.* J Emerg Med, 2011. **40**(3): p. 348-54.
52. Caldwell, H. and W. Young, *Oxytocin and vasopressin: genetics and behavioral implications*, in *Handbook of neurochemistry and molecular neurobiology*. 2006, Springer. p. 573-607.
53. Pelletier, J.S., et al., *Cardiac effects of vasopressin.* J Cardiovasc Pharmacol, 2014. **64**(1): p. 100-7.
54. Nemenoff, R.A., *Vasopressin signaling pathways in vascular smooth muscle.* Front Biosci, 1998. **3**: p. d194-207.
55. Maturi, M.F., et al., *Coronary vasoconstriction induced by vasopressin. Production of myocardial ischemia in dogs by constriction of nondiseased small vessels.* Circulation, 1991. **83**(6): p. 2111-21.
56. Wenzel, V., et al., *Effects of intravenous arginine vasopressin on epicardial coronary artery cross sectional area in a swine resuscitation model.* Resuscitation, 2005. **64**(2): p. 219-26.
57. Kozniewska, E. and K. Romaniuk, *Vasopressin in vascular regulation and water homeostasis in the brain.* J Physiol Pharmacol, 2008. **59 Suppl 8**: p. 109-16.
58. Kumazawa, M., et al., *The effects of transient cerebral ischemia on vasopressin-induced vasoconstriction in rabbit cerebral vessels.* Anesth Analg, 2008. **106**(3): p. 910-5, table of contents.
59. Cooke, C.R., et al., *Cardiovascular effects of vasopressin following V(1) receptor blockade compared to effects of nitroglycerin.* Am J Physiol Regul Integr Comp Physiol, 2001. **281**(3): p. R887-93.
60. Altura, B.M. and B.T. Altura, *Actions of vasopressin, oxytocin, and synthetic analogs on vascular smooth muscle.* Fed Proc, 1984. **43**(1): p. 80-6.
61. Faraci, F.M., et al., *Effects of arginine vasopressin on cerebral microvascular pressure.* Am J Physiol, 1988. **255**(1 Pt 2): p. H70-6.
62. Wenzel, V., et al., *Vasopressin improves vital organ blood flow after prolonged cardiac arrest with postcountershock pulseless electrical activity in pigs.* Crit Care Med, 1999. **27**(3): p. 486-92.
63. Wenzel, V., et al., *Survival with full neurologic recovery and no cerebral pathology after prolonged cardiopulmonary resuscitation with vasopressin in pigs.* J Am Coll Cardiol, 2000. **35**(2): p. 527-33.
64. Nozari, A., S. Rubertsson, and L. Wiklund, *Differences in the pharmacodynamics of epinephrine and vasopressin during and after experimental cardiopulmonary resuscitation.* Resuscitation, 2001. **49**(1): p. 59-72.
65. Krismer, A.C., et al., *Vasopressin during cardiopulmonary resuscitation: a progress report.* Crit Care Med, 2004. **32**(9 Suppl): p. S432-5.
66. Voelckel, W.G., et al., *Comparison of epinephrine and vasopressin in a pediatric porcine model of asphyxial cardiac arrest.* Crit Care Med, 2000. **28**(12): p. 3777-83.
67. Callaway, C.W., et al., *Part 8: Post-Cardiac Arrest Care: 2015 American Heart Association Guidelines Update for Cardiopulmonary Resuscitation and Emergency Cardiovascular Care.* Circulation, 2015. **132**(18 Suppl 2): p. S465-82.

68. Luscher, T.F. and M. Barton, *Endothelins and endothelin receptor antagonists: therapeutic considerations for a novel class of cardiovascular drugs.* Circulation, 2000. **102**(19): p. 2434-40.
69. Rubanyi, G.M. and M.A. Polokoff, *Endothelins: molecular biology, biochemistry, pharmacology, physiology, and pathophysiology.* Pharmacol Rev, 1994. **46**(3): p. 325-415.
70. Schneider, M.P., E.I. Boesen, and D.M. Pollock, *Contrasting actions of endothelin ET(A) and ET(B) receptors in cardiovascular disease.* Annu Rev Pharmacol Toxicol, 2007. **47**: p. 731-59.
71. Gross, P.M., et al., *Intraventricular endothelin-1 uncouples the blood flow: metabolism relationship in periventricular structures of the rat brain: involvement of L-type calcium channels.* Neuropeptides, 1992. **22**(3): p. 155-65.
72. DeBehnke, D., *The effects of graded doses of endothelin-1 on coronary perfusion pressure and vital organ blood flow during cardiac arrest.* Acad Emerg Med, 2000. **7**(3): p. 211-21.
73. Holzer, M., et al., *Endothelin-1 elevates regional cerebral perfusion during prolonged ventricular fibrillation cardiac arrest in pigs.* Resuscitation, 2002. **55**(3): p. 317-27.
74. Parker, J.D., et al., *Human endothelin-1 clearance kinetics revealed by a radiotracer technique.* J Pharmacol Exp Ther, 1999. **289**(1): p. 261-5.
75. Shiba, R., et al., *Elimination of intravenously injected endothelin-1 from the circulation of the rat.* J Cardiovasc Pharmacol, 1989. **13 Suppl 5**: p. S98-101; discussion S102.
76. Hilwig, R.W., et al., *Endothelin-1 vasoconstriction during swine cardiopulmonary resuscitation improves coronary perfusion pressures but worsens postresuscitation outcome.* Circulation, 2000. **101**(17): p. 2097-102.
77. Krep, H., et al., *Endothelin type A-antagonist improves long-term neurological recovery after cardiac arrest in rats.* Crit Care Med, 2000. **28**(8): p. 2873-80.
78. Krep, H., et al., *Treatment with an endothelin type A receptor-antagonist after cardiac arrest and resuscitation improves cerebral hemodynamic and functional recovery in rats.* Crit Care Med, 2000. **28**(8): p. 2866-72.
79. Mehta, P.K. and K.K. Griendling, *Angiotensin II cell signaling: physiological and pathological effects in the cardiovascular system.* Am J Physiol Cell Physiol, 2007. **292**(1): p. C82-97.
80. Yan, C., et al., *Functional interplay between angiotensin II and nitric oxide: cyclic GMP as a key mediator.* Arterioscler Thromb Vasc Biol, 2003. **23**(1): p. 26-36.
81. Griendling, K.K., D. Sorescu, and M. Ushio-Fukai, *NAD(P)H oxidase: role in cardiovascular biology and disease.* Circ Res, 2000. **86**(5): p. 494-501.
82. Little, C.M. and C.G. Brown, *Angiotensin II administration improves cerebral blood flow in cardiopulmonary arrest in swine.* Stroke, 1994. **25**(1): p. 183-8.
83. Venkat, P., M. Chopp, and J. Chen, *New insights into coupling and uncoupling of cerebral blood flow and metabolism in the brain.* Croat Med J, 2016. **57**(3): p. 223-8.
84. Forstermann, U. and W.C. Sessa, *Nitric oxide synthases: regulation and function.* Eur Heart J, 2012. **33**(7): p. 829-37, 837a-837d.
85. Toda, N. and T. Okamura, *Cerebral vasoconstrictor mediators.* Pharmacol Ther, 1993. **57**(2-3): p. 359-75.
86. Rastaldo, R., et al., *Nitric oxide and cardiac function.* Life Sci, 2007. **81**(10): p. 779-93.

87. Jin, R.C. and J. Loscalzo, *Vascular Nitric Oxide: Formation and Function.* J Blood Med, 2010. **2010**(1): p. 147-162.
88. Bolotina, V.M., et al., *Nitric oxide directly activates calcium-dependent potassium channels in vascular smooth muscle.* Nature, 1994. **368**(6474): p. 850-3.
89. Millatt, L.J., E.M. Abdel-Rahman, and H.M. Siragy, *Angiotensin II and nitric oxide: a question of balance.* Regul Pept, 1999. **81**(1-3): p. 1-10.
90. Miyata, N. and R.J. Roman, *Role of 20-hydroxyeicosatetraenoic acid (20-HETE) in vascular system.* J Smooth Muscle Res, 2005. **41**(4): p. 175-93.
91. Garry, P.S., et al., *The role of the nitric oxide pathway in brain injury and its treatment--from bench to bedside.* Exp Neurol, 2015. **263**: p. 235-43.
92. Kida, K., et al., *Beneficial effects of nitric oxide on outcomes after cardiac arrest and cardiopulmonary resuscitation in hypothermia-treated mice.* Anesthesiology, 2014. **120**(4): p. 880-9.
93. Tsui, S.S., et al., *Nitric oxide production affects cerebral perfusion and metabolism after deep hypothermic circulatory arrest.* Ann Thorac Surg, 1996. **61**(6): p. 1699-707.
94. Hiramatsu, T., et al., *Cerebral metabolic recovery from deep hypothermic circulatory arrest after treatment with arginine and nitro-arginine methyl ester.* J Thorac Cardiovasc Surg, 1996. **112**(3): p. 698-707.
95. Schultz, J.C., et al., *Sodium nitroprusside-enhanced cardiopulmonary resuscitation improves resuscitation rates after prolonged untreated cardiac arrest in two porcine models.* Crit Care Med, 2011. **39**(12): p. 2705-10.
96. Yannopoulos, D., et al., *Sodium nitroprusside enhanced cardiopulmonary resuscitation improves survival with good neurological function in a porcine model of prolonged cardiac arrest.* Crit Care Med, 2011. **39**(6): p. 1269-74.
97. Kleschyov, A.L., et al., *Does nitric oxide mediate the vasodilator activity of nitroglycerin?* Circulation Research, 2003. **93**(9): p. E104-E112.
98. Ebmeyer, U., T. Esser, and G. Keilhoff, *Low-dose nitroglycerine improves outcome after cardiac arrest in rats.* Resuscitation, 2014. **85**(2): p. 276-83.
99. Wenzel, V., et al., *Vasopressin combined with nitroglycerin increases endocardial perfusion during cardiopulmonary resuscitation in pigs.* Resuscitation, 1998. **38**(1): p. 13-7.
100. Wenzel, V., et al., *Vasopressin combined with epinephrine decreases cerebral perfusion compared with vasopressin alone during cardiopulmonary resuscitation in pigs.* Stroke, 1998. **29**(7): p. 1462-7; discussion 1467-8.
101. Lurie, K.G., et al., *Combination drug therapy with vasopressin, adrenaline (epinephrine) and nitroglycerin improves vital organ blood flow in a porcine model of ventricular fibrillation.* Resuscitation, 2002. **54**(2): p. 187-94.
102. Kono, S., et al., *Vasopressin with delayed combination of nitroglycerin increases survival rate in asphyxia rat model.* Resuscitation, 2002. **54**(3): p. 297-301.
103. Varvarousi, G., et al., *Epinephrine, vasopressin, and nitroglycerin improve neurologic outcome in porcine asphyxial cardiac arrest.* Am J Emerg Med, 2012. **30**(8): p. 1549-54.
104. Samdani, A.F., T.M. Dawson, and V.L. Dawson, *Nitric oxide synthase in models of focal ischemia.* Stroke, 1997. **28**(6): p. 1283-8.
105. Iadecola, C., *Bright and dark sides of nitric oxide in ischemic brain injury.* Trends Neurosci, 1997. **20**(3): p. 132-9.

106. Cannon, R.O., 3rd, et al., *Effects of inhaled nitric oxide on regional blood flow are consistent with intravascular nitric oxide delivery.* The Journal of clinical investigation, 2001. **108**(2): p. 279-287.
107. Segawa, D., et al., *The effect of nitric oxide synthase inhibitor on reperfusion injury of the brain under hypothermic circulatory arrest.* J Thorac Cardiovasc Surg, 1998. **115**(4): p. 925-30.
108. Evora, P.R., *Methylene Blue Is a Guanylate Cyclase Inhibitor That Does Not Interfere with Nitric Oxide Synthesis.* Tex Heart Inst J, 2016. **43**(1): p. 103.
109. Mayer, B., F. Brunner, and K. Schmidt, *Inhibition of nitric oxide synthesis by methylene blue.* Biochem Pharmacol, 1993. **45**(2): p. 367-74.
110. Miclescu, A., S. Basu, and L. Wiklund, *Cardio-cerebral and metabolic effects of methylene blue in hypertonic sodium lactate during experimental cardiopulmonary resuscitation.* Resuscitation, 2007. **75**(1): p. 88-97.
111. Young, J.D., et al., *Effect of methylene blue on the vasodilator action of inhaled nitric oxide in hypoxic sheep.* Br J Anaesth, 1994. **73**(4): p. 511-6.
112. Nanri, K., et al., *The selective inhibitor of neuronal nitric oxide synthase, 7-nitroindazole, reduces the delayed neuronal damage due to forebrain ischemia in rats.* Stroke, 1998. **29**(6): p. 1248-53; discussion 1253-4.
113. Jiang, M.H., et al., *7-Nitroindazole reduces nitric oxide concentration in rat hippocampus after transient forebrain ischemia.* Eur J Pharmacol, 1999. **380**(2-3): p. 117-21.
114. Jiang, M.H., et al., *Different effects of eNOS and nNOS inhibition on transient forebrain ischemia.* Brain Res, 2002. **946**(1): p. 139-47.
115. Layland, J., et al., *Adenosine: physiology, pharmacology, and clinical applications.* JACC Cardiovasc Interv, 2014. **7**(6): p. 581-91.
116. Frobert, O., et al., *Adenosine concentration in the porcine coronary artery wall and A2A receptor involvement in hypoxia-induced vasodilatation.* J Physiol, 2006. **570**(Pt 2): p. 375-84.
117. Mustafa, S.J., et al., *Adenosine receptors and the heart: role in regulation of coronary blood flow and cardiac electrophysiology.* Handbook of experimental pharmacology, 2009(193): p. 161-188.
118. Xu, K., et al., *Adenosine treatment delays postischemic hippocampal CA1 loss after cardiac arrest and resuscitation in rats.* Brain Res, 2006. **1071**(1): p. 208-17.
119. Mallet, M.L., *Proarrhythmic effects of adenosine: a review of the literature.* Emergency medicine journal : EMJ, 2004. **21**(4): p. 408-410.
120. Abu-Laban, R.B., et al., *Aminophylline in bradyasystolic cardiac arrest: a randomised placebo-controlled trial.* Lancet, 2006. **367**(9522): p. 1577-84.
121. Northover, B.J., *The effect of drugs on the constriction of isolated depolarized blood vessels in response to calcium or barium.* Br J Pharmacol, 1968. **34**(2): p. 417-28.
122. Jackson, W.F., *Ion channels and vascular tone.* Hypertension, 2000. **35**(1 Pt 2): p. 173-8.
123. Gelmers, H.J., *Calcium-channel blockers: effects on cerebral blood flow and potential uses for acute stroke.* Am J Cardiol, 1985. **55**(3): p. 144B-148B.
124. Kalogeris, T., et al., *Cell biology of ischemia/reperfusion injury.* Int Rev Cell Mol Biol, 2012. **298**: p. 229-317.
125. Zakhari, S., *Mechanism of action of calcium antagonists on myocardial and smooth muscle membranes.* Drugs Exp Clin Res, 1986. **12**(9-10): p. 817-29.

126. Schindler, I., et al., *Effects of nimodipine on regional blood flow in heart and brain during cardiopulmonary resuscitation in pigs.* Anesth Analg, 1994. **78**(1): p. 87-93.
127. Forsman, M., et al., *Effects of nimodipine on cerebral blood flow and cerebrospinal fluid pressure after cardiac arrest: correlation with neurologic outcome.* Anesth Analg, 1989. **68**(4): p. 436-43.
128. Lindner, K.H., et al., *Effects of diltiazem on oxygen delivery and consumption after asphyxial cardiac arrest and resuscitation.* Crit Care Med, 1992. **20**(5): p. 650-8.
129. White, B.C., et al., *Effect of flunarizine on canine cerebral cortical blood flow and vascular resistance post cardiac arrest.* Ann Emerg Med, 1982. **11**(3): p. 119-26.
130. Edmonds, H.L., Jr., et al., *Improved short-term neurological recovery with flunarizine in a canine model of cardiac arrest.* Am J Emerg Med, 1985. **3**(2): p. 150-5.
131. Kasikcioglu, H.A. and N. Cam, *A review of levosimendan in the treatment of heart failure.* Vasc Health Risk Manag, 2006. **2**(4): p. 389-400.
132. Kelm, R.F., et al., *Effects of levosimendan on hemodynamics, local cerebral blood flow, neuronal injury, and neuroinflammation after asphyctic cardiac arrest in rats.* Crit Care Med, 2014. **42**(6): p. e410-9.
133. DiPadova, C., et al., *Effects of ranitidine on blood alcohol levels after ethanol ingestion. Comparison with other H2-receptor antagonists.* Jama, 1992. **267**(1): p. 83-6.
134. *A randomized clinical study of a calcium-entry blocker (lidoflazine) in the treatment of comatose survivors of cardiac arrest.* N Engl J Med, 1991. **324**(18): p. 1225-31.
135. Roine, R.O., et al., *Nimodipine after resuscitation from out-of-hospital ventricular fibrillation. A placebo-controlled, double-blind, randomized trial.* JAMA, 1990. **264**(24): p. 3171-7.
136. Schampel, A. and S. Kuerten, *Danger: High Voltage-The Role of Voltage-Gated Calcium Channels in Central Nervous System Pathology.* Cells, 2017. **6**(4): p. 43.
137. Nishizawa, Y., *Glutamate release and neuronal damage in ischemia.* Life Sci, 2001. **69**(4): p. 369-81.
138. Hu, P., et al., *Effects of the AMPA-receptor antagonist, NBQX, on neuron loss in dentate hilus of the hippocampal formation after 8, 10, or 12 min of cerebral ischemia in the rat.* J Cereb Blood Flow Metab, 1997. **17**(2): p. 147-52.
139. Diemer, N.H., et al., *Extended studies on the effect of glutamate antagonists on ischemic CA-1 damage.* Acta Neurochir Suppl, 1996. **66**: p. 73-5.
140. Nellgard, B., I. Gustafson, and T. Wieloch, *Lack of protection by the N-methyl-D-aspartate receptor blocker dizocilpine (MK-801) after transient severe cerebral ischemia in the rat.* Anesthesiology, 1991. **75**(2): p. 279-287.
141. Fleischer, J.E., et al., *MK-801, an excitatory amino acid antagonist, does not improve neurologic outcome following cardiac arrest in cats.* J Cereb Blood Flow Metab, 1989. **9**(6): p. 795-804.
142. Matsumoto, M., et al., *AMPA and NMDA receptor antagonists do not decrease hippocampal glutamate concentrations during transient global ischemia.* Anesthesiology, 1992. **77**(4): p. 764-71.
143. Brambrink, A.M., et al., *Effects of the AMPA receptor antagonist NBQX on outcome of newborn pigs after asphyxic cardiac arrest.* J Cereb Blood Flow Metab, 1999. **19**(8): p. 927-38.

144. Aoki, M., et al., *Effects of MK-801 and NBQX on acute recovery of piglet cerebral metabolism after hypothermic circulatory arrest.* J Cereb Blood Flow Metab, 1994. **14**(1): p. 156-65.
145. Aoki, M., et al., *Effects of cerebroplegic solutions during hypothermic circulatory arrest and short-term recovery.* J Thorac Cardiovasc Surg, 1994. **108**(2): p. 291-301.
146. Kroetz, D.L. and D.C. Zeldin, *Cytochrome P450 pathways of arachidonic acid metabolism.* Curr Opin Lipidol, 2002. **13**(3): p. 273-83.
147. Huang, H., M. Al-Shabrawey, and M.H. Wang, *Cyclooxygenase- and cytochrome P450-derived eicosanoids in stroke.* Prostaglandins Other Lipid Mediat, 2016. **122**: p. 45-53.
148. Hall, C.N., et al., *Capillary pericytes regulate cerebral blood flow in health and disease.* Nature, 2014. **508**(7494): p. 55-60.
149. Dalkara, T., Y. Gursoy-Ozdemir, and M. Yemisci, *Brain microvascular pericytes in health and disease.* Acta Neuropathol, 2011. **122**(1): p. 1-9.
150. Harder, D.R., et al., *Formation and action of a P-450 4A metabolite of arachidonic acid in cat cerebral microvessels.* Am J Physiol, 1994. **266**(5 Pt 2): p. H2098-107.
151. Imig, J.D., et al., *Formation and actions of 20-hydroxyeicosatetraenoic acid in rat renal arterioles.* Am J Physiol, 1996. **270**(1 Pt 2): p. R217-27.
152. Lange, A., et al., *20-hydroxyeicosatetraenoic acid-induced vasoconstriction and inhibition of potassium current in cerebral vascular smooth muscle is dependent on activation of protein kinase C.* Journal of Biological Chemistry, 1997. **272**(43): p. 27345-27352.
153. Zeng, Q., et al., *20-HETE increases NADPH oxidase-derived ROS production and stimulates the L-type Ca2+ channel via a PKC-dependent mechanism in cardiomyocytes.* Am J Physiol Heart Circ Physiol, 2010. **299**(4): p. H1109-17.
154. Bao, Y.Y., et al., *20-Hydroxyeicosatetraenoic Acid Induces Apoptosis in Neonatal Rat Cardiomyocytes Through Mitochondrial-Dependent Pathways.* Journal of Cardiovascular Pharmacology, 2011. **57**(3): p. 294-301.
155. Renic, M., et al., *Protective effect of 20-HETE inhibition in a model of oxygen-glucose deprivation in hippocampal slice cultures.* Am J Physiol Heart Circ Physiol, 2012. **302**(6): p. H1285-93.
156. Lakhkar, A., et al., *20-HETE-induced mitochondrial superoxide production and inflammatory phenotype in vascular smooth muscle is prevented by glucose-6-phosphate dehydrogenase inhibition.* American Journal of Physiology-Heart and Circulatory Physiology, 2016. **310**(9): p. H1107-H1117.
157. Lozano, H., et al., *The effects of prostaglandin inhibition on whole-body ischemia-reperfusion in swine.* Am J Emerg Med, 2008. **26**(1): p. 45-53.
158. Rayar, A.M., et al., *Update on COX-2 Selective Inhibitors: Chemical Classification, Side Effects and their Use in Cancers and Neuronal Diseases.* Curr Top Med Chem, 2017. **17**(26): p. 2935-2956.
159. Liu, J.Y., et al., *Metabolic profiling of murine plasma reveals an unexpected biomarker in rofecoxib-mediated cardiovascular events.* Proc Natl Acad Sci U S A, 2010. **107**(39): p. 17017-22.
160. Newton, D.J., et al., *Vasoactive characteristics of bupivacaine and levobupivacaine with and without adjuvant epinephrine in peripheral human skin.* BJA: British Journal of Anaesthesia, 2005. **94**(5): p. 662-667.

161. Li, X., et al., *Role of continuous high thoracic epidural anesthesia in hippocampal apoptosis after global cerebral ischemia in rats.* Cell Physiol Biochem, 2014. **34**(4): p. 1227-40.
162. Runciman, W.B., L.E. Mather, and D.G. Selby, *Cardiovascular effects of propofol and of thiopentone anaesthesia in the sheep.* Br J Anaesth, 1990. **65**(3): p. 353-9.
163. Nemoto, E.M., S. Frinak, and F. Taylor, *Postischemic brain oxygenation with barbiturate therapy in rats.* Crit Care Med, 1979. **7**(8): p. 339-45.
164. Snyder, B.D., et al., *Failure of thiopental to modify global anoxic injury.* Stroke, 1979. **10**(2): p. 135-41.
165. Ebmeyer, U., et al., *Thiopental combination treatments for cerebral resuscitation after prolonged cardiac arrest in dogs. Exploratory outcome study.* Resuscitation, 2000. **45**(2): p. 119-31.
166. Chae, J.E., et al., *Ionic mechanisms of desflurane on prolongation of action potential duration in rat ventricular myocytes.* Yonsei Med J, 2012. **53**(1): p. 204-12.
167. Warltier, D.C. and P.S. Pagel, *Cardiovascular and respiratory actions of desflurane: is desflurane different from isoflurane?* Anesth Analg, 1992. **75**(4 Suppl): p. S17-29; discussion S29-31.
168. Loepke, A.W., et al., *Desflurane improves neurologic outcome after low-flow cardiopulmonary bypass in newborn pigs.* Anesthesiology, 2002. **97**(6): p. 1521-7.
169. Ferimer, H.N., K.L. Kutina, and J.C. LaManna, *Methyl isobutyl amiloride delays normalization of brain intracellular pH after cardiac arrest in rats.* Crit Care Med, 1995. **23**(6): p. 1106-11.
170. Lauro, K.L., H. Kabert, and J.C. LaManna, *Methyl isobutyl amiloride alters regional brain reperfusion after resuscitation from cardiac arrest in rats.* Brain Res, 1999. **831**(1-2): p. 64-71.
171. Ames, A., 3rd, et al., *Cerebral ischemia. II. The no-reflow phenomenon.* Am J Pathol, 1968. **52**(2): p. 437-53.
172. Bottiger, B.W., et al., *The cerebral 'no-reflow' phenomenon after cardiac arrest in rats--influence of low-flow reperfusion.* Resuscitation, 1997. **34**(1): p. 79-87.
173. Fischer, M. and K.A. Hossmann, *No-reflow after cardiac arrest.* Intensive Care Med, 1995. **21**(2): p. 132-41.
174. Adrie, C., et al., *Coagulopathy after successful cardiopulmonary resuscitation following cardiac arrest: implication of the protein C anticoagulant pathway.* J Am Coll Cardiol, 2005. **46**(1): p. 21-8.
175. Gando, S., et al., *Tissue factor and tissue factor pathway inhibitor levels during and after cardiopulmonary resuscitation.* Thromb Res, 1999. **96**(2): p. 107-13.
176. Wada, T., et al., *Coagulofibrinolytic changes in patients with disseminated intravascular coagulation associated with post-cardiac arrest syndrome--fibrinolytic shutdown and insufficient activation of fibrinolysis lead to organ dysfunction.* Thromb Res, 2013. **132**(1): p. e64-9.
177. Gray, E., J. Hogwood, and B. Mulloy, *The anticoagulant and antithrombotic mechanisms of heparin.* Handb Exp Pharmacol, 2012(207): p. 43-61.
178. Olson, S.T. and I. Bjork, *Predominant contribution of surface approximation to the mechanism of heparin acceleration of the antithrombin-thrombin reaction. Elucidation from salt concentration effects.* J Biol Chem, 1991. **266**(10): p. 6353-64.

179. Levi, M. and T. van der Poll, *Recombinant human activated protein C: current insights into its mechanism of action.* Crit Care, 2007. **11 Suppl 5**: p. S3.
180. Fischer, M., et al., *Thrombolysis using plasminogen activator and heparin reduces cerebral no-reflow after resuscitation from cardiac arrest: an experimental study in the cat.* Intensive Care Med, 1996. **22**(11): p. 1214-23.
181. Xu, L., et al., *Effect of enoxaparin and aspirin on hemodynamic disturbances after global cerebral ischemia in rats.* Resuscitation, 2010. **81**(12): p. 1709-13.
182. Johansson, J., et al., *Antithrombin administration during experimental cardiopulmonary resuscitation.* Resuscitation, 2004. **62**(1): p. 71-8.
183. Bruckner, M., et al., *High dose infusion of activated protein C (rhAPC) fails to improve neuronal damage and cognitive deficit after global cerebral ischemia in rats.* Neurosci Lett, 2013. **551**: p. 28-33.
184. Mekaj, Y.H., F.T. Daci, and A.Y. Mekaj, *New insights into the mechanisms of action of aspirin and its use in the prevention and treatment of arterial and venous thromboembolism.* Therapeutics and Clinical Risk Management, 2015. **11**.
185. Tsui, S.S., et al., *Thromboxane A2-receptor blockade improves cerebral protection for deep hypothermic circulatory arrest.* Eur J Cardiothorac Surg, 1997. **12**(2): p. 228-35.
186. McCarty, M.F., J.H. O'Keefe, and J.J. DiNicolantonio, *Pentoxifylline for vascular health: a brief review of the literature.* Open Heart, 2016. **3**(1): p. e000365.
187. Tanahashi, N., et al., *Pentoxifylline ameliorates postischemic delayed hypoperfusion of the cerebral cortex following cardiac arrest in cats.* J Neurol Sci, 1995. **132**(2): p. 105-9.
188. Sirin, B.H., et al., *Pentoxifylline reduces injury of the brain in transient ischaemia.* Acta Cardiol, 1998. **53**(2): p. 89-95.
189. Guo, X.D., et al., *Effect of urokinase on cerebral perfusion after cardiopulmonary resuscitation in rabbits.* Eur Rev Med Pharmacol Sci, 2014. **18**(8): p. 1158-62.
190. Lin, S.R., *The effect of dextran and streptokinase on cerebral function and blood flow after cardiac arrest. An experimental study on the dog.* Neuroradiology, 1978. **16**: p. 340-2.
191. Spinelli, E., et al., *Thrombolytic-Enhanced Extracorporeal Cardiopulmonary Resuscitation After Prolonged Cardiac Arrest.* Crit Care Med, 2016. **44**(2): p. e58-69.
192. Aoki, M., et al., *Effects of aprotinin on acute recovery of cerebral metabolism in piglets after hypothermic circulatory arrest.* Ann Thorac Surg, 1994. **58**(1): p. 146-53.
193. Bottiger, B.W. and E. Martin, *Thrombolytic therapy during cardiopulmonary resuscitation and the role of coagulation activation after cardiac arrest.* Curr Opin Crit Care, 2001. **7**(3): p. 176-83.
194. Lederer, W., et al., *Recombinant tissue plasminogen activator during cardiopulmonary resuscitation in 108 patients with out-of-hospital cardiac arrest.* Resuscitation, 2001. **50**(1): p. 71-6.
195. Abu-Laban, R.B., et al., *Tissue plasminogen activator in cardiac arrest with pulseless electrical activity.* N Engl J Med, 2002. **346**(20): p. 1522-8.
196. Schreiber, W., et al., *Thrombolytic therapy after cardiac arrest and its effect on neurological outcome.* Resuscitation, 2002. **52**(1): p. 63-9.
197. O'Connell, K.E., et al., *Practical murine hematopathology: a comparative review and implications for research.* Comp Med, 2015. **65**(2): p. 96-113.

198. Sakamoto, T., et al., *Hemodilution elevates cerebral blood flow and oxygen metabolism during cardiopulmonary bypass in piglets.* Ann Thorac Surg, 2004. **77**(5): p. 1656-63; discussion 1663.
199. Halstead, J.C., et al., *Avoidance of hemodilution during selective cerebral perfusion enhances neurobehavioral outcome in a survival porcine model.* Eur J Cardiothorac Surg, 2007. **32**(3): p. 514-20.
200. Yano, H. and M. Takaori, *Effect of hemodilution on capillary and arteriolovenous shunt flow in organs after cardiac arrest in dogs.* Crit Care Med, 1990. **18**(10): p. 1146-51.
201. Liu, X., et al., *Buffer administration during CPR promotes cerebral reperfusion after return of spontaneous circulation and mitigates post-resuscitation cerebral acidosis.* Resuscitation, 2002. **55**(1): p. 45-55.
202. Yoon, S., M. Zuccarello, and R.M. Rapoport, *pCO(2) and pH regulation of cerebral blood flow.* Frontiers in physiology, 2012. **3**: p. 365-365.
203. Leonov, Y., et al., *Hypertension with hemodilution prevents multifocal cerebral hypoperfusion after cardiac arrest in dogs.* Stroke, 1992. **23**(1): p. 45-53.
204. Albaeni, A., et al., *The association between post resuscitation hemoglobin level and survival with good neurological outcome following Out Of Hospital cardiac arrest.* Resuscitation, 2016. **99**: p. 7-12.
205. Chow, M.S., et al., *Effects of diaspirin cross-linked hemoglobin (DCLHb) during and post-CPR in swine.* J Pharmacol Exp Ther, 2001. **297**(1): p. 224-9.
206. Hamadate, N., et al., *Liposome-encapsulated hemoglobin ameliorates impairment of fear memory and hippocampal dysfunction after cerebral ischemia in rats.* J Pharmacol Sci, 2010. **114**(4): p. 409-19.
207. Hayman, E.G., et al., *Cerebral Edema After Cardiopulmonary Resuscitation: A Therapeutic Target Following Cardiac Arrest?* Neurocrit Care, 2018. **28**(3): p. 276-287.
208. Krep, H., et al., *Effects of hypertonic versus isotonic infusion therapy on regional cerebral blood flow after experimental cardiac arrest cardiopulmonary resuscitation in pigs.* Resuscitation, 2004. **63**(1): p. 73-83.
209. Kaakinen, T., et al., *Hypertonic saline dextran improves outcome after hypothermic circulatory arrest: a study in a surviving porcine model.* Ann Thorac Surg, 2006. **81**(1): p. 183-90.
210. Noppens, R.R., et al., *Effects of a single-dose hypertonic saline hydroxyethyl starch on cerebral blood flow, long-term outcome, neurogenesis, and neuronal survival after cardiac arrest and cardiopulmonary resuscitation in rats*.* Crit Care Med, 2012. **40**(7): p. 2149-56.
211. Fischer, M. and K.A. Hossmann, *Volume expansion during cardiopulmonary resuscitation reduces cerebral no-reflow.* Resuscitation, 1996. **32**(3): p. 227-40.
212. Wallisch, J.S., et al., *The aquaporin-4 inhibitor AER-271 blocks acute cerebral edema and improves early outcome in a pediatric model of asphyxial cardiac arrest.* Pediatr Res, 2019. **85**(4): p. 511-517.
213. Patil, K.D., H.R. Halperin, and L.B. Becker, *Cardiac arrest: resuscitation and reperfusion.* Circ Res, 2015. **116**(12): p. 2041-9.
214. Lee, T.F., et al., *Effects of postresuscitation N-acetylcysteine on cerebral free radical production and perfusion during reoxygenation of hypoxic newborn piglets.* Pediatr Res, 2008. **64**(3): p. 256-61.

215. Langley, S.M., et al., *The free radical spin trap alpha-phenyl-tert-butyl nitrone attenuates the cerebral response to deep hypothermic ischemia.* J Thorac Cardiovasc Surg, 2000. **119**(2): p. 305-13.
216. Liachenko, S., P. Tang, and Y. Xu, *Deferoxamine improves early postresuscitation reperfusion after prolonged cardiac arrest in rats.* J Cereb Blood Flow Metab, 2003. **23**(5): p. 574-81.
217. Langley, S.M., et al., *Preoperative high dose methylprednisolone attenuates the cerebral response to deep hypothermic circulatory arrest.* Eur J Cardiothorac Surg, 2000. **17**(3): p. 279-86.
218. Schubert, S., et al., *Large-dose pretreatment with methylprednisolone fails to attenuate neuronal injury after deep hypothermic circulatory arrest in a neonatal piglet model.* Anesth Analg, 2005. **101**(5): p. 1311-8.
219. Varvarousi, G., et al., *Combination pharmacotherapy improves neurological outcome after asphyxial cardiac arrest.* Resuscitation, 2012. **83**(4): p. 527-32.
220. Mulligan, K.A., et al., *Synergistic effects of vasopressin plus epinephrine during cardiopulmonary resuscitation.* Resuscitation, 1997. **35**(3): p. 265-71.
221. Prengel, A.W., et al., *Effects of combined administration of vasopressin, epinephrine, and norepinephrine during cardiopulmonary resuscitation in pigs.* Crit Care Med, 2005. **33**(11): p. 2587-91.
222. Mayr, V.D., et al., *Developing a vasopressor combination in a pig model of adult asphyxial cardiac arrest.* Circulation, 2001. **104**(14): p. 1651-6.
223. Halvorsen, P., et al., *Neural injury after use of vasopressin and adrenaline during porcine cardiopulmonary resuscitation.* Ups J Med Sci, 2015. **120**(1): p. 11-9.
224. Ruiz, E., et al., *Cerebral resuscitation after cardiac arrest using hetastarch hemodilution, hyperbaric oxygenation and magnesium ion.* Resuscitation, 1986. **14**(4): p. 213-23.
225. Cerchiari, E.L., et al., *Effects of combined superoxide dismutase and deferoxamine on recovery of brainstem auditory evoked potentials and EEG after asphyxial cardiac arrest in dogs.* Resuscitation, 1990. **19**(1): p. 25-40.
226. Griffiths, P.D., et al., *In vivo measurement of cerebral blood flow: a review of methods and applications.* Vascular Medicine, 2001. **6**(1): p. 51-60.
227. Ostergaard, L., et al., *The role of the microcirculation in delayed cerebral ischemia and chronic degenerative changes after subarachnoid hemorrhage.* J Cereb Blood Flow Metab, 2013. **33**(12): p. 1825-37.
228. Rossano, J.W., M.Y. Naim, V.M. Nadkarni and R.A. Berg, *Epidemiology of Pediatric Cardiac Arrest*, in *Pediatric and Congenital Cardiology, Cardiac Surgery and Intensive Care*. 2013, Springer. p. 1275-1287.
229. Nadkarni, V.M., et al., *First documented rhythm and clinical outcome from in-hospital cardiac arrest among children and adults.* Jama-Journal of the American Medical Association, 2006. **295**(1): p. 50-57.
230. Fink, E.L., et al., *Experimental model of pediatric asphyxial cardiopulmonary arrest in rats.* Pediatr Crit Care Med, 2004. **5**(2): p. 139-44.
231. Manole, M.D., et al., *Brain tissue oxygen monitoring identifies cortical hypoxia and thalamic hyperoxia after experimental cardiac arrest in rats.* Pediatric Research, 2014. **75**(2): p. 295-301.

232. Hill, R.A., et al., *Regional Blood Flow in the Normal and Ischemic Brain Is Controlled by Arteriolar Smooth Muscle Cell Contractility and Not by Capillary Pericytes.* Neuron, 2015. **87**(1): p. 95-110.
233. Itoh, Y. and N. Suzuki, *Control of brain capillary blood flow.* J Cereb Blood Flow Metab, 2012. **32**(7): p. 1167-76.
234. Levy, D.E., J.B. Brierley, and F. Plum, *Ischaemic brain damage in the gerbil in the absence of 'no-reflow'.* J Neurol Neurosurg Psychiatry, 1975. **38**(12): p. 1197-1205.
235. Fischer, E.G., et al., *Reassessment of cerebral capillary changes in acute global ischemia and their relationship to the "no-reflow phenomenon".* Stroke, 1977. **8**(1): p. 36-9.
236. Bai, J. and P.D. Lyden, *Revisiting cerebral postischemic reperfusion injury: new insights in understanding reperfusion failure, hemorrhage, and edema.* Int J Stroke, 2015. **10**(2): p. 143-52.
237. del Zoppo, G.J., *Virchow's triad: the vascular basis of cerebral injury.* Rev Neurol Dis, 2008. **5 Suppl 1**: p. S12-21.
238. Kamoun, W.S., et al., *Simultaneous measurement of RBC velocity, flux, hematocrit and shear rate in vascular networks.* Nat Methods, 2010. **7**(8): p. 655-60.
239. Hauck, E.F., et al., *Capillary flow and diameter changes during reperfusion after global cerebral ischemia studied by intravital video microscopy.* J Cereb Blood Flow Metab, 2004. **24**(4): p. 383-91.
240. Stefanovic, B., et al., *Functional reactivity of cerebral capillaries.* J Cereb Blood Flow Metab, 2008. **28**(5): p. 961-72.
241. Adams, D.L., et al., *Vascular Supply of the Cerebral Cortex is Specialized for Cell Layers but Not Columns.* Cereb Cortex, 2015. **25**(10): p. 3673-81.
242. Iadecola, C., *Neurovascular regulation in the normal brain and in Alzheimer's disease.* Nat Rev Neurosci, 2004. **5**(5): p. 347-60.
243. Dezfulian, C., et al., *Mechanistic characterization of nitrite-mediated neuroprotection after experimental cardiac arrest.* J Neurochem, 2016. **139**(3): p. 419-431.
244. Morgan, R.W., et al., *A hemodynamic-directed approach to pediatric cardiopulmonary resuscitation (HD-CPR) improves survival.* Resuscitation, 2017. **111**: p. 41-47.
245. Itoh, Y., *Blockade of thromboxane A2 receptor ameliorates delayed postischemic hypoperfusion of the brain in cats.* Keio J Med, 1994. **43**(2): p. 88-93.
246. Lee, J.K., et al., *Cerebral blood flow and cerebrovascular autoregulation in a swine model of pediatric cardiac arrest and hypothermia.* Crit Care Med, 2011. **39**(10): p. 2337-45.
247. Smrcka, M., et al., *"No-reflow" phenomenon as a cause of hypoperfusion after severe head injury?* Bratisl Lek Listy, 2003. **104**(7-8): p. 236-8.
248. Pluta, R., et al., *Platelet occlusion phenomenon after short- and long-term survival following complete cerebral ischemia in rats produced by cardiac arrest.* J Hirnforsch, 1994. **35**(4): p. 463-71.
249. Tanahashi N, F.Y., Tomita M, Kobari M, Takeda H, Yokoyama M, *Pentoxifylline ameliorates postischemic delayed hypoperfusion of the cerebral cortex following cardiac arrest in cats.* J Neurol Sci, 1995. **132**(2): p. 105-9.
250. Kuzman, D., et al., *Effect of pH on red blood cell deformability.* Pflugers Arch, 2000. **440**(5 Suppl): p. R193-4.

251. Crumrine, R.C. and J.C. LaManna, *Regional cerebral metabolites, blood flow, plasma volume, and mean transit time in total cerebral ischemia in the rat.* J Cereb Blood Flow Metab, 1991. **11**(2): p. 272-82.
252. Drabek, T., et al., *Global and regional differences in cerebral blood flow after asphyxial versus ventricular fibrillation cardiac arrest in rats using ASL-MRI.* Resuscitation, 2014. **85**(7): p. 964-71.
253. Kozberg, M.G., et al., *Resolving the transition from negative to positive blood oxygen level-dependent responses in the developing brain.* Proc Natl Acad Sci U S A, 2013. **110**(11): p. 4380-5.
254. Seregi, A., M. Keller, and G. Hertting, *Are cerebral prostanoids of astroglial origin? Studies on the prostanoid forming system in developing rat brain and primary cultures of rat astrocytes.* Brain Res, 1987. **404**(1-2): p. 113-20.
255. Du, L., et al., *Innate gender-based proclivity in response to cytotoxicity and programmed cell death pathway.* J Biol Chem, 2004. **279**(37): p. 38563-70.
256. Armstead, W.M., J. Riley, and M.S. Vavilala, *K channel impairment determines sex and age differences in epinephrine-mediated outcomes after brain injury.* J Neurosci Res, 2017.
257. Samuelsson, B., *Arachidonic acid metabolism: role in inflammation.* Z Rheumatol, 1991. **50 Suppl 1**: p. 3-6.
258. Ding, X.Z., R. Hennig, and T.E. Adrian, *Lipoxygenase and cyclooxygenase metabolism: new insights in treatment and chemoprevention of pancreatic cancer.* Mol Cancer, 2003. **2**: p. 10.
259. Panigrahy, D., et al., *Cytochrome P450-derived eicosanoids: the neglected pathway in cancer.* Cancer Metastasis Rev, 2010. **29**(4): p. 723-35.
260. Liu, M., P.D. Hurn, and N.J. Alkayed, *Cytochrome P450 in neurological disease.* Curr Drug Metab, 2004. **5**(3): p. 225-34.
261. McGiff, J.C. and J. Quilley, *20-HETE and the kidney: resolution of old problems and new beginnings.* Am J Physiol, 1999. **277**(3 Pt 2): p. R607-23.
262. Imig, J.D., *Epoxide hydrolase and epoxygenase metabolites as therapeutic targets for renal diseases.* American Journal of Physiology-Renal Physiology, 2005. **289**(3): p. F496-F503.
263. Kehl, F., et al., *20-HETE contributes to the acute fall in cerebral blood flow after subarachnoid hemorrhage in the rat.* Am J Physiol Heart Circ Physiol, 2002. **282**(4): p. H1556-65.
264. Lu, L., et al., *20-HETE Inhibition by HET0016 Decreases the Blood-Brain Barrier Permeability and Brain Edema After Traumatic Brain Injury.* Front Aging Neurosci, 2018. **10**: p. 207.
265. Han, X., et al., *20-HETE synthesis inhibition promotes cerebral protection after intracerebral hemorrhage without inhibiting angiogenesis.* J Cereb Blood Flow Metab, 2018: p. 271678x18762645.
266. Zhang, H., et al., *Upregulation of 20-HETE Synthetic Cytochrome P450 Isoforms by Oxygen-Glucose Deprivation in Cortical Neurons.* Cell Mol Neurobiol, 2017. **37**(7): p. 1279-1286.
267. Gebremedhin, D., et al., *Expression of CYP 4A omega-hydroxylase and formation of 20-hydroxyeicosatetreanoic acid (20-HETE) in cultured rat brain astrocytes.* Prostaglandins Other Lipid Mediat, 2016. **124**: p. 16-26.

268. Yang, Z.J., et al., *Attenuation of neonatal ischemic brain damage using a 20-HETE synthesis inhibitor.* J Neurochem, 2012. **121**(1): p. 168-79.
269. Li, L., et al., *Cerebral microcirculatory alterations and the no-reflow phenomenon in vivo after experimental pediatric cardiac arrest.* J Cereb Blood Flow Metab, 2017: p. 271678x17744717.
270. Mu, Y., et al., *Intravenous formulation of N-hydroxy-N'-(4-n-butyl-2-methylphenyl)formamidine (HET0016) for inhibition of rat brain 20-hydroxyeicosatetraenoic acid formation.* Drug Metab Dispos, 2008. **36**(11): p. 2324-30.
271. Nishimura, N., et al., *Penetrating arterioles are a bottleneck in the perfusion of neocortex.* Proc Natl Acad Sci U S A, 2007. **104**(1): p. 365-70.
272. Kulik, T., et al., *Regulation of cerebral vasculature in normal and ischemic brain.* Neuropharmacology, 2008. **55**(3): p. 281-8.
273. Kontos, H.A., et al., *Responses of cerebral arteries and arterioles to acute hypotension and hypertension.* Am J Physiol, 1978. **234**(4): p. H371-83.
274. Kobari, M., et al., *Blood flow velocity in the pial arteries of cats, with particular reference to the vessel diameter.* J Cereb Blood Flow Metab, 1984. **4**(1): p. 110-4.
275. Qi, X., et al., *(2-Hydroxypropyl)-beta-Cyclodextrin Is a New Angiogenic Molecule for Therapeutic Angiogenesis.* PLoS One, 2015. **10**(5): p. e0125323.
276. Sterz, F., et al., *Hypertension with or without hemodilution after cardiac arrest in dogs.* Stroke, 1990. **21**(8): p. 1178-84.
277. Stefaniotou, A., et al., *The effects of nitroglycerin during cardiopulmonary resuscitation.* Eur J Pharmacol, 2014. **734**: p. 42-9.
278. Zhu, J., et al., *Additive Neuroprotection of a 20-HETE Inhibitor with Delayed Therapeutic Hypothermia after Hypoxia-Ischemia in Neonatal Piglets.* Dev Neurosci, 2015. **37**(4-5): p. 376-89.
279. Manole, M.D., et al., *Brain tissue oxygen monitoring identifies cortical hypoxia and thalamic hyperoxia after experimental cardiac arrest in rats.* Pediatr Res, 2014. **75**(2): p. 295-301.
280. van Gijn, J., R.S. Kerr, and G.J. Rinkel, *Subarachnoid haemorrhage.* Lancet, 2007. **369**(9558): p. 306-18.
281. Donnelly, M.K., et al., *20-HETE is associated with unfavorable outcomes in subarachnoid hemorrhage patients.* Journal of Cerebral Blood Flow and Metabolism, 2015. **35**(9): p. 1515-1522.
282. Zacharia, B.E., et al., *Epidemiology of aneurysmal subarachnoid hemorrhage.* Neurosurg Clin N Am, 2010. **21**(2): p. 221-33.
283. *Epidemiology of aneurysmal subarachnoid hemorrhage in Australia and New Zealand: incidence and case fatality from the Australasian Cooperative Research on Subarachnoid Hemorrhage Study (ACROSS).* Stroke, 2000. **31**(8): p. 1843-50.
284. Lee, K.H., T. Lukovits, and J.A. Friedman, *"Triple-H" therapy for cerebral vasospasm following subarachnoid hemorrhage.* Neurocrit Care, 2006. **4**(1): p. 68-76.
285. Taylor, T.N., et al., *Lifetime cost of stroke in the United States.* Stroke, 1996. **27**(9): p. 1459-66.
286. Macdonald, R.L., *Delayed neurological deterioration after subarachnoid haemorrhage.* Nat Rev Neurol, 2014. **10**(1): p. 44-58.

287. Mahaney, K.B., et al., *Acute postoperative neurological deterioration associated with surgery for ruptured intracranial aneurysm: incidence, predictors, and outcomes.* J Neurosurg, 2012. **116**(6): p. 1267-78.
288. van der Schaaf, I.C., et al., *Study design and outcome measures in studies on aneurysmal subarachnoid hemorrhage.* Stroke, 2002. **33**(8): p. 2043-6.
289. Dorsch, N., *A clinical review of cerebral vasospasm and delayed ischaemia following aneurysm rupture.* Acta Neurochir Suppl, 2011. **110**(Pt 1): p. 5-6.
290. Crowley, R.W., et al., *Angiographic vasospasm is strongly correlated with cerebral infarction after subarachnoid hemorrhage.* Stroke, 2011. **42**(4): p. 919-23.
291. Laskowitz, D.T. and B.J. Kolls, *Neuroprotection in subarachnoid hemorrhage.* Stroke, 2010. **41**(10 Suppl): p. S79-84.
292. Macdonald, R.L., et al., *Clazosentan to overcome neurological ischemia and infarction occurring after subarachnoid hemorrhage (CONSCIOUS-1): randomized, double-blind, placebo-controlled phase 2 dose-finding trial.* Stroke, 2008. **39**(11): p. 3015-21.
293. Liu, P., J.B. De Vis, and H. Lu, *Cerebrovascular reactivity (CVR) MRI with CO2 challenge: A technical review.* Neuroimage, 2018.
294. Dernbach, P.D., et al., *Altered cerebral autoregulation and CO2 reactivity after aneurysmal subarachnoid hemorrhage.* Neurosurgery, 1988. **22**(5): p. 822-6.
295. Balbi, M., et al., *Inversion of neurovascular coupling after subarachnoid hemorrhage in vivo.* J Cereb Blood Flow Metab, 2017. **37**(11): p. 3625-3634.
296. Schmieder, K., et al., *CO2 reactivity in patients after subarachnoid haemorrhage.* Acta Neurochir (Wien), 1997. **139**(11): p. 1038-41.
297. da Costa, L., et al., *Impaired cerebrovascular reactivity in the early phase of subarachnoid hemorrhage in good clinical grade patients does not predict vasospasm.* Acta Neurochir Suppl, 2015. **120**: p. 249-53.
298. Hassler, W. and F. Chioffi, *CO2 reactivity of cerebral vasospasm after aneurysmal subarachnoid haemorrhage.* Acta Neurochir (Wien), 1989. **98**(3-4): p. 167-75.
299. Gebremedhin, D., et al., *Production of 20-HETE and its role in autoregulation of cerebral blood flow.* Circ Res, 2000. **87**(1): p. 60-5.
300. Siler, D.A., et al., *Protective role of p450 epoxyeicosanoids in subarachnoid hemorrhage.* Neurocritical care, 2015. **22**(2): p. 306-319.
301. Crago, E.A., et al., *Cerebrospinal fluid 20-HETE is associated with delayed cerebral ischemia and poor outcomes after aneurysmal subarachnoid hemorrhage.* Stroke, 2011. **42**(7): p. 1872-1877.
302. Dunn, K.M., et al., *Elevated production of 20-HETE in the cerebral vasculature contributes to severity of ischemic stroke and oxidative stress in spontaneously hypertensive rats.* American journal of physiology. Heart and circulatory physiology, 2008. **295**(6): p. H2455-H2465.
303. Crago, E.A., et al., *Cerebrospinal fluid 20-HETE is associated with delayed cerebral ischemia and poor outcomes after aneurysmal subarachnoid hemorrhage.* Stroke, 2011. **42**(7): p. 1872-7.
304. Park, C.W., et al., *Autoregulatory response and CO2 reactivity of the basilar artery.* Stroke, 2003. **34**(1): p. 34-9.
305. Miller, T.M., et al., *Rapid, simultaneous quantitation of mono and dioxygenated metabolites of arachidonic acid in human CSF and rat brain.* J Chromatogr B Analyt Technol Biomed Life Sci, 2009. **877**(31): p. 3991-4000.

306. MacVicar, B.A. and E.A. Newman, *Astrocyte regulation of blood flow in the brain.* Cold Spring Harb Perspect Biol, 2015. **7**(5).
307. Marji, J.S., M.H. Wang, and M. Laniado-Schwartzman, *Cytochrome P-450 4A isoform expression and 20-HETE synthesis in renal preglomerular arteries.* Am J Physiol Renal Physiol, 2002. **283**(1): p. F60-7.
308. Fan, F., et al., *Molecular mechanisms and cell signaling of 20-hydroxyeicosatetraenoic acid in vascular pathophysiology.* Front Biosci (Landmark Ed), 2016. **21**: p. 1427-63.
309. Yi, X., et al., *20-Hydroxyeicosatetraenoic Acid as a Predictor of Neurological Deterioration in Acute Minor Ischemic Stroke.* Stroke, 2016. **47**(12): p. 3045-3047.
310. Widder, B., et al., *Transcranial Doppler CO2 test for the detection of hemodynamically critical carotid artery stenoses and occlusions.* Eur Arch Psychiatry Neurol Sci, 1986. **236**(3): p. 162-8.
311. Oldag, A., et al., *Near-infrared spectroscopy and transcranial sonography to evaluate cerebral autoregulation in middle cerebral artery steno-occlusive disease.* J Neurol, 2016. **263**(11): p. 2296-2301.
312. Portegies, M.L., et al., *Cerebral vasomotor reactivity and risk of mortality: the Rotterdam Study.* Stroke, 2014. **45**(1): p. 42-7.
313. Bragin, D.E., et al., *Rheological effects of drag-reducing polymers improve cerebral blood flow and oxygenation after traumatic brain injury in rats.* J Cereb Blood Flow Metab, 2017. **37**(3): p. 762-775.
314. van den Brule, J.M.D., J.G. van der Hoeven, and C.W.E. Hoedemaekers, *Cerebral Perfusion and Cerebral Autoregulation after Cardiac Arrest.* Biomed Res Int, 2018. **2018**: p. 4143636.
315. Nemoto, E.M., et al., *Role of microvascular shunts in the loss of cerebral blood flow autoregulation.* Adv Exp Med Biol, 2014. **812**: p. 43-49.
316. Brown, C.G., et al., *The effect of high-dose phenylephrine versus epinephrine on regional cerebral blood flow during CPR.* Ann Emerg Med, 1987. **16**(7): p. 743-8.
317. Safar, P., et al., *Improved cerebral resuscitation from cardiac arrest in dogs with mild hypothermia plus blood flow promotion.* Stroke, 1996. **27**(1): p. 105-13.
318. Voelckel, W.G., et al., *Effects of epinephrine and vasopressin in a piglet model of prolonged ventricular fibrillation and cardiopulmonary resuscitation.* Crit Care Med, 2002. **30**(5): p. 957-62.
319. Pytte, M., et al., *Haemodynamic effects of adrenaline (epinephrine) depend on chest compression quality during cardiopulmonary resuscitation in pigs.* Resuscitation, 2006. **71**(3): p. 369-78.
320. Semenas, E., H.S. Sharma, and L. Wiklund, *Adrenaline increases blood-brain-barrier permeability after haemorrhagic cardiac arrest in immature pigs.* Acta Anaesthesiol Scand, 2014. **58**(5): p. 620-9.
321. Debaty, G., et al., *Enhanced perfusion during advanced life support improves survival with favorable neurologic function in a porcine model of refractory cardiac arrest.* Crit Care Med, 2015. **43**(5): p. 1087-95.
322. Hardig, B.M., et al., *Physiologic effect of repeated adrenaline (epinephrine) doses during cardiopulmonary resuscitation in the cath lab setting: A randomised porcine study.* Resuscitation, 2016. **101**: p. 77-83.

323. Angelos, M.G., K.R. Ward, and P.D. Beckley, *Norepinephrine-induced hypertension following cardiac arrest: effects on myocardial oxygen use in a swine model.* Ann Emerg Med, 1994. **24**(5): p. 907-14.
324. Ikeda, Y., et al., *Arginine vasopressin release inhibitor RU51599 attenuates brain oedema following transient forebrain ischaemia in rats.* Acta Neurochir (Wien), 1997. **139**(12): p. 1166-71; discussion 1171-2.
325. Nozari, A., S. Rubertsson, and L. Wiklund, *Improved cerebral blood supply and oxygenation by aortic balloon occlusion combined with intra-aortic vasopressin administration during experimental cardiopulmonary resuscitation.* Acta Anaesthesiol Scand, 2000. **44**(10): p. 1209-19.
326. Krep, H., M. Fischer, and A. Hoeft, *Endothelin-1 elevates regional cerebral perfusion during prolonged ventricular fibrillation cardiac arrest in pigs.* Resuscitation, 2003. **57**(3): p. 317-8.
327. Lin, H.W., et al., *Protein kinase C delta modulates endothelial nitric oxide synthase after cardiac arrest.* J Cereb Blood Flow Metab, 2014. **34**(4): p. 613-20.
328. Sistino, J.J., et al., *Safety of heparin-coated circuits in primates during deep hypothermic cardiopulmonary bypass.* J Extra Corpor Technol, 1993. **25**(1): p. 15-21.
329. Lin, S.R., et al., *The effect of combined dextran and streptokinase on cerebral function and blood flow after cardiac arrest: and experimental study on the dog.* Invest Radiol, 1978. **13**(6): p. 490-8.
330. Sterz, F., et al., *Effects of U74006F on multifocal cerebral blood flow and metabolism after cardiac arrest in dogs.* Stroke, 1991. **22**(7): p. 889-95.
331. Lin, S.R., et al., *Effect of dextran on cerebral function and blood after cardiac arrest. An experimental study on the dog.* Stroke, 1979. **10**(1): p. 13-20.
332. Nozari, A., et al., *Maximisation of cerebral blood flow during experimental cardiopulmonary resuscitation does not ameliorate post-resuscitation hypoperfusion.* Resuscitation, 1999. **40**(1): p. 27-35.